Intrinsic and extrinsic drivers of T_{reg} fragility in the tumor microenvironment

by

Abigail E. Overacre-Delgoffe

B.Sc., The University of Oklahoma, 2012

Submitted to the Graduate Faculty of

The School of Medicine in partial fulfillment

of the requirements for the degree of

Doctor of Philosophy

University of Pittsburgh

2018

UNIVERSITY OF PITTSBURGH

SCHOOL OF MEDICINE

This dissertation was presented

by

Abigail E. Overacre-Delgoffe

It was defended on

February 20, 2018

and approved by

Robert L. Ferris M.D., Director, UPMC Hillman Cancer Center, Hillman Professor of Oncology, Professor of Otolaryngology, Immunology, and Radiation Oncology

Lisa H. Butterfield PhD, Professor, Medicine, Surgery, Immunology, and Clinical & Translational Science

Janet S. Lee PhD, Professor, Medicine

Michael T. Lotze M.D., Professor, Surgery & Immunology

Dissertation Advisor: **Dario A.A. Vignali PhD**, Frank Dixon Chair in Cancer Immunology, Vice Chair and Professor, Immunology

Intrinsic and extrinsic drivers of T_{reg} fragility in the tumor microenvironment

Abigail E. Overacre-Delgoffe, PhD

University of Pittsburgh, 2018

Regulatory T cells (T_{regs}) are required to maintain immune homeostasis through suppressive mechanisms. Characterized by the transcription factor Foxp3, they exert function in a variety of ways, including producing adenosine, and secreting suppressive cytokines. While mandatory for prevention of autoimmunity, T_{regs} contribute to cancer progression by suppressing the anti-tumor immune response. Depletion of the entire T_{reg} pool is not a viable option for therapy, as mice and humans lacking this population succumb to systemic autoimmunity. Therefore, it is critical to uncover novel mechanisms to target T_{reg} function specifically within the tumor microenvironment (TME) and determine means by which they can in turn be regulated or counter-regulated.

Neuropilin-1 (Nrp1) is required to maintain T_{reg} function and stability within the TME through binding of Semaphorin-4a, and when deleted from T_{regs}, mice show significantly reduced tumor growth or clearance (**Appendix A**). However, Nrp1 is dispensable for T_{reg} function in the periphery, making this an attractive target in cancer immunotherapy. Interestingly, *Nrp1*$^{-/-}$ T_{regs} maintain Foxp3 expression but lose suppressive function, resulting in T_{reg} 'fragility', a term I have coined to describe this phenomenon (**Chapter 3**). Rather, these cells secrete the pro-inflammatory cytokine IFNγ and cripple surrounding WT T_{regs}, leading to infectious fragility and enhanced anti-tumor immunity. Strikingly, IFNγ-mediated T_{reg} fragility is required for response to PD-1 blockade in mice, and seems to be partially responsible for response to other

immunotherapies, including antibodies and vaccines (**Chapter 4**). Nrp1 also prevents T_{reg} fragility by acting as a driver of T_{reg} metabolic plasticity within the tumor microenvironment. Indeed, while WT T_{regs} are distinct metabolically in order to survive in a nutrient-depleted environment within the tumor, *Nrp1*$^{-/-}$ T_{regs} are dependent on glycolysis (**Chapter 5**). This is thought to be due to an increase in Hif1α which supports glycolysis and increases IFNγ in T_{regs}. Lastly, I have shown that Nrp1 supports T_{reg} stability through maintaining hypomethylation at the Foxp3 locus in the tumor microenvironment, as *Nrp1*$^{-/-}$ T_{regs} are hypermethylated, but maintain Foxp3 expression (**Appendix B**).

Taken together, my findings have uncovered new mechanisms that drive T_{reg} fragility in tumors that are critical for response to immunotherapy.

Table of contents

LIST OF TABLES

LIST OF FIGURES

PREFACE

The training leading up to my PhD has been a wonderful experience, and is one that I will look back on fondly for many years to come.

My mentor, Dr. Dario Vignali, has had a tremendous impact on my life both as a scientist and as an individual. None of this would have been possible without him taking a chance on a biochemist with absolutely no immunology experience and his being endlessly patient. He has provided priceless guidance, insight into how to be a successful scientist, freedom to explore within my project, and support at every step along the way. I feel as though sometimes I am a ‘mini-Dario’ and that is a title I am very proud of. It has been an honor to be his student and I hope to continue to make him proud throughout my scientific career.

My thesis committee has been integral in my success within the program. I’d like to thank Drs. Lisa Butterfield, Bob Ferris, Janet Lee, and Mike Lotze for their incredible support and scientific insight. They provided exceptional guidance in both my PhD projects and my career development. I value their input greatly.

I am immensely thankful for a number of postdoctoral associates I have had the pleasure of getting to know throughout my training. Matt and Maria Bettini set an excellent example of work ethic in the lab while enjoying every minute. They also were supportive of me in the lab from my very first day, which greatly shaped my decision to

join the lab. Meghan Turnis taught me how to work with mouse tumor models, and for that I am thankful. Deepali Sawant has been a great friend to me within in the lab and I enjoyed our scientific and family discussions. Cliff Guy was the first postdoc I worked with in the lab and was extremely patient with me. I am thankful for his training and his “baptism by fire” approach, and for having so much confidence in me.

I am also thankful for other members of the lab who provided training and career support to me. Creg Workman continuously mentored me through all aspects of lab, from technical details of an experiment to motivating me during tough revisions of a paper. Tullia Bruno has been an excellent mentor from both a scientific and career perspective, and has also become a very dear friend over the years.

Greg Delgoffe has played an instrumental role in my success as a scientist. He is the best example of someone who loves every aspect of the job, from the 6am mouse harvests, to the 11pm flow. He has constantly supported me through every peak and valley of graduate school. I’m lucky to call him my “partner in crime” in life, and I treasure our adventures together every day.

A number of other people within the lab have made my time here more enjoyable. Andrea Workman aided me in cloning and was always fun to talk to in and out of lab. Kate Vignali provided unlimited insight and help in cloning, and I always enjoyed our lively conversations about politics or family. Sherry Zhang has been an amazing colleague and friend along this journey—her excellence and commitment has made me a better scientist. Becky Dadey has been a great friend and supporter to me over the years, and I cherish our relationship. I always enjoy the fun discussions and

excitement Hiro Yano has for science. Erin Brunazzi has been a great friend to me and without her help, my work would not have been possible.

My friends and family have been so supportive over the years—their encouragement has given me the confidence needed to complete this program. I have developed great friendships with many people throughout the Immunology Department, including Lyndsay Avery, Rachael Gordon, and Uzo Uche, and I am thankful for their support and fun scientific discussions.

ABBREVIATIONS

2-NBDG: (2-(N-(7-Nitrobenz-2-oxa-1,3-diazol-4-yl)Amino)-2-Deoxyglucose)

ADCC: antibody dependent cell mediated cytotoxicity

Akt: protein kinase B

ATP: adenosine triphosphate

B16: transplantable mouse melanoma cell line

BAC: bacterial artificial chromosome

Bcl2: B cell lymphoma 2

CCL2: C-C motif chemokine ligand 2

CCR4: C-C motif receptor 4

CNS2: conserved non-coding sequence 2

CpG: C-phosphate-G site

Cre: cre recombinase

CTLA4: cytotoxic T lymphocyte associate protein 4

Cxcr3: C-X-C chemokine receptor 3

DAPI: 4’,6-diamidino-2-phenylindole

DC: dendritic cell

DKO: double knock out

dLN; draining lymph node

DNMT: DNA methyltransferase

DT: diphtheria toxin

DTR: diphtheria toxin receptor

ECAR: extracellular acidification rate

EL4: transplantable mouse lymphoma cell line

Eomes: eomesodermin

Foxo: forkhead box O

Foxp3: forkhead box P3

GBM: malignant gliobastoma

GFP: green fluorescent protein

GITR: glucocorticoid induced TNFR-related protein (TNFRSF18)

Hif1α: hypoxia inducible factor 1α

HNSCC: head and neck squamous cell carcinoma

i.p.: intraperitoneal

i.v.: intravenous

ICOS: inducible T cell costimulatory

IFNgR1 or IFNγR1: Interferon-γ receptor

IFNγ: Interferon-γ

Ig: immunoglobulin

IL10: interleukin 10

IL2: interleukin 2

IL35: interleukin 35

IL7r: Interleukin-7 receptor

IPEX: immune dysregulation, polyendocrinopathy, enteropathy, X-linked

IR: inhibitory receptor

IRES: internal ribosomal entry site

IRF4: interferon regulatory factor 4

iT_{reg}: induced T_{reg} (*in vitro*)

Klf2: kruppel like factor 2

LAG3: lymphocyte activation gene 3

LARC: late advanced rectal cancer

MC38: transplantable mouse adenocarcinoma cell line

MSA: microsuppression assay

MSA-IL-2: mouse serum albumin fused to IL-2

mTOR: mechanistic target of rapamycin

ndLN: non-draining lymph node

NK cell: natural killer cell

NOD: non-obese diabetic mice

Nrp1: neuropilin-1

OCR: oxygen consumption rate

OXPHOS: oxidative phosphorylation

PBL: peripheral blood lymphocytes

PD-1 program cell death protein 1

pDC: plasmacytoid dendritic cell

PDK: pyruvate dehydrogenase kinase

PGC1α: PPAR-gamma coactivator 1 α

PI3K: phosphoinositide 3-kinase

PTEN: phosphatase and tensin homolog

pT_{reg}: peripherally derived T_{reg}

qPCR: quantitative polymerase chain reaction

RNASeq: RNA Sequencing

Rorγt: RAR related orphan receptor γ

s.c.: subcutaneous

SEM: standard error of the mean

Sema4a: Semaphorin-4a

SRC: spare respiratory capacity

Stat: signal transducer and activator of transcription

Tbx21: T-box transcriptional factor 21 (encodes T-bet)

T_{conv}: conventional T cells

TCR: T cell receptor

T_{eff}: effector T cell

Tet2: Tet methylcytosine dioxygenase 2

Tg: transgenic

TGFβ: transforming growth factor β

T_H: T helper cell

TIL: tumor infiltrating lymphocytes

TME: tumor microenvironment

TMRE: tetramethylrhodamine

T_{reg}: regulatory T cell

Trp1: tyrosinase related protein 1

TSDR: T_{reg} specific demethylated region

tT_{reg}: thymically derived T_{reg}

UTR: untranslated region

VEGF: vascular endothelial growth factor

WT: wildtype

YFP: yellow fluorescent protein

1.0 INTRODUCTION

Portions of this chapter (1.6 and 1.7) were compiled and submitted to *Current Opinion in Immunology* in the following manuscript:

Overacre AE, Vignali, DA. "T_{reg} stability: to be or not to be?" Curr Opin Immunol. 2016 Jan 14;39:39-43. doi: 10/1016/j.coi.2015.12.009.

1.1 CANCER

1.1.1 Hallmarks

Cancer is a chronic, often fatal group of diseases that can occur in a variety of tissues, each with a distinct microenvironment. It is the second leading cause of death globally [1] and the single leading cause of death in those dying in the US under the age of 85. Cancer related deaths are expected to increase substantially over the next 2 decades. Cancer development occurs when normal cells are altered and take on a multitude of new 'hallmarks', including the ability to resist cell death, inducing angiogenesis, sustained proliferative signaling, evading growth suppressors, activating invasion and metastasis, and enabling replicative immortality. In addition, tumor cells can gain the ability to deregulate cellular energetics, enable genome instability and mutation, and

prevent immune clearance through avoiding immune-mediated destruction and promotion of ‘pro-tumor’ inflammation [2, 3].

1.1.2 Cancer Immunoediting

While traditional treatment methods (chemotherapy, surgery, radiation, hormonal therapy) are somewhat successful in a proportion of patients, many, primarily those with metastatic disease, are not responsive. This is thought to be in part due to the tumor’s ability to evade the immune system [4]. Immunosurveillance, the process by which the immune system identifies and eliminates newly transformed cells that could be cancerous and is thought to be a major contributor of cancer prevention. IFNγ, whether produced naturally or administered exogenously, plays a critical role in immunosurveillance by acting directly on the tumor cells to induce autophagy, limit new protein production, promote antigen processing and presentation in the context of MHC molecules. It also acts on immune cells, leading to the production of chemokines that attract additional cells to the tumor site [5, 6, 7]. While immunosurveillance is effective at eliminating many tumor cells, others acquire additional mutations as a result of immune pressure (so-called immune editing) and become less immunogenic, leading to an equilibrium between the tumor and immune cells. This stage of cancer is often not detected clinically and can last for decades [8]. Once equilibrium is reached, select tumor cells are able to escape the immune system by becoming less ‘visible’ to the immune system through downregulation of MHC or antigen expression, or by recruiting immunosuppressive cells to the microenvironment, such as regulatory T cells.

Therefore, tactics to educate and stimulate the immune system against tumor cells has gained interest.

1.2 IMMUNOTHERAPY

1.2.1 Coley's Toxins

Coley's toxins were first used in the late 1800s, when William Coley injected *Streptococcal pyogenes* into a patient with an inoperable tumor in hopes of awakening the "resisting mechanisms" or immune system [9]. He had previously observed tumor regression after a patient had come down with a skin infection and high fever, which inspired him to try this approach. His first patient responded to therapy and led to more than 40 years of Coley treating patients with *Streptococcal pyogenes* or *Serratia marcescens*. He later became known as one of the "Fathers of Immunotherapy"; however, his immunotherapeutic approach was halted due to unreliable success rates in the 1960s by the FDA with the rise of radiation and chemotherapy.

1.2.2 Vaccines

Therapeutic vaccines were first utilized in the late 1800s by combining a patient's irradiated tumor cells with an adjuvant to stimulate the immune system [10]. A GM-CSF transduced tumor vaccine (GVAX) was later developed; however, while it showed limited efficacy in the clinic as a monotherapy, it has since been combined with

checkpoint inhibitors for the treatment of patients with prostate cancer as well as listeria-expressing mesothelin for pancreatic cancer [11, 12, 13, 14]. Therapeutic vaccinations have been developed in other cancers such as melanoma by loading DCs with tumor peptides and in breast cancer through development of a vaccine against the HER2 antigen [15, 16].

1.2.3 Adoptive Cell Therapy

Adoptive cell therapy (ACT) is the isolation, expansion, and re-administration of a patient's own immune effector cells to target their cancer [17]. The most successful application of this is the development of chimeric antigen receptor (CAR) T cell therapy. CAR T was initially used in relapsed pediatric liquid tumors (ALL) with response occurring in most of the patients [18, 19]. Since this time, CAR T has been FDA approved for pediatric ALL and has recently been used in adult ALL as well.

1.2.4 Antibodies

Immunotherapy developed a renewed focus of cancer therapy 7 years ago, when an antibody targeting the inhibitory receptor, CTLA-4 (Ipilimumab), showed a ~20% increase in overall survival in metastatic melanoma patients and was FDA approved. Interest in immunotherapy grew rapidly a few years later when another antibody targeting PD-1 (Nivolumab) was approved with better than anticipated patient responses, showing a 40% objective response rate in melanoma patients [20, 21, 22, 23, 24]. The underlying mechanisms of resistance to immunotherapy are not fully understood.

One potential roadblock is the presence of suppressive cell populations, primarily T_{regs}[25].

1.3 REGULATORY T CELLS

1.3.1 T_{reg} Characteristics and Function

T_{regs} function as the master regulators of the immune system, providing the much needed 'breaks' to reign in the immune response in order to maintain homeostasis and prevent autoimmunity. Initially identified as 'suppressor cells' [26], these cells were later characterized by expression of the transcription factor *Foxp3* in mice [27]. These cells can develop in the thymus (tT_{regs}), arise in the periphery (pT_{regs}), or be generated *in vitro* with the addition of TGFβ (iT_{regs}) [28]. I will primarily focus on tT_{regs} (herein denoted as 'T_{regs}'); however, the role of pT_{regs} in tumors, their stabilizing factors, and whether they become fragile in tumors remains unclear and warrants further investigation.

T_{reg} function is exerted through a variety of mechanisms such as (1) cytokine secretion (including IL-10 and IL-35), (2) metabolic disruption through CD39:CD73 adenosine production pathways or IL-2 deprivation, (3) direct cytolysis through Granzyme B delivery through perforin pores, and (4) dendritic cell targeting through upregulation of LAG3 and CTLA4 [29]. In the absence of T_{regs} or when the *Foxp3* locus is disrupted, rampant autoimmunity ensues. This presents as IPEX (immune disregulation polyendocrinopathy, enteropathy, x-linked) in patients and is lethal without allogenic bone marrow transplantation [30, 31]. A similar disease occurs in mice bearing the *Scurfy*

mutation [32, 33] but can be prevented through T_{reg} cell transfer within 48 hours of birth [34]. While T_{regs} are critical for preventing autoimmunity, they also suppress the anti-tumor immune response and promote tumor outgrowth [35]. Indeed, a higher CD8:T_{reg} ratio is predictive of response to combination radiation and anti-CTLA4 in mice [36]. Furthermore, many cancer types show a positive correlation between higher T_{reg} percentages and poor prognosis in patients [37, 38].

1.3.2 Targeting T_{regs}

T_{regs} have been targeted therapeutically, primarily through depletion strategies, in both mice and in the clinic with limited success. T_{reg} depletion in tumor models has been studied in *Foxp3*$^{DTR\text{-}GFP}$ mice, where, while the majority of mice clear the tumor, they ultimately succumb to systemic autoimmunity [39]. In the clinic, T_{reg} depletion has been the primary strategy, resulting in limited response or off target effects. Depletion strategies targeting the IL-2 pathway through use of antibodies like anti-CD25 or other small molecules led to off-target effects such as depletion of effector T cells or loss of DC-mediated T cell activation [40, 41]. Striking a balance between sustained T_{reg} depletion and autoimmunity prevention has proven difficult, further highlighting the need to target T_{reg} function specifically within the TME rather than eliminating the cell population systemically.

Intratumoral T_{regs} bear a distinct transcriptional and functional profile in comparison to those found in the periphery, including upregulation of activation and suppressive molecules, such as CD44, CD39, and ICOS [42]. Other markers promoting T_{reg} function are significantly increased in the tumor microenvironment in both mouse

models and patient samples, such as the surface receptor, Neuropilin-1 (Nrp1) [43]. While Nrp1 can be expressed on a number of cell types, it is highly upregulated on T_{regs} and supports T_{reg} function through binding of Semaphorin-4a (Sema4a). Upon Sema4a:Nrp1 ligation, PTEN is recruited to the immunological synapse and limits Akt activity, thus increasing translocation of FOXO1/3a to the nucleus [43]. In the absence of Nrp1 signaling, either through Nrp1 blockade or genetic deletion (using *Nrp1*$^{L/L}$*Foxp3*$^{Cre\text{-}YFP}$ mice), intratumoral T_{regs} show reduced cell survival and expression of suppressive markers such as CD73 and IL-10, and significantly impaired suppressive function, while maintaining Foxp3 expression. As a result, *Nrp1*$^{L/L}$*Foxp3*$^{Cre\text{-}YFP}$ mice cleared tumors similarly to mice lacking T_{regs}; however, the mice displayed no signs of autoimmunity. Nrp1^{+} T_{regs} are also increased in metastatic melanoma and head and neck squamous cell carcinoma patients compared to healthy donors. Furthermore, patients with a larger population of Nrp1^{+} T_{regs} correlated with reduced disease-free survival in comparison to those with a smaller population [44]. The distinction between peripheral and intratumoral T_{regs} suggests that there are specific markers one could target within the TME leading to T_{reg} instability (dysfunction and loss of Foxp3 expression) or T_{reg} fragility (dysfunction while maintaining Foxp3 expression).

1.3.3 Challenges

A critical concern in targeting or utilizing T_{regs} therapeutically is their stability, as defined by the maintenance of *Foxp3* expression and suppressive activity, while not exhibiting pro-inflammatory effector function. While continued *Foxp3* expression has been the primary determinant of T_{reg} stability, it has become apparent that this alone does not

define ‘stability’. Indeed, there are many additional factors and mechanisms that need to be considered, including epigenetic modifications and expression of activating or regulatory factors, as examples of T_{reg} instability and loss of function have been described despite continued *Foxp3* expression [45, 46]. I will primarily focus on thymically-derived T_{regs} (tT_{regs}) [28]. The stability of induced T_{reg} populations, such as peripherally derived T_{regs} (pT_{regs}), has been discussed elsewhere [45, 47, 48]

1.4 NEUROPILIN-1

Neuropilin-1 (Nrp1) is a type 1 transmembrane receptor that is composed of a large extracellular domain, a single transmembrane domain, and a short intracellular domain. Nrp1 can bind to Semaphorins and VEGF through the extracellular domain and results in enhanced axonal guidance and angiogenesis respectively [49, 50, 51].

Nrp1 is expressed on many immune cell types, including DCs and T cells [52, 53]. More recently, our lab has highlighted a role for Nrp1 in immune cells, specifically that it contributes to T_{reg} stability upon binding of Sema4a [43]. While Nrp1 can be expressed on other immune populations, such as $CD8^+$ T cells, it is highly upregulated on T_{regs} and is thought to be a distinguishing marker of thymically derived T_{regs} from peripheral T_{regs} in mice [54, 55]. Nrp1 is upregulated on intratumoral T_{regs} and contribute to their suppressive function through binding to Sema4a binding, which can be expressed by T cells, NK cells, and DCs [43]. Upon binding to Sema4a, Nrp1 recruits PTEN to the immunological synapse, thereby restraining Akt activity, leading to Foxo1/3a translocation to the nucleus and subsequent stabilization of Foxp3. Nrp1 is also expressed on human T_{regs}

in patient PBL and tumor samples, but is expressed at very low levels in healthy donor PBL in contrast to mice. It is thought to contribute to their suppressive function in the TME as patients with higher percentages of $Nrp1^+$ T_{regs} have a poorer disease-free survival in both HNSCC and metastatic melanoma [44].

1.5 INTERFERON-γ

Interferon-γ (IFNγ) is a type II interferon composed of homodimerized glycosylated monomers that is secreted primarily by T cells, NK cells, and NKT cells that activates macrophages, endothelia, and surrounding T cells. IFNγ can be induced through IFNγ in a feed-forward loop or through IL12 and IL18 uptake [56, 57]. IFNγ binds IFNγR1/2 and signals through Jak1/2 to phosphorylate Stat1. This in turn homodimerizes, translocates to the nucleus, and binds gamma-interferon activated sites (GAS) [58]. IFNγ was first appreciated in tumor immunology when a methylcholanthrene (Meth A) tumor cell line grew more rapidly *in vivo* following treatment with an IFNγ antibody [6, 59]. Other studies have shown that IFNγ can act directly on tumor cells through the use of *Ifngr1*$^{-/-}$ cell lines that grew more rapidly *in vivo* in comparison to WT lines. Interestingly, mice with *Ifngr1*$^{-/-}$ tumors are resistant to anti-CTLA4. In addition, patients with tumors that lack IFNγ signaling are also less responsive to CTLA4 therapy, suggesting that this may be a mechanism of resistance to immunotherapy [60].

While it has been previously shown that T_{regs} can produce IFNγ in the presence of IL12 and are less suppressive *in vitro*, the role of $IFN\gamma^+$ T_{regs} in the tumor microenvironment remained unclear. I have now shown that IFNγ can also lead to loss of T_{reg} function that

may be required for response to checkpoint blockade [44]. Indeed, loss of the IFNγR on T_{regs} led to complete resistance to PD-1 blockade in mice. In addition, treating either mouse or human T_{regs} with IFNγ led to reduced suppression, suggesting that it is sufficient to drive T_{reg} loss of function.

1.6 WHAT DOES T_{REG} STABILITY MEAN AND HOW IS IT ASSESSED?

Fundamentally, I would argue that T_{reg} stability should be defined by the maintenance of all of the following characteristics: (1) sustained Foxp3 expression, (2) potent suppressive activity, and (3) lack of effector activity (eg. production of IL2 and pro-inflammatory cytokines, cytolysis, B cell help, etc). While there are observations that challenge this definition, such as the expression of lineage defining transcriptions factors *T-box 21* (*Tbet*) [61], *Interferon regulatory factor 4* (*IRF4*) [62] and *Signal transducer and activator of transcription 3* (*STAT3*) [63] by T_{regs}, these fundamental characteristics are nonetheless maintained.

Stable *Foxp3* expression is thought to be maintained by specific epigenetic modifications. For instance, a Conserved Noncoding Sequence 2 (CNS2, also known as T_{reg} Specific Demethylated Region, TSDR) in the 5' UTR of *Foxp3,* comprised of a series of CpG motifs is hypomethylated in T_{regs} but hypermethylated in naive or effector T cells [45, 64]. This hypomethylated pattern is maintained in an IL-2 dependent manner [45]. A fully methylated locus is considered to be closed and thus not transcriptionally active, while an unmethylated locus is open and active [65]. Indeed, the increased CNS2 methylation seen in TGFβ-induced T_{regs} is thought to underlie their instability [48]. A

genome wide analysis has suggested that hypomethylation at other loci such as *Il2ra* (CD25), *Ikzf4* (Eos), *Ctla4* (Cytotoxic T-lymphocyte-associated protein 4) and *Tnfrsf18* (GITR), may also be important for T_{reg} stability [48]. Although all of these loci show a similar hypomethylation pattern to *Foxp3* in T_{regs}, *Foxp3* CNS2 demethylation is reliant on DNA methyltransferases, such as DNMT1 [66], while the other loci are not. Furthermore, it was recently shown that Tet methylcytosine dioxygenase 2 (Tet2) is required for *Foxp3* CNS2 hypomethylation [67, 68]. In fact, overexpression of Tet2 leads to hypomethylation and stability of *Foxp3* regardless of IL-2 expression. These reports suggest a role for epigenetic alterations in maintaining *Foxp3* expression and T_{reg} stability.

T_{reg} stability has been a controversial topic for a number of years [69]. Many studies have suggested that T_{reg} development leads to a terminally differentiated population, albeit with a number of different suppressive functions determined by the surrounding milieu [70]. Indeed, some have suggested that T_{regs} are one of the more stable cell lineages, based on lineage tracing experiments with *Foxp3*$^{CreERT2\text{-}GFP}$*Rosa*$^{LSL.YFP}$ mice. These mice allow for tamoxifen-inducible expression of Foxp3-driven Cre in T_{regs}, which permanently marks these cells with YFP regardless of subsequent Foxp3 expression [64]. Using this approach, very few if any T_{regs} appear to lose *Foxp3* expression and become "exT_{regs}" up to 5 months after tamoxifen injection. In addition, the majority of T_{regs} maintained *Foxp3* expression even under IL-2 deprivation, and although some cells had a minor decrease in *Foxp3* expression, they maintained their suppressive activity and exhibited a normal pattern of cytokine secretion. T_{reg} stability has also been tested in a limited number of disease scenarios, such as *Listeria monocytogenes* and diabetes.

When given a sub-lethal dose of *Listeria monocytogenes*, T_H1 transcription factors such as *Tbet* and *Cxcr3* were increased in both *Foxp3*$^+$ and *Foxp3*$^-$ T cells, but *Foxp3* expression was largely maintained [64]. To assess T_{reg} stability in an autoimmune setting, pure GFP$^+$ cells from BDC2.5 TCR-transgenic *Foxp3*^{GFP} NOD mice were transferred to lymphoreplete NOD Thy1.1 mice. Transferred T_{regs} infiltrated islets by 4 weeks after injection, and were almost exclusively *Foxp3*$^+$.

However, other studies have suggested that T_{regs} can lose *Foxp3* expression and take on a pro-inflammatory, memory-like phenotype in certain disease environments [71]. Using a *Foxp3*$^{Cre\text{-}GFP}$*Rosa*$^{LSL.YFP}$ BAC transgenic mouse in which Cre is expressed by all T_{regs} and YFP marks all cells that have *Foxp3*, it was noted that a small percentage of mature T_{regs} had lost *Foxp3* expression (10-20%) [72, 73]. These exT_{regs} had increased *Foxp3* CNS2 methylation compared with stable T_{reg} counterparts, suggesting instability. These cells displayed an activated-memory phenotype as noted by increased CD44 expression and IFNγ secretion. When *Foxp3*$^{Cre\text{-}GFP}$*Rosa* $^{LSL.YFP}$ NOD mice were analyzed to assess the role of exT_{regs} in a disease setting, a moderate percentage of exT_{regs} was observed in the islets (30-35%) [72]. These cells were also capable of inducing autoimmune diabetes, as shown following adoptive transfer of BDC2.5 TCR transgenic T_{regs}. Interestingly, when purified and cultured *in vitro,* up to 20% of the T_{regs} lost *Foxp3* expression.

The topic of *Foxp3* stability remains controversial. However, there are a number of potential reasons why different conclusions may have been reported. First, the mouse strains used to assess T_{reg} stability are designed differently. Whereas a *Foxp3*^{Cre} BAC transgenic mouse labels all cells that express *Foxp3* early in development,

Foxp3^{CreERT2} mice label *Foxp3*$^{+}$ cells only upon tamoxifen injection. In addition, BAC transgenic mice sometimes don't exhibit entirely faithful promoter expression that is identical to the endogenous promoter due to the location of insertion and the influence of local control elements. Second, different methods were used to isolate T_{regs}, such as double versus single sorting, before transfer into a new host. It is possible that the observed exT_{regs} could have been generated by cellular stress or derived from contamination, either from *Foxp3*$^{-}$ cells or cells that transiently upregulated *Foxp3* during development. Third, it is also possible that T cells transiently upregulate *Foxp3* during development leading to 'false labeling' of cells that are not destined to become *bona fide* T_{regs}, as indicated by hypermethylation at the *Foxp3* CNS2. Some *Foxp3*$^{+}$ T cells also transiently lose *Foxp3* expression, which leads to a partially methylated CNS2. However, upon reactivation, these cells reacquire a hypomethylated CNS2, indicating lineage commitment [74]. Indeed, it was previously shown that a small subset of naïve cells transiently co-expresses RORγt and *Foxp3*, producing either T_H17 or T_{reg} cells depending on the surrounding environment [75]. Transient *Foxp3* expression has also been observed in human T cells, although these cells have no suppressive function [76]. While a few reports suggest that a small percentage of exT_{regs} exist, two points remain: (1) Are they simply undergoing transient expression of *Foxp3*? (2) If they are a separate subset, do they impact specific diseases? Regardless of whether one considers T_{regs} stable or occasionally unstable, an overriding question is how is T_{reg} stability maintained?

1.7 HOW IS T_{REG} STABILITY MAINTAINED?

While Foxp3 is required for maintaining T_{reg} stability, there are several reports suggesting that T_{reg} stability is supported and enforced by other factors, such as IL-2, Foxo1/3a, Eos, a member of the Ikaros family of transcription factors, and Nrp1.

Once *Foxp3* is upregulated, expression must be maintained to preserve T_{reg} function and stability. Many factors are involved in this, including the IL-2/STAT5 pathway. In fact, *Foxp3* expression is significantly diminished in *Il2rb*$^{-/-}$ (CD25) mice, while STAT5 deletion prevents T_{reg} development. Indeed, STAT5 binds to the *Foxp3* promotor region, leading to stabilization of the locus [77]. *Foxp3* is also modulated by other members of the Forkhead box family, *Foxo1* and *Foxo3a* [78]. *Foxo1/3a* prevent T_{regs} from taking on effector functions [79, 80]. In the absence of *Foxo1*, T_{reg} development is diminished, and those that do develop are unable to suppress *in vitro.* Indeed, in the absence of *Foxo1*, T cells express more IFNγ, leading to severe autoimmunity *in vivo* [81]. This is further exacerbated in the absence of both *Foxo1* and *Foxo3a* [82]. Stable T_{regs} show reduced Akt expression, leading to enhanced *Foxo1* and *Foxo3a* in the nucleus, where they stabilize *Foxp3* expression by binding to the promotor region and regulating other transcription factors [83].

Eos, a zinc-finger transcription factor, was identified as a critical facilitator of T_{reg} stability [84]. Indeed, *Eos*-limited T_{regs} exhibited enhanced expression of IL-2 and IFNγ along with reduced suppressive capacity, but showed no difference in the expression of *Foxp3.* Forced overexpression of *Eos* prevented T_{reg} reprogramming, even in destabilizing environments, maintaining CTLA-4 expression and preventing CD40L, IL-2 and IL-17 expression. *Eos*$^{-}$*Foxp3*$^{+}$ T_{regs} (Eos-labile) were later identified *in vivo* and

were also shown to have reduced regulatory function [85]. Eos-labile T_{regs} were capable of functional reprogramming, shown through adoptive transfers into *Cd40lg*$^{-/-}$ mice, which lack efficient priming of naïve CD8 cells. Indeed, when transferred into CD40L-deficient hosts, a subset of T_{regs} downregulated Eos and upregulated CD40L to provide help for CD8 priming. Therefore, both Eos-labile and Eos-stable T_{regs} suppress and maintain *Foxp3* expression, but the former maintains the ability to reprogram and display helper activity in certain environments. However, whether Eos-labile and Eos-stable T_{regs} are two distinct subsets, or if Eos expression enhances stability, is unknown.

A pathway that is important for maintaining T_{reg} stability in a manner that appears to be independent of *Foxp3* expression is the Neuropilin-1:Semaphorin-4a axis [43]. The majority of mouse T_{regs} express high levels of Nrp1 [86] and this contributes to their function and stability [43, 87]. Nrp1 has also been shown to increased angiogenesis and CD8 activation in a VEGF-dependent manner [43, 87]. When Nrp1 was blocked *in vitro*, T_{regs} were capable of suppressing in classic contact-dependent suppression assays, but were incapable of suppressing across a permeable transwell, where suppression is mediated by IL-10 and IL-35 [88] . *Nrp1*$^{L/L}$*Foxp3*^{Cre} mice showed no signs of autoimmunity and remained healthy well past one year of age, indicating that Nrp1-deficient T_{regs} were capable of maintaining immune homeostasis. However, when injected with transplantable tumors (B16, EL4, MC38), tumor growth was substantially reduced. While tumor clearance was also observed in most cases, no autoimmunity or inflammatory lesions were observed. Therefore, Nrp1-deficient T_{regs} lost stability and suppressive capacity in the tumor microenvironment, while maintaining stability in the periphery, likely due to destabilizing factors that were confined to the tumor

microenvironment. Blocking antibodies to Nrp1 or Sema4a were also found to limit tumor growth. Nrp1-deficient T_{regs} maintained *Foxp3* expression, but showed alterations in other critical T_{regs} markers, such as a decrease in ICOS, IL-10 and CD73. Further mechanistic analysis showed that Nrp1:Sema4a ligation leads to the recruitment of PTEN, which limits Akt activity, leading to increased nuclear translocation of Foxo1 and Foxo3a, thereby stabilizing *Foxp3* expression. This leads to an enhancement of quiescence and survival factors (Klf2, Bcl2) and effector molecules (IL-10, CD73), while limiting lineage-defining transcription factors (T-bet, IRF4, Rorγt) and effector molecules (IFN-γ). These data suggest that T_{reg} stability can occur independently of *Foxp3* expression.

In summary, I would argue that T_{reg} stability can be defined by the maintenance of three critical traits: (a) stable Foxp3 expression, (b) efficient suppressive activity, and (c) a lack of effector activity. Several factors appear to contribute to and are required for the maintenance of this stable phenotype, including demethylation of the *Foxp3* CNS2 locus, the transcription factors Foxo1/3a and Eos, and the Nrp1:Sema4a axis.

However, many questions remain. (1) Are there other factors or mechanisms that are required for the maintenance of T_{reg} stability? (2) What is the functional relevance of *Foxp3* CNS2 hypomethylation, given that this is not always required for Foxp3 expression? (3) Is T_{reg} stability engrained during development or does it have to be continually and actively reinforced in the periphery? (4) Do exT_{regs} or destabilized *Foxp3*$^{+}$ T_{regs} have distinct and unique functions, and if so, how can one track or target these cells in humans? (5) How can one utilize or target T_{reg} stability in disease?

Limiting or enhancing T_{reg} stability provides a novel therapeutic strategy for a wide variety of diseases. For example, inducing T_{reg} instability in tumors could lead to an improved response to immunotherapies, while enhancing T_{reg} stability could limit transplant rejection, autoimmunity, and inflammatory disease. Clearly, more research is required to further understand how T_{reg} stability is maintained and its functional relevance in various disease settings.

2.0 METHODS

2.1 EXPERIMENTAL MODEL AND SUBJECT DETAILS

2.1.1 Mice

Nrp1$^{L/L}$ mice were obtained from D. Cheresh (UC San Diego). *Foxp3*$^{Cre\text{-}YFP/Cre\text{-}YFP}$, *Foxp3*$^{DTR\text{-}GFP/DTR\text{-}GFP}$, *Foxp3*$^{-/-}$ mice were obtained from A.Y. Rudensky (Memorial Sloan Kettering). [27, 39, 89]. *Ifngr1*$^{-/-}$, *Ifng*$^{-/-}$, *Ifngr1*$^{L/L}$, *Hif1a*$^{L/L}$ and *Rosa*$^{L\text{-}Tomato\text{-}L\text{-}GFP}$ mice were obtained from Jackson Laboratories [90, 91, 92]. All animal experiments were performed in the American Association for the Accreditation of Laboratory Animal Care-accredited, specific-pathogen-free facilities in Animal Resource Center, St. Jude Children's Research Hospital (SJCRH), and Division of Laboratory Animal Resources, University of Pittsburgh School of Medicine (UPSOM). Female and male mice were used. Animal protocols were approved by the Institutional Animal Care and Use Committees of SJCRH and UP.

2.1.2 Human T-cell populations

All HNSCC and melanoma tissues were acquired under a University of Pittsburgh Cancer Institute Institutional Review Board (IRB)-approved protocol with written informed consent obtained from each patient in conjunction with the University of Pittsburgh Cancer Institute HNSCC and Melanoma SPOREs. There were no restrictions on cancer subtype, smoking status, age, race, or prior adjuvant therapy. Control donor peripheral blood (PBL) was collected through an approved MTA protocol with the Western Pennsylvania Bloodbank. Human HNSCC PBL and TIL samples (unmatched) as well as healthy donor PBL samples were provided by R. Ferris from patients with high-risk, advanced (stage III or IV) resectable HNSCC treated with surgery. Most tumors were from oral cavity or laryngeal sites, and all were HPV-negative. Tumor specimens were obtained at the time of surgical resection, prior to adjuvant therapy. TIL were isolated, frozen, and thawed prior to staining for NRP1. Freshly processed samples were used in functional assays. Human melanoma TIL and PBL samples were provided by J. Kirkwood from an accrual trail (96-099) of patients with metastatic melanoma.

2.2 METHOD DETAILS

2.2.1 Antibodies and flow cytometry

Single cell suspensions were stained with antibodies against CD4 (clone# GK1.5, Biolegend), CD8α (clone# YTS156.7.7, Biolegend; clone# H35-17.2, eBioscience), TCRβ (clone# H57-597, Biolegend), Thy1.1 (clone# OX-7, Biolegend), Thy1.2 (clone# 30-H12, Biolegend), Foxp3 (clone# FJK-16s, eBioscience; clone# 150D, Biolegend), IFNγ (clone# XMG1.2, Biolegend), ICOS (clone# C398.4A, Biolegend), phospho-Stat1 (Clone# 4a, BD Biosciences) and phospho-Stat4 (Clone# 38, BD Biosciences). Surface staining was performed on ice for 15min. For cytokine expression analysis, cells were activated with 0.1ng/ml PMA (Sigma) and 0.5ng/ml Ionomycin (Sigma) in RPMI containing 10% FBS and Monensin (eBioscience) for 8hr. For intracellular staining of cytokines and transcription factors, cells were stained with surface markers, fixed in Fix/Perm buffer (eBioscience) for 15 minutes, washed in permeabilization buffer (eBioscience) twice and stained intracellular factors in permeabilization buffer for 30min on ice. For phosphoprotein staining, cells were fixed with 1.5% PFA (Alfa Aesar) at 37°C for 15min, permeabilized with ice cold Methanol for 1hr, and stained on ice for 1hr. Cells were sorted on Aria II (BD Biosciences) or analyzed on Fortessa (BD Biosciences), and data analysis was performed on FlowJo (Tree Star).

2.2.2 Fusion Proteins

The sequence encoding the extracellular domains of *Sema4a* and *Nrp1*were cloned in-frame to pX-Ig to create a Sema4a- or Nrp1-mouse IgG1 fusion protein construct (Sema4a-IgG1 and Nrp1-IgG1). J558L B cells were electroporated with this construct, and high-producing clones were selected by single-cell sorting. High-producing clones were seeded into Sartorious Bioreactors and collected for protein G purification and concentration. Sulphate latex 4-µm beads (Life Technologies) were conjugated with isotype control (mouse IgG1, MOPC21, R&D Systems) or Sema4a-Ig overnight with 3 pg protein per bead, blocked with 10% FBS, and stored in media. Mouse Sema-3a-Fc, Sema4a-Fc, mouse Nrp1, and human Sema4a-Fc was purchased from R&D Systems.

2.2.3 Tumor models

Mice were injected with either B16.F10 melanoma (1.25×10^5 cells or 50,000 cells intradermally), MC38 adenocarcinoma ($5x10^5$ cells subcutaneously). Tumors were measured every 3 days with digital calipers and tumor size was calculated; this was performed in blinded manner but not randomized. 100ug Diptheria Toxin was injected every 3 days starting on day 7 in *Foxp3*$^{\text{DTR-GFP/DTR-GFP}}$ and *Foxp3*$^{\text{DTR-GFP/+}}$ mice. Sema4aIg was injected every 3 days starting on day 5 (400ug, 200ug, 200ug), and anti-CD8 (YTS) was injected every 3 days starting on day 5 (200ug). *Foxp3*$^{\textit{Cre-YFP}}$ and *Ifngr1*$^{\text{L/L}}$*Foxp3*$^{\text{Cre-YFP}}$ mice were treated with either anti-PD1 (clone G4) or isotype (Armenian Hamster IgG), “AIPV”, anti-LAG3, or anti-GITR. Tumors and non-tumor

draining lymph nodes were collected for analysis on day 12. TILs were prepared with enzymatic (collagenase IV and dispase, 1mg/mL) and mechanical disruption. In Appendix A, therapeutic B16 experiments were conducted by injecting 1.25×10^5 B16 melanoma cells intradermally and waiting until tumors were palpable (5 days). On day 5, mice began to receive intraperitoneal injections of either rat IgG2a, or anti-Nrp1 (R&D Systems clone 761704, MAB59941) (400 µg initial dose and 200 µg every 3 days). Prophylactic experiments included anti-Sema4a (R&D Systems clone 757129) and Sema4a-IgG1 consisting of twice weekly injections of 100 µg of protein starting on the day of tumor inoculation. To achieve reasonable power, at least 3 mice were used per group per experiment. Group means were compared with Student's t tests. Tumor growth over time was analyzed using two-way ANOVA with multiple comparisons. Event-free survival (moribund) estimates were calculated with the Kaplan-Meier method. Groups of mice were compared by log-rank test. All p values are two-sided, and statistical significance was assessed at the 0.05 level. Analyses were conducted using GraphPad Prism software.

2.2.4 *Foxp3*$^{-/-}$ model

CD45.1^{+} *Foxp3*$^{+/-}$ female mice were bred with *CD45.1*$^{+}$*Foxp3*$^{+/+}$ male mice in timed matings. Male progeny were genotyped at birth for *Foxp3*$^{-/-}$ status. T_{regs} from *Thy1.1*$^{+}$ *Foxp3*$^{Cre\text{-}YFP/Cre\text{-}YFP}$, *Thy1.2*$^{+}$ *Nrp1*$^{L/L}$*Foxp3*$^{Cre\text{-}YFP/Cre\text{-}YFP}$, *Thy1.2*$^{+}$ *Ifng*$^{-/-}$ *Nrp1*$^{L/L}$*Foxp3*$^{Cre\text{-}YFP/Cre\text{-}YFP}$, *Thy1.1*$^{+}$ *Ifngr1*$^{-/-}$*Foxp3*$^{Cre\text{-}YFP/Cre\text{-}YFP}$ mice were purified by FACS and 10^6 cells injected intraperitoneally into *Foxp3*$^{-/-}$ male pups within 2 days of birth [34]. When a 50:50 mixture of T_{regs} was injected the total was maintained at 10^6 cells.

Mice were monitored for the autoimmune phenotype 'scurfy' (scaly skin, eye inflammation, runted phenotype, and lack of mobility) [34]. Any mice exhibiting any autoimmune or inflammatory symptoms prior to B16 injection, even if mild, were removed from further study. Mice were injected with $1.25x10^5$ B16.F10 cells at 4 weeks of age and tumor growth was monitored every 3 days.

2.2.5 Gene expression profiling by RNAseq and bioinformatics analyses

Tregs ($5x10^3$) were either single (n=3) or double sorted (n=2) and cDNAs were prepared using the SMARTer® Ultra™ Low Input RNA Kit for Sequencing - v3 user manual (Clontech Laboratories). I reasoned that double sorting results in higher purity but has lower yield and may alter the expression profile. Though melanoma genes were found at lower levels in double sorted samples no other substantial differences, such as activation of stress response genes, were observed. T_{regs} were sorted on the following markers: $Foxp3^{Cre\text{-}YFP/Cre\text{-}YFP}$ ($Nrp1^{+/+}$) on YFP, $Nrp1^{L/L}Foxp3^{Cre\text{-}YFP/Cre\text{-}YFP}$ ($Nrp1^{-/-}$) on YFP, $Nrp1^{L/L}Foxp3^{Cre\text{-}YFP/DTR\text{-}GFP}$ ($Nrp1^{-/-}$) on YFP, and $Nrp1^{L/L}Foxp3^{Cre\text{-}YFP/DTR\text{-}GFP}$ ($Nrp1^{+/+}$) on GFP. Sequencing libraries were prepared using Nextera XT DNA Library Preparation kit (Illumina), normalized at 2nM using Tris-HCl (10mM, pH 8.5) with 0.1% Tween20, diluted and denatured to a final concentration of 1.8nM using the Illumina Denaturing and Diluting libraries for the NextSeq 500 protocol Revision D (Illumina). Cluster generation and 75bp paired-end dual-indexed sequencing was performed on Illumina NextSeq 500 system.

RNAseq data was aligned to the mm10 genome using the STAR aligner [93] and quantified using featureCounts [94]. The raw counts data were processed using the

“voom” function [95] in the limma R package [96, 97], which normalizes the data and assigns a weight for each measurement for subsequent linear model fitting. Unsupervised analysis of the data revealed a small cluster of melanoma specific genes that I reasoned were caused by contaminations. Following a previous approach [98], Dr. Maria Chikina removed five melanoma specific genes from all downstream analysis (Mlana, Syt4, Tyr, Tyrp1, Dct). To filter for low expression genes. Dr. Chikina defined a cutoff of 90 reads per gene based on visual inspection of the bimodal count distribution. Only genes that met this threshold in at least 5 samples (~11,000 out of ~23,000) were kept for further analysis. Differential expression was assessed using the limma moderated T statistic. The differences between the intratumoral Treg populations were subtle and in order to increase the power of my study Dr. Chikina included technical factors as covariates in my differential expression analysis. Following the approach outlined in a recent human RNAseq study [98]. Dr. Chikina included three Picard [99]("picard,") RNAseq metrics ("PCT_INTERGENIC_BASES" "MEDIAN_3PRIME_BIAS", "MEDIAN_CV_COVERAGE") [99] as well GC correlation (computed as the sample specific Pearson correlation between each gene's GC content and its expression value). Normalization for replicate number and technical parameters was also applied directly to the voom result to obtain "normalized counts", which were used for data visualization. Geneset enrichment was performed using the “RankSumWithCorrelation” function in the limma R package, which automatically corrects enrichment statistic inflation due to correlation among genes (with the immune genesets restricted to those relevant to T cells). p-values were combined from the “*Nrp1*$^{L/L}$*Foxp3*$^{Cre\text{-}YFP/Cre\text{-}YFP}$ (Nrp1$^{-/-}$) vs *Foxp3*$^{Cre\text{-}YFP/Cre\text{-}YFP}$ (Nrp1$^{+/+}$)” and “*Nrp1*$^{L/L}$*Foxp3*$^{Cre\text{-}YFP/DTR\text{-}GFP}$ (Nrp1$^{+/+}$) vs

Nrp1$^{L/L}$*Foxp3*$^{Cre\text{-}YFP/DTR\text{-}GFP}$ (Nrp1$^{-/-}$) using the Fisher's "log sum" method [Fisher] to define significant genes. Genesets with a q-value FDR of <0.2 were considered significant. In order to assess the alterations in Treg specific expression profile I relied on the Treg signature genes defined in a previous study [100]. For pathway analysis bar charts, results of geneset enrichment analysis were depicted with colors representing the effect size and height representing the corresponding p-values. The effect size is defined as AUC (area under receiver operating curve) – 0.5 which provides a normalized ranksum statistic that is comparable across genesets of different sizes. The plot is restricted to the top 10 pathways (based on their Nrp1$^{+/+}$ vs Nrp1$^{-/-}$ significance) from the "canonical" mSigDB geneset. Dr. Maria Chikina additionally restricted this analysis to genesets and pathways that were deemed relevant to intercellular signaling (defined at least half of the genes in the geneset having an extracellular or membrane annotation).

2.2.6 *In vitro assays*

Splenic CD4^{+}YFP^{-} (CD4^{+}Foxp3^{-} T cells) cells from *Foxp3*$^{Cre\text{-}YFP}$ mice were sorted as responder cells and labeled with 5μM CellTrace Violet (Life Technology). CD4^{-}CD8^{-} splenocytes from *Foxp3*$^{Cre\text{-}YFP}$ mice were treated with 20μg/mL mitomycin C (Sigma) at 37°C for 30min, washed five times with PBS, and then used as antigen presenting cells (APCs). Responder cells (4x10^{3}), APCs (8x10^{3}), and different concentrations of T_{regs} (1:2-1:16 T_{reg}:T_{eff} ratio, 500-2000 T_{regs}) were activated with 2μg/ml anti-CD3 (Biolegend) in a 96-well round bottom plate with 100ul RPMI for 3 days [101]. Suppression was calculated as previously described [102]. Briefly, cells were acquired by BD Fortessa, and

the division index of responder cells was analyzed using FlowJo based on the division of CellTrace Violet. Suppression was then calculated with the formula % Suppression = (1-DIT_{reg}/DICtrl) x 100% (DIT_{reg} stands for the division index of responder cells with Tregs, and DICtrl stands for the division index of responder cells activated without T_{regs}). Human microsuppression assays were performed similarly to mouse assays with the following changes: 0.5μg/ml anti-CD3 is used for activation, and cells are cultured in assay conditions (200uL) for 4 days.

For co-culture assays, sorted T_{reg} populations were cultured together in a 96 well round-bottom plate or in a 96 well transwell plate (Millipore) for 72 hours prior to being resorted and used in a suppression assay. Cells were treated with 100ng/mL PMA (Sigma), 500ng/mL Ionomycin (Sigma) and 1000IU hIL-2 (Prometheus) for co-culture. For some experiments, sorted T_{regs} were cultured in the presence of 0.3-20ng/mL anti-IFNγ (BioXcell) or 0-200ng/mL IFNγ (Biolegend) to the microsuppression assay.

For the hypoxia assays, T_{regs} were stimulated with PMA/Ionomycin and IL-2 for 3 days in normoxic (5% CO_2 and 20% O_2) or hypoxic (5.5% CO_2 and 1.5% O_2) conditions at 37˚C. Cells were then stained in the same condition in the absence of cytokine.

2.2.7 Microscopy

Foxo3a was carried out on freshly isolated T_{reg} cells that were left unstimulated in media overnight or stimulated with immobilized anti-CD3 and anti-CD28 in the presence or absence of immobilized Sema4a-IgG1 or its isotype control. Cells were collected, fixed in 1% PFA, and permeabilized with 0.1% Triton X-100 in TBS. After

blocking with normal mouse serum, cells were stained with anti-Foxo3a (Cell Signaling Technologies) overnight in Tris-buffered 1% BSA. After several washes, cells were stained with Alexa Fluor 647 conjugated anti-rabbit IgG (Life Technologies), and then washed several times. Cells were then loaded with 4′,6-diamidino-2-phenylindole (DAPI) and phalloidin-Alexa Fluor 546 or 488 before microscopy. Random fields of 10 to 30 cells were visualized using spinning-disc laser-scanning confocal microscopy. Blinded masks were generated using phalloidin and DAPI staining to determine cytoplasmic and nuclear volume, respectively, and only then was the Foxo3a staining visualized. The nuclear and cytoplasmic volumes of Foxo3a fluorescence of 20 to 30 stacks were calculated using Slidebook (3i) software in arbitrary fluorescence units and analyzed in Graphpad Prism.

2.2.8 Metabolism Assays

Lymphocytes were isolated from ndLN and TIL of *Foxp3*$^{\text{Cre-YFP}}$ and *Nrp1*$^{\text{L/L}}$*Foxp3*$^{\text{Cre-YFP}}$ mice. To assess mitochondrial mass and function, cells were stained with MitoTracker FM and TMRE respectively. To visualize hypoxic cells within the tumor, mice were injected with 2mg pimonidazole in 100uL PBS IV 1 hour prior to sacrifice and staining was done using Hypoxiprobe 549 at 1:400 for histology and 1:1000 for flow cytometry. For metabolic function assays, cells were loaded on a Cell-Tak coated Seahorse culture plate (60,000-100,000 cells per well) in DMEM supplemented with 1% BSA, 25mM glucose, 1mM pyruvate, and 2mM glutamine and were analyzed on a Seahorse XFe96 (Agilent). Basal extracellular acidification (ECAR) and oxygen consumption (OCR) rates were taken for 30 minutes prior to stimulation with oligomycin (2uM), FCCP (0.5uM), 2-

DG (100mM) and rotenone/antimycin A (100uM) to determine maximum respiratory values.

2.2.9 Bisulfite Sequencing

$CD4^+Foxp3^-$ and $CD4^+Foxp3^+$ T cells were sorted from ndLN or TIL of *Foxp3*$^{Cre=YFP}$ or *Nrp1*$^{L/L}$*Foxp3*$^{Cre-YFP}$ mice on day 12 after B16 inoculation. Bisulfite conversion was performed on half the samples (with the other half as unconverted controls) using either the Zymo EZ DNA Methylation Kit (#D5001) on gDNA for 14 hours or using the Zymo EZ DNA Methylation-Direct Kit (#D5020) directly on cells as outlined in the protocol. Methyl-specific PCR (primers below) was performed on samples, prior to TOPO cloning (10+ colonies picked per sample) and minipreps (Clontech Nucleospin Plasmid EasyPure Kit). A portion of the miniprep product was digested with EcoR1 to verify band size. 200ng of the miniprep products were resuspended in 10uL with 2.5uL of primers T7 (forward) or SP6 (reverse), both kept at 20mM, and were sent for Sanger sequencing. Analysis was done using DNAStar.

Amp 1/2 Untreated Primer (f): GAGGCTGACATTCCAGAGCCAGC

Amp 1/2 Untreated Primer (r): GAGGACCTGAATTGGATATGGTCTGTCTAG

Amp 1/2 Treated Primer (f): CTAACATTCCAAAACCAACAAAAAACC

Amp 1/2 Treated Primer (r): GGATTTGAATTGGATATGGTTTGTTTAG

T7 Primer: GGC TTG TCG ACA TTA ATA CGA CTC ACT ATA GGG

SP6 Primer: GGC ATT TAG GTG ACA CTA TAG

2.2.10 Quantification and statistical analysis

Statistics were performed using Prism v6.07. Students t-tests were used in to determine statistical significance between groups from flow cytometry analysis. Kaplan Meier was used to determine significance between tumor associated survival. Two-way ANOVA was used to determine significance between groups over time in tumor growth experiments. “n” represents the number of mice used in the experiment, with the number of individual experiments listed in the legend. Graphs show individual samples. Samples are shown with the mean with or without error bars showing the SEM. Significance was defined as p=0.05.

2.2.11 Data and software availability (Chapter 3)

The RNASeq datasets from Chapter 3 have been deposited in the Gene Expression Omnibus (GEO) under code GSE97939.

2.3 Resources

Table 1. Key resources table

REAGENT or	SOURCE	IDENTIFIER
Antibodies		
CD4	Biolegend	GK1.5
CD8	Biolegend	YTS156.7.7
TCRβ	Biolegend	H57-597

Thy1.1	Biolegend	OX-7
Thy1.2	Biolegend	30-H12
Foxp3	Biolegend	FJK-16s
IFNγ	Biolegend	XMG1.2
Nrp1	Biolegend	3E12
ICOS	Biolegend	C398.4A
pAKT	Cell Signaling	D9E
pSTAT1	BD Biosciences	4a
pSTAT4	BD Biosciences	38
CD3 (human)	Biolegend	HIT3a
CD4 (human)	eBioscience	RPA-T4
CD25 (human)	Biolegend	BC96
CD127 (human)	Biolegend	A019D5
Foxp3 (human)	eBioscience	PCH101
IFNγR (human)	eBioscience	GIR-208
Nrp1 (human)	Abcam	EPR3113
Hif1α (human/mouse)	R&D	241812
PD1 (blocking)	In house	G4
Arm. Hamst. IgG	Bioxcell	BE0091
Rat IgG2a	Bioxcell	2A3
CD8 (depleting)	Bioxcell	53-6.72
Chemicals, Peptides, and Recombinant Proteins		
Diptheria Toxin	Sigma	D0564
Sema4aIg	In house	In house
Critical Commercial Assays		
SMARTer® Ultra™ Low Input RNA Kit for Sequencing - v3	Clontech	634850
Nextera XT DNA Library Preparation kit	Illumina	FC-131-1096

Deposited Data		
RNASeq	GEO	GSE97939
Experimental Models: Cell Lines		
B16.F10	M.J. Turk	Dartmouth College
MC38	J.P. Allison	MD Anderson
Experimental Models: Organisms/Strains		
Foxp3$^{Cre\text{-}YFP}$	A.Y. Rudensky	Memorial Sloan Kettering
Nrp1$^{L/L}$	D. Cheresh	UC San Diego
Foxp3$^{DTR\text{-}GFP}$	A.Y. Rudensky	Memorial Sloan Kettering
Rosa$^{L\text{-}Tom\text{-}L\ GFP}$	Jackson Labs	007576
Ifng$^{-/-}$	Jackson Labs	002287
Ifngr1$^{-/-}$	Jackson Labs	003288
Ifngr1$^{L/L}$	Jackson Labs	025394
Foxp3$^{-/-}$	A.Y. Rudensky	Memorial Sloan Kettering
Software and Algorithms		
mSigDB	Subramanian et al 2005	http://www.pnas.org/content/102/43/15545.abstract
Fisher	Fisher, RA 1925	http://www.haghish.com/resources/materials/Statistical_Methods_for_Research_Workers.pdf
Picard	Broad Institute	https://broadinstitute.github.io/picard/
Normalization	Battle et al 2014	http://genome.cshlp.org/content/early/2013/10/02/gr.155192.113.abstract

3.0 INTERFERON-γ DRIVES T_{REG} FRAGILITY TO PROMOTE ANTI-TUMOR IMMUNITY

Data within this chapter were compiled and published in *Cell* in 2017 in the following manuscript:

Overacre-Delgoffe AE, Chikina M, Dadey RE, Yano H, Brunazzi EA, Shayan G, Horne W, Moskovitz JM, Kolls JK, Sander C, Shuai Y, Normolle DP, Kirkwood JM, Ferris RL, Delgoffe GM, Bruno TB, Workman CJ, Vignali DAA. "Interferon-γ drives T_{reg} fragility to promote anti-tumor immunity." Cell. 2017 June 1;169(6):1130-1141. doi: 10.1016/j.cell.2017.05.005.

3.1 SUMMARY

Regulatory T cells (T_{regs}) are a barrier to anti-tumor immunity. Neuropilin-1 (Nrp1) is required to maintain intratumoral T_{reg} stability and function but is dispensable for peripheral homeostasis. T_{reg}-restricted Nrp1 deletion results in profound tumor resistance due to T_{reg} functional fragility. Drivers of T_{reg} fragility, the mechanistic basis

of Nrp1-dependency, and relevance for human cancer and immunotherapy remain unknown. I show that a high percentage of intratumoral NRP1^{+} T_{regs} correlates with poor prognosis in melanoma and HNSCC. Using a mouse model of melanoma where Nrp1-deficient (*Nrp1*$^{-/-}$) and wild-type (*Nrp1*$^{+/+}$) T_{regs} could be assessed in a competitive environment, I found that a high proportion of intratumoral *Nrp1*$^{-/-}$ T_{regs} produce interferon-γ (IFNγ), which drives the fragility of surrounding WT T_{regs}, boosts anti-tumor immunity, and facilitates tumor clearance.

3.2 INTRODUCTION

Regulatory T cells (T_{regs}), characterized by their expression of the forkhead box transcription factor, *Foxp3*, are required to maintain immune homeostasis and prevent excessive tissue damage [29, 39, 103, 104]. Humans that lack a functional T_{reg} population develop a lethal autoimmune disorder, termed Immune dysregulation, Polyendocrinopathy, Enteropathy, X-linked (IPEX) syndrome, which can be recapitulated in mice through *Foxp3* deletion. While T_{regs} are required to limit autoimmunity and maintain immune regulation, they can be deleterious in cancer through suppression of anti-tumor immunity [105, 106, 107]. Indeed, high numbers of T_{regs} and a low CD8^{+} T cell:T_{reg} ratio are considered poor prognostic factors for many tumor types, including melanoma, head and neck squamous cell carcinoma (HNSCC), ovarian cancer and colorectal carcinoma [37, 108, 109, 110, 111]. Although targeting intratumoral T_{regs} could be an effective therapeutic approach for multiple tumor types, perturbation of

peripheral T_{reg} number or function could lead to life-threatening autoimmune or inflammatory complications. Therefore, identifying pathways that could be targeted to selectively undermine intratumoral T_{regs} is essential.

It has been previously shown that Neuropilin-1 (Nrp1) is expressed by ~90% of tumor infiltrating T_{regs} in mouse models of cancer and is critical for their function in the tumor microenvironment [43]. Indeed, mice with a T_{reg}-restricted deletion of Nrp1 are highly resistant to B16 melanoma, which is normally refractory to immune-mediated clearance, yet remarkably do not exhibit any autoimmune or inflammatory disease. Although Nrp1-deficient T_{regs} have been previously described as 'unstable', due to their loss of function [43], previous studies and data included here clearly show that they retain Foxp3 expression. Thus, this phenotype is now referred to as T_{reg} 'fragility' consistent with their retention of Foxp3 expression yet loss of function *ex vivo* (as exhibited by loss of suppressive activity *in vitro*) and tumor tolerance *in vivo* (as exhibited by tumor growth reduction/clearance). While it has been previously shown that Nrp1 plays a role in maintaining intratumoral T_{reg} function, many questions remain including the fate of these fragile T_{regs} and their contribution to anti-tumor immunity, the drivers of T_{reg} fragility, the expression, contribution, and impact of NRP1 on human intratumoral T_{regs}, and the broader implications for T_{reg} function and cancer immunotherapy.

3.3 RESULTS

3.3.1 Increased NRP1 expression on T_{regs} in human cancer

While Nrp1 has been shown to prevent T_{reg} fragility in mice, its presence and role in human T_{regs} remains unclear. Previous studies have been controversial, with some suggesting peripheral human T_{regs} do not express NRP1 while other suggest that $NRP1^+$ T_{regs} are potent suppressors [22, 112, 113, 114, 115, 116, 117, 118]. Indeed, very few human T_{regs} in peripheral blood lymphocytes (PBL) from healthy donors express NRP1 (Fig. 1A and B). Remarkably, most patients with metastatic melanoma and head and neck squamous cell carcinoma (HNSCC) possessed a reasonably high percentage of intratumoral $NRP1^+$ T_{regs} (Fig. 1A and B). This varied considerably from 3-90% in melanoma and 35-90% in HNSCC. The percentage of $NRP1^+$ T_{regs} in PBL was also substantially enhanced. Interestingly, NRP1 expression in intratumoral T_{regs} appeared to correlate with poor prognosis in both melanoma and HNSCC (Fig. 1C).

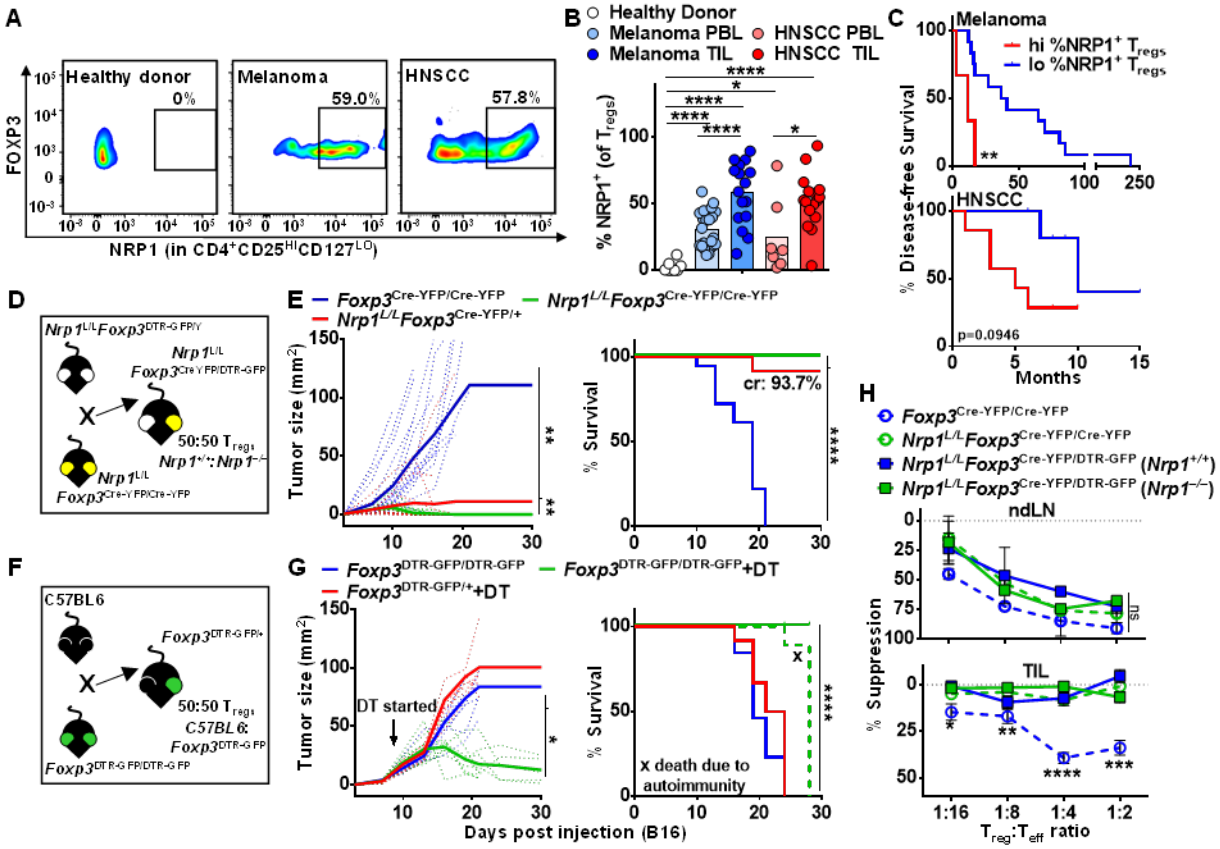

Figure 1: Decreased Nrp1 expression leads to tumor regression and enhanced survival.

(**A-C**) Flow cytometry analysis of human T_{regs}. Lymphocytes were harvested from PBL of healthy donors (n=8) or from PBL of healthy donor and TIL of Head and Neck Squamous Cell Carcinoma (HNSCC) and metastatic melanoma (3-5 experiments, n=16-23) and frozen or stained fresh. Frozen TIL and PBL were thawed and stained directly without stimulation. (**D-G**) Mice breeding scheme and tumor growth curves. *Foxp3*$^{Cre\text{-}YFP/Cre\text{-}YFP}$, *Nrp1*$^{L/L}$*Foxp3*$^{Cre\text{-}YFP/Cre\text{-}YFP}$, *Nrp1*$^{L/L}$*Foxp3*$^{Cre\text{-}YFP/DTR\text{-}GFP}$, *Foxp3*$^{DTR\text{-}GFP/DTR\text{-}GFP}$, and *Foxp3*$^{DTR\text{-}GFP/+}$ mice were injected with B16.F10 melanoma tumor cells ID on day 0. Tumor growth was measured with digital calipers every three days. Mice were removed from study when tumor growth reached a diameter of 2cm in any direction or when necrosis was observed, and survival plots were generated (4 experiments, n=9-18). (**F-G**) Mice breeding scheme and tumor growth curves. *Foxp3*$^{DTR\text{-}GFP/DTR\text{-}GFP}$, and *Foxp3*$^{DTR\text{-}GFP/+}$ mice were treated with 100μg Diptheria Toxin IP every three days starting on day 7. (**H**) Microsuppression assays. T_{regs} were isolated on day 12 post B16 injection from ndLN and

TIL of *Foxp3*$^{Cre\text{-}YFP/Cre\text{-}YFP}$, *Nrp1*$^{L/L}$*Foxp3*$^{Cre\text{-}YFP/Cre\text{-}YFP}$, and *Nrp1*$^{L/L}$*Foxp3*$^{Cre\text{-}YFP/DTR\text{-}GFP}$ mice and cultured with effector T cells and APCs for 72 hours in a classical microsuppression assay. T_{regs} were pooled from 3 mice with 5-6 mice per group per experiment. Proliferation was measured and percent suppression was calculated as described in methods. Data represent 3-5 (A-C), 4 (D-G), or 3 (H) independent experiments. Error bars represent the mean ± SEM. Students unpaired t test (Fig. 1B, H), 2 way ANOVA (Fig. 1E, G), and Kaplan-Meier tests (Fig. 1E, G) were used (*$p < 0.05$, **$p < 0.01$, ***$p < 0.001$, ****$p < 0.0001$).

3.3.2 *Nrp1*$^{-/-}$ T_{regs} block wild type T_{reg} function and promote anti-tumor immunity

It has been previously shown that anti-Nrp1 substantially limits the growth of a B16 mouse model of human melanoma [43]. Given the heterogeneous nature of NRP1 expression on human tumor infiltrating Tregs, where only a proportion express NRP1, I questioned what impact Nrp1 loss on only a proportion of mouse Tregs might have on the function of the remaining wild-type (WT) counterparts, and by extension anti-tumor immunity and tumor growth. Also, as Nrp1-deficient Tregs show a reduction in suppressive function but also an increase in effector phenotype [43], I questioned whether these cells had an active role in re-shaping the tumor microenvironment, or whether reduced tumor growth was instead due to reduction of a major suppressive cell population.

Foxp3 is on the X chromosome and is thus subject to X inactivation [119, 120, 121], rendering only one allele active in each T_{reg}. Consequently in heterozygous *Nrp1*$^{L/L}$*Foxp3*$^{Cre\text{-}YFP/DTR\text{-}GFP}$ female mice, 50% of T_{regs} have a Cre-mediated deletion of *Nrp1*, are marked with YFP [herein referred to as *Nrp1*$^{-/-}$ T_{regs}] and exhibit functional fragility, and the other 50% express DTR-GFP and are WT T_{regs}, as they carry the *Nrp1*$^{L/L}$ allele but not *Foxp3*$^{Cre\text{-}YFP}$ [herein referred to as *Nrp1*$^{+/+}$ T_{regs}] (Fig. 1D). I first assessed tumor growth in heterozygous *Nrp1*$^{L/L}$Foxp3$^{Cre\text{-}YFP/DTR\text{-}GFP}$ female mice, with *Nrp1*$^{L/L}$*Foxp3*$^{Cre\text{-}YFP/Cre\text{-}YFP}$ [all T_{regs} are *Nrp1*$^{-/-}$] and *Foxp3*$^{Cre\text{-}YFP/Cre\text{-}YFP}$ [all T_{regs} are WT/*Nrp1*$^{+/+}$] female mice as controls. Strikingly, *Nrp1*$^{L/L}$*Foxp3*$^{Cre\text{-}YFP/DTR\text{-}GFP}$ mice exhibited dramatically reduced tumor growth, enhanced survival, and increased intratumoral lymphocyte and CD8^{+} T cell number, phenocopying *Nrp1*$^{L/L}$*Foxp3*$^{Cre\text{-}YFP/Cre\text{-}}$

^{YFP} mice (Fig. 1E and Fig. 2A) [43]. This occurred despite the presence of *Nrp1*$^{+/+}$ T_{regs} in similar numbers to *Nrp1*$^{-/-}$ T_{regs} in the tumor (Fig. 2A). A previous study had suggested that the absence of Nrp1 leads to reduced influx of T_{regs} into certain tumor types [122]. However, there did not seem to be a significant difference in the number of intratumoral *Nrp1*$^{-/-}$ versus *Nrp1*$^{+/+}$ $T_{regs,}$ even in *Nrp1*$^{L/L}$*Foxp3*$^{Cre\text{-}YFP/DTR\text{-}GFP}$ mice (Fig. 2A). One might also argue that the *Nrp1*$^{L/L}$*Foxp3*$^{Cre\text{-}YFP}$ mutation causes a basal inflammatory state that impacts the establishment of a tumor mass. To rule this out and any potential impact Nrp1 loss may have on T_{reg} development, migration and function, the impact of *Nrp1* temporal deletion in T_{regs} following the establishment of B16 tumor growth was determined. *Nrp1*$^{L/L}$*Foxp3*^{CreERT2}, but not *Foxp3*^{CreERT2}, mice exhibited substantially reduced tumor growth following *Nrp1* deletion induced by daily tamoxifen treatment on Days 7-11 (Fig. 2B-C).

To rule out the possibility that the inability of *Nrp1*$^{+/+}$ T_{regs} to block anti-tumor immunity and tumor clearance was due to their reduced number in heterozygous *Nrp1*$^{L/L}$*Foxp3*$^{Cre\text{-}YFP/DTR\text{-}GFP}$ mice, I also assessed tumor growth in heterozygous *Foxp3*$^{DTR\text{-}GFP/+}$ female mice in which diphtheria toxin (DT) treatment reduced peripheral and intratumoral T_{reg} number by approximately half (Fig. 1F and Fig. 2D). In stark contrast to tumor growth in heterozygous *Nrp1*$^{L/L}$*Foxp3*$^{Cre\text{-}YFP/DTR\text{-}GFP}$ mice, DT-treated heterozygous *Foxp3*$^{DTR\text{-}GFP/+}$ mice exhibited tumor growth that was indistinguishable from the untreated control mice (Fig. 1G). While *Foxp3*$^{DTR\text{-}GFP/DTR\text{-}GFP}$ mice treated with DT largely cleared their tumors, they ultimately succumbed to autoimmunity due to an absence of T_{regs} in contrast to heterozygous *Nrp1*$^{L/L}$*Foxp3*$^{Cre\text{-}YFP/DTR\text{-}GFP}$ and *Nrp1*$^{L/L}$*Foxp3*$^{Cre\text{-}YFP/Cre\text{-}YFP}$ female mice that never exhibited an autoimmune or

inflammatory phenotype (Fig. 1D and 1E, and data not shown) [43]. Taken together, my data suggest that if half the T_{regs} are depleted tumors grow unrestrained, as the reduced number of WT T_{regs} are still capable of blocking anti-tumor immunity. In contrast, if half the T_{regs} lose *Nrp1*, tumors are controlled, suggesting that *Nrp1*$^{-/-}$ T_{regs} are playing an active role in re-shaping the tumor microenvironment. I hypothesized that *Nrp1*$^{-/-}$ T_{regs} not only lost their suppressive activity but may also negatively impact the function of surrounding intratumoral *Nrp1*$^{+/+}$ T_{regs}. In order to assess this possibility, I determined the suppressive capacity of *Nrp1*$^{+/+}$ (GFP^{+}) and *Nrp1*$^{-/-}$ (YFP^{+}) T_{regs} from *Nrp1*$^{L/L}$*Foxp3*$^{\text{Cre-YFP/DTR-GFP}}$ heterozygous and control mice using a microsuppression assay [101]. While all T_{reg} populations isolated from non-draining lymph nodes (ndLN) were equally capable of suppressing effector T cells (Fig. 1H), *Nrp1*$^{-/-}$ T_{regs} isolated from homozygous*Nrp1*$^{L/L}$*Foxp3*$^{Cre\text{-}YFP/Cre\text{-}YFP}$ and heterozygous *Nrp1*$^{L/L}$*Foxp3*$^{\text{Cre-YFP/DTR-GFP}}$ tumors lacked suppressive activity (Fig. 1H). Interestingly, intratumoral *Nrp1*$^{+/+}$ T_{regs} isolated from heterozygous *Nrp1*$^{L/L}$*Foxp3*$^{\text{Cre-YFP/DTR-GFP}}$ mice were also unable to suppress.

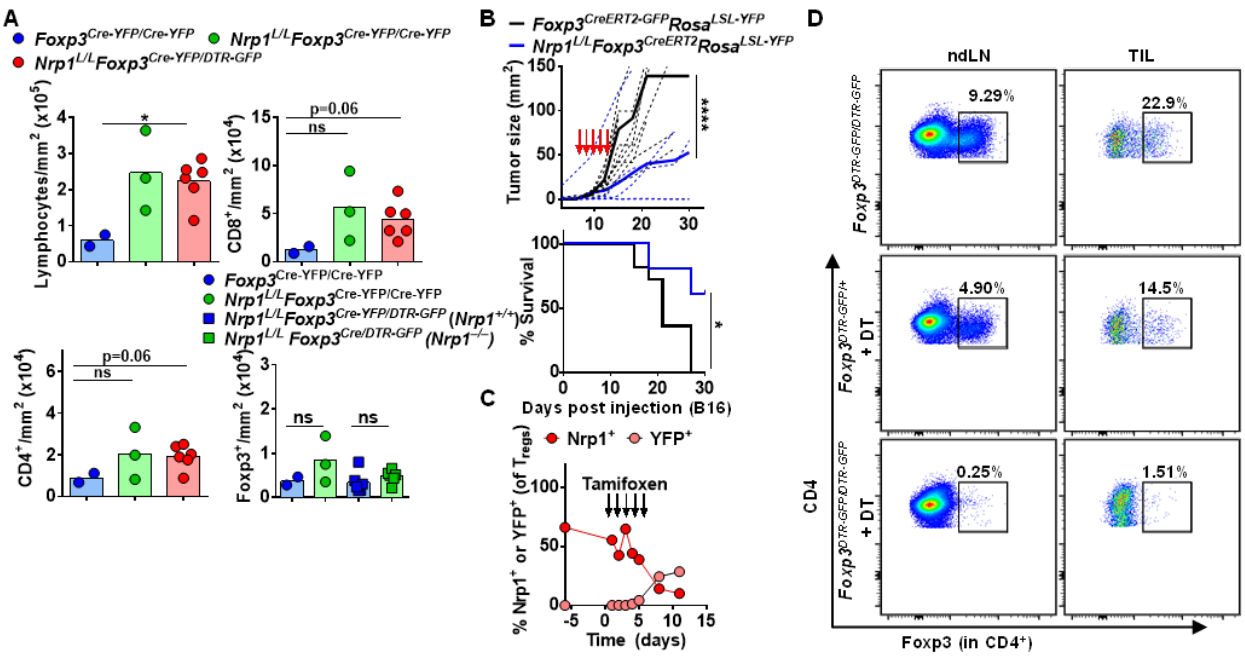

Figure 2: Temporal Nrp1 deletion leads to reduced tumor growth.

(**A**) Cell numbers in the tumor. Lymphocytes were isolated from TIL of *Foxp3*$^{\text{Cre-YFP/Cre-YFP}}$, *Nrp1*$^{\text{L/L}}$*Foxp3*$^{\text{Cre-YFP/Cre-YFP}}$, and *Nrp1*$^{\text{L/L}}$*Foxp3*$^{\text{Cre-YFP/DTR-GFP}}$ mice, stained and quantified for cell numbers (n=2-6). (**B**) Tumor growth curve. *Foxp3*$^{\text{CreERT2-GFP}}$*Rosa*$^{\text{LSL-YFP}}$ or *Nrp1*$^{\text{L/L}}$*Foxp3*$^{\text{CreERT2-GFP}}$*Rosa*$^{\text{LSL-YFP}}$ mice were injected with B16.F10 ID on day 0 and treated with Tamoxifen on days 7-11. Tumors were measured every 3 days (n=5-11). (**C**) Analysis of temporal deletion of Nrp1. *Foxp3*$^{\text{CreERT2-GFP}}$*Rosa*$^{\text{LSL-YFP}}$ or *Nrp1*$^{\text{L/L}}$*Foxp3*$^{\text{CreERT2-GFP}}$*Rosa*$^{\text{LSL-YFP}}$ mice were bled on days indicated and stained. Mice were treated with Tamoxifen on days 1-5 (n=3). (**D**) Analysis of T_{reg} depletion with DT treatment. Lymphocytes were isolated from ndLN and TIL of *Foxp3*$^{\text{DTR-GFP/DTR-GFP}}$, *Foxp3*$^{\text{DTR-GFP/DTR-GFP}}$ + DT, and *Foxp3*$^{\text{DTR-GFP/+}}$ + DT mice (n=3-6). Data represent 2-4 independent experiments. Student unpaired t test (S1A), 2-way ANOVA and Kaplan-Meier tests (S1B) were used. (*p < 0.05, ****p<0.0001).

It is possible that *Nrp1*$^{-/-}$ T_{regs} impact the tumor microenvironment by losing *Foxp3* and becoming so-called ex-T_{regs} with an altered functional phenotype [71, 73, 123]. Ex-T_{regs} have been previously reported in lymphopenia and diabetes. Around ~10-20% of T_{regs} lost Foxp3 and became pathogenic in nature. Still, other groups performed similar assays and found that Foxp3 was very stable *in vivo* [64]. The key distinctions between these two contradicting ideas were the disease and mouse models. First, exT_{regs} were identified in settings of autoimmunity (NOD mice for example), whereas the lack of exT_{regs} was reported in steady state conditions or in infection. Second, exT_{regs} were uncovered utilizing a BAC transgenic mouse while subsequent studies showing a stable lineage utilized an inducible Cre system. This is a critical distinction as BAC transgenic mice sometimes display unfaithful promoter expression and also label all cells from early in development, leading to confounding results if Foxp3 is transiently upregulated during this time. By using an inducible Cre, one can 'tag' the cells after they have developed and moved into the periphery, presumably allowing one to label mature, stable T_{regs}.

I analyzed *Foxp3* fate mapping mice in which T_{regs} either possessed (*Foxp3*$^{Cre\text{-}YFP}$*Rosa*$^{L\text{-}Tom\text{-}L\text{-}GFP}$) or lacked *Nrp1* expression (*Nrp1*$^{L/L}$*Foxp3*$^{Cre\text{-}YFP}$*Rosa*$^{L\text{-}Tom\text{-}L\text{-}GFP}$) (Fig. 3A). In this mouse model, non-T_{regs} are Tomato^{+}GFP^{-}YFP^{-}, *Foxp3*$^{+}$ T_{regs} are Tomato^{-} GFP^{+}YFP^{+} and *Foxp3*$^{-}$ ex-T_{regs} are Tomato^{-}GFP^{+}YFP^{-}. Interestingly, there were very few (<5%) ex-T_{regs} present in the periphery or in the tumor, regardless of Nrp1 expression (Fig. 3B and C). These data suggest that the absence of Nrp1 does not affect *Foxp3* expression and does not result in the generation of ex-T_{regs}.

Previous reports have shown that T_{regs} can display alternative functions *in vivo* while maintaining *Foxp3* expression [85, 124]. Two hallmarks of T_{reg} fragility are elevated pAkt and reduced ICOS expression [43]. Elevated pAkt and reduced ICOS were observed in *Nrp1*$^{-/-}$ T_{regs} in *Nrp1*$^{L/L}$*Foxp3*$^{Cre\text{-}YFP/Cre\text{-}YFP}$ mice and *Nrp1*$^{L/L}$*Foxp3*$^{Cre\text{-}YFP/DTR\text{-}GFP}$ heterozygous mice relative to *Nrp1*$^{+/+}$ T_{regs} in *Foxp3*$^{Cre\text{-}YFP/Cre\text{-}YFP}$ mice as expected (Fig. 3D and E). However, elevated pAkt and, to a lesser extent, reduced ICOS was also observed in *Nrp1*$^{+/+}$ T_{regs} in *Nrp1*$^{L/L}$*Foxp3*$^{Cre\text{-}YFP/DTR\text{-}GFP}$ heterozygous mice. Taken together, these data suggest that *Nrp1*$^{-/-}$ T_{regs} have a negative impact on the suppressive function of intratumoral *Nrp1*$^{+/+}$ T_{regs}.

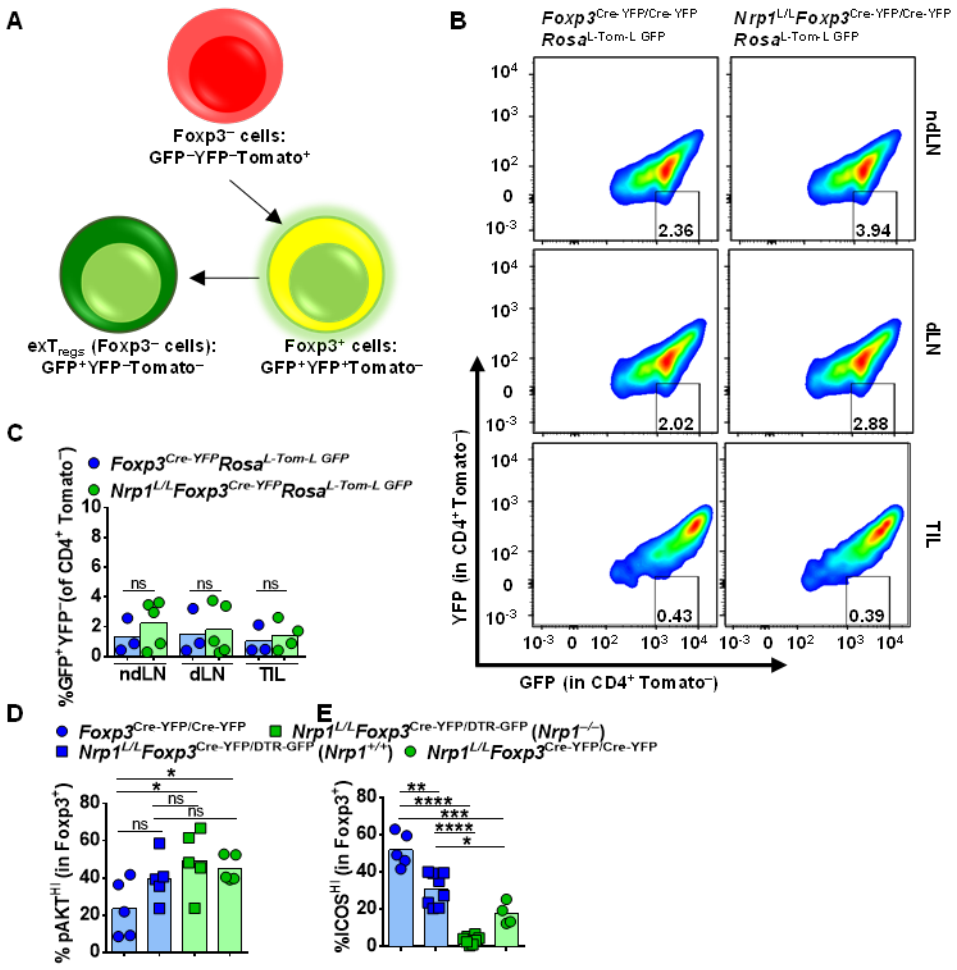

Figure 3: Nrp1$^{-/-}$ T$_{regs}$ maintain Foxp3 expression.

exT$_{reg}$ analysis. (**A-C**) Lymphocytes were isolated from ndLN, dLN, and TIL of *Foxp3*$^{Cre\text{-}YFP/Cre\text{-}YFP}$*Rosa*$^{L\text{-}Tom\text{-}L\ GFP}$ and *Nrp1*$^{L/L}$*Foxp3*$^{Cre\text{-}YFP/Cre\text{-}YFP}$*Rosa*$^{L\text{-}Tom\text{-}L\ GFP}$ mice and stained (n=3-5). (**D-E**) Lymphocytes were isolated from TIL of *Foxp3*$^{Cre\text{-}YFP/Cre\text{-}YFP}$, *Nrp1*$^{L/L}$*Foxp3*$^{Cre\text{-}YFP/Cre\text{-}YFP}$, *Nrp1*$^{L/L}$*Foxp3*$^{Cre\text{-}YFP/+}$ mice and stained. T$_{regs}$ from *Nrp1*$^{L/L}$*Foxp3*$^{Cre\text{-}YFP/+}$ mice were stained with Foxp3 and Nrp1^{+} and Nrp1^{-} T$_{regs}$ were distinguished as YFP^{+}Foxp3^{+} (Nrp1^{-}) and YFP^{-}Foxp3^{+} (Nrp1^{+}). This was also verified by Nrp1 staining (n=5). Data represent 2-3 independent experiments. Student unpaired t test was used. (ns, not significant, *p < 0.05, **p < 0.01, ***p < 0.001, ****p < 0.0001).

3.3.3 Fragile and wild type T_{regs} have a reciprocal impact on their transcriptome

I next used transcriptomic analysis of *Nrp1*$^{+/+}$ and *Nrp1*$^{-/-}$ T_{regs} from *Foxp3*$^{Cre\text{-}YFP/Cre\text{-}YFP}$, *Nrp1*$^{L/L}$*Foxp3*$^{Cre\text{-}YFP/Cre\text{-}YFP}$ and *Nrp1*$^{L/L}$*Foxp3*$^{Cre\text{-}YFP/DTR\text{-}GFP}$ mice to evaluate the cell intrinsic and extrinsic impact of *Nrp1* loss (Fig. 4). Significant alterations in the T_{reg} transcriptome were observed between *Nrp1*$^{+/+}$ and *Nrp1*$^{-/-}$ T_{regs}. Principal Component Analysis (PCA) based on differentially expressed genes clearly separated T_{eff} and T_{regs} based on both location and genotype. Interestingly, intratumoral *Nrp1*$^{+/+}$ and *Nrp1*$^{-/-}$ T_{regs} from heterozygous *Nrp1*$^{L/L}$*Foxp3*$^{Cre\text{-}YFP/DTR\text{-}GFP}$ mice were similar to each other and yet distinct from their genotypically identical counterparts from control *Foxp3*$^{Cre\text{-}YFP/Cre\text{-}YFP}$ and *Nrp1*$^{L/L}$*Foxp3*$^{Cre\text{-}YFP/Cre\text{-}YFP}$ mice (Fig. 5A).

Pathway analysis highlighted a potential role for IFNγ/IL-12-related transcriptional programs. Of particular interest was an increase in *Ifng* and its targets in *Nrp1*$^{-/-}$ T_{regs} in *Nrp1*$^{L/L}$*Foxp3*$^{Cre\text{-}YFP/Cre\text{-}YFP}$ and *Nrp1*$^{L/L}$*Foxp3*$^{Cre\text{-}YFP/DTR\text{-}GFP}$ as well as in *Nrp1*$^{+/+}$ T_{regs} in *Nrp1*$^{L/L}$*Foxp3*$^{Cre\text{-}YFP/DTR\text{-}GFP}$ mice (Fig. 5B-C), implicating a role for the IFNγ pathway in modulating T_{reg} function and function in the tumor microenvironment. When T_{reg} signature genes were assessed wherein it became evident that all four populations were district and yet bore a transcriptional relationship (Fig. 6A-D). These data suggest that *Nrp1*$^{+/+}$ and *Nrp1*$^{-/-}$ T_{regs} in heterozygous *Nrp1*$^{L/L}$*Foxp3*$^{Cre\text{-}YFP/DTR\text{-}GFP}$ mice impact each other's transcriptome in a reciprocal manner.

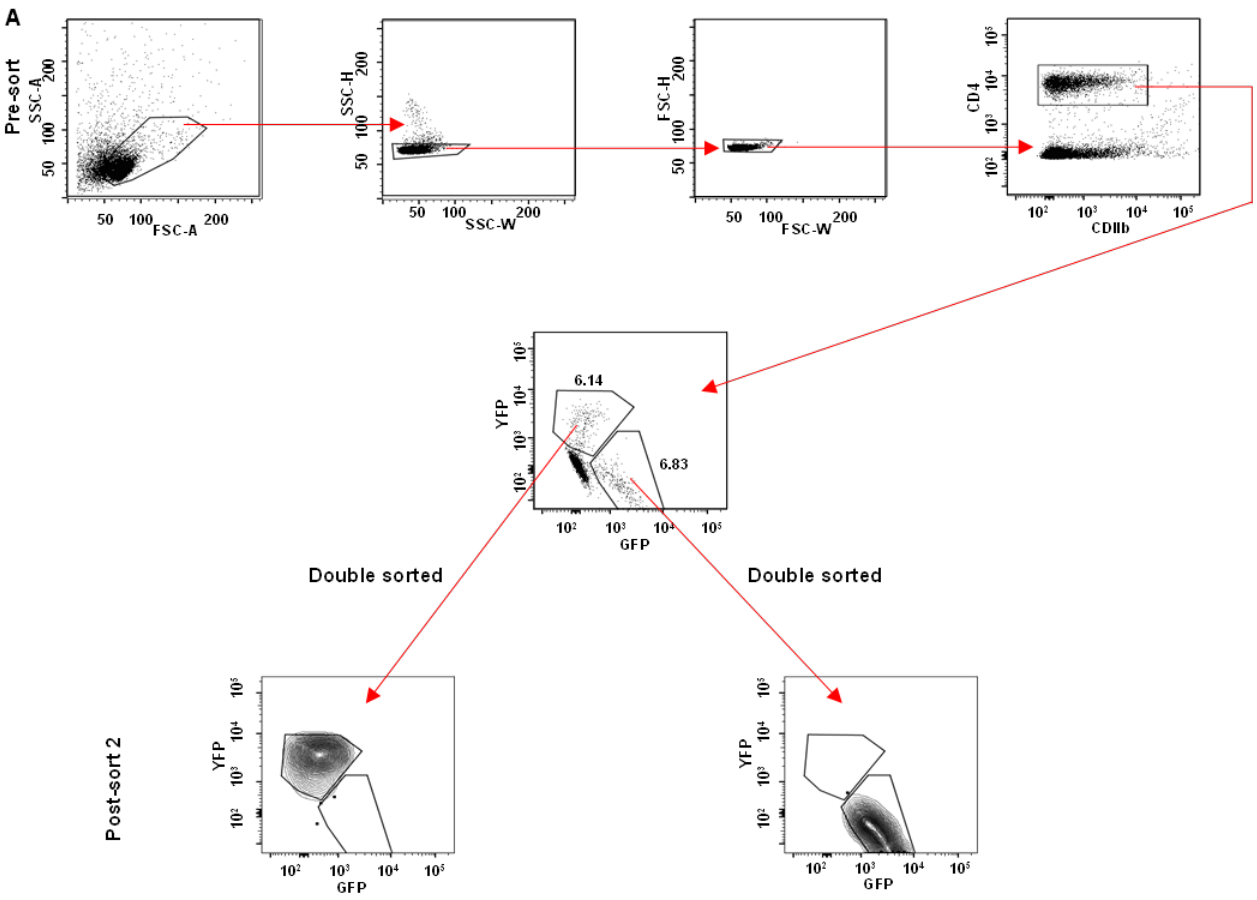

Figure 4: RNASeq sorting scheme.

RNASeq double sorting scheme. T_{regs} were isolated from ndLN and TIL of *Foxp3*$^{Cre\text{-}YFP/Cre\text{-}YFP}$, *Nrp1*$^{L/L}$*Foxp3*$^{Cre\text{-}YFP/Cre\text{-}YFP}$, and *Nrp1*$^{L/L}$*Foxp3*$^{Cre\text{-}YFP/DTR\text{-}GFP}$ mice and checked for purity. Cells were either single or double sorted. No significant difference was noted between single or double sorted samples. Data represent 5 independent experiments.

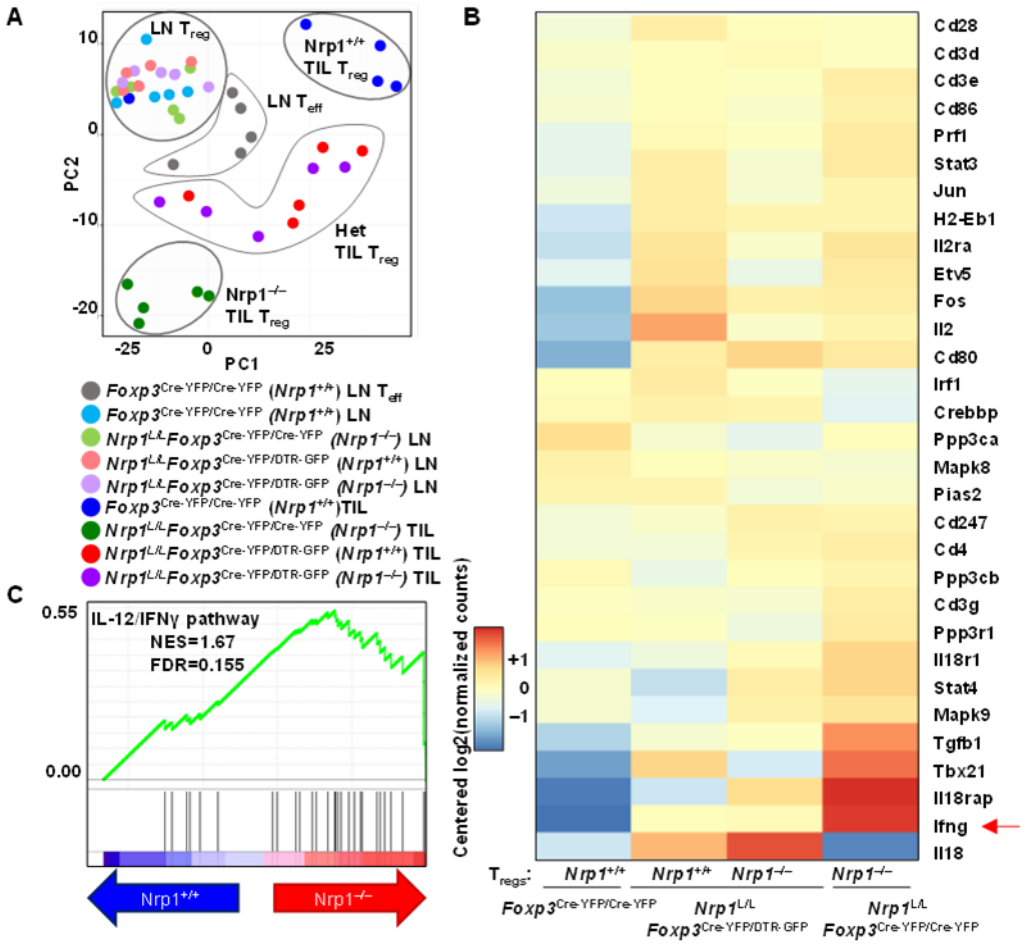

Figure 5: Nrp1 alters the T_{reg} transcriptome.

RNASeq analysis. (**A-C**) T_{regs} were purified based on $CD4^+$, and GFP or YFP expression from *Foxp3*$^{Cre\text{-}YFP/Cre\text{-}YFP}$, *Nrp1*$^{L/L}$*Foxp3*$^{Cre\text{-}YFP/Cre\text{-}YFP}$, and *Nrp1*$^{L/L}$*Foxp3*$^{Cre\text{-}YFP/DTR\text{-}GFP}$ mice on D12, cDNA and libraries were generated using the Clontech SmartER Ultra-Low and Illumina Nextera XT Library Prep kits. Samples were normalized to 2nM and sequenced on a NextSeq500. (**A**) Differentially expressed genes are determined by the genes that have q-value of 0.2 between any two of the four T_{reg} groups in the TIL. PCA was computed using the "prcomp()" R functions using the normalized voom data restricted to the same differentially expressed genes as shown in figure. (**B-C**) Significant genes were cross-referenced with those that were annotated to "plasma membrane" or "extracellular part" in the Cellular Component Gene Ontology. The Gene Ontology annotations were obtained from mSigDB. A number of genes associated with the Ifng/Il12/Il18 pathways were upregulated in the *Nrp1*$^{-/-}$ samples. Data represent 5 independent experiments with 3-5 mice pooled per experiment.

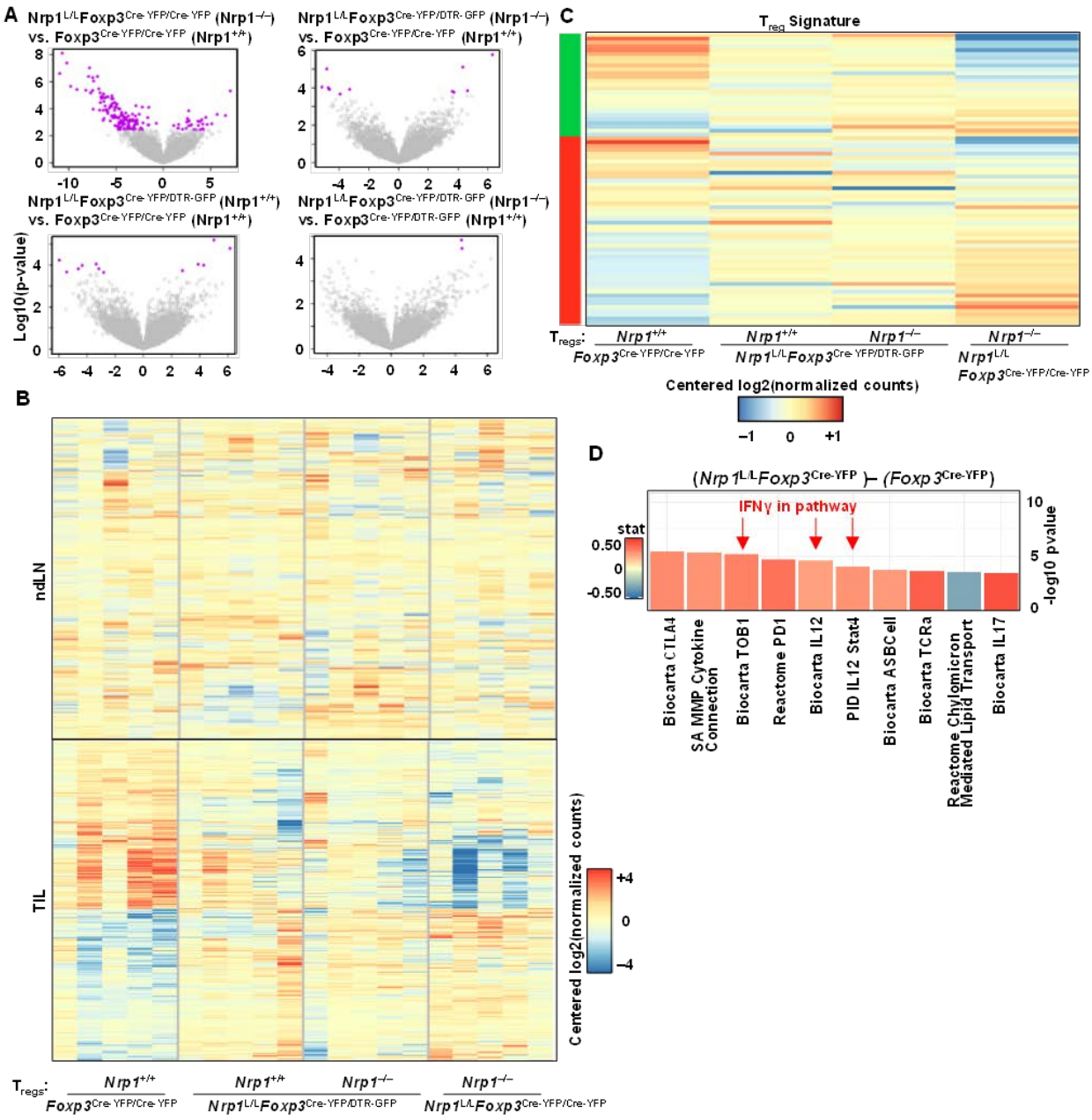

Figure 6: Nrp1$^{-/-}$ display an altered T_{reg} signature.

RNASeq analysis. T_{regs} were isolated from ndLN and TIL of *Foxp3*$^{Cre\text{-}YFP/Cre\text{-}YFP}$, *Nrp1*$^{L/L}$*Foxp3*$^{Cre\text{-}YFP/Cre\text{-}YFP}$, and *Nrp1*$^{L/L}$*Foxp3*$^{Cre\text{-}YFP/DTR\text{-}GFP}$ mice and checked for purity. (**A**) Volcano plots. (**B**) Global heatmap. All genes that passed a threshold of q-value FDR <0.2 are shown. (**C**) T_{reg} signature gene heatmap. Green/red coloring represents genes that are upregulated/downregulated in T_{regs}. (**D**) Bar chart of top differentially expressed pathways. Data represent 5 experiments.

While previous reports have suggested that a small subset of T_{regs} produce IFNγ during inflammation [125, 126, 127], the expression of IFNγ by T_{regs} in tumors and its impact on their suppressive function remains unclear. Using flow cytometry, I found that there was increased expression of IFNγ by *Nrp1*$^{-/-}$ T_{regs} in both *Nrp1*$^{L/L}$*Foxp3*$^{Cre\text{-}YFP/Cre\text{-}YFP}$ and *Nrp1*$^{L/L}$*Foxp3*$^{Cre\text{-}YFP/DTR\text{-}GFP}$ mice (Fig. 7A-B). Interestingly, an increased percentage of *Nrp1*$^{+/+}$ T_{regs} from *Nrp1*$^{L/L}$*Foxp3*$^{Cre\text{-}YFP/DTR\text{-}GFP}$ mice also expressed IFNγ. Interferon-γ receptor 1 (IFNγR) expression showed an elevated trend in *Nrp1*$^{-/-}$ T_{regs} in *Nrp1*$^{L/L}$*Foxp3*$^{Cre\text{-}YFP/Cre\text{-}YFP}$ mice, and both *Nrp1*$^{-/-}$ and *Nrp1*$^{+/+}$ T_{regs} in *Nrp1*$^{L/L}$*Foxp3*$^{Cre\text{-}YFP/DTR\text{-}GFP}$ heterozygous mice (Fig. 7B). In order to determine whether modulation of IFNγ and IFNγR expression also occurred following blockade of the Nrp1:Sema4a axis, I treated B16 tumor-bearing mice with Sema4aIg [43]. Indeed, Sema4aIg treatment decreased tumor size, and led to an unstable T_{reg} phenotype as assessed by increased IFNγ production and higher IFNγR expression (Fig. 7C-E). In addition to increases in IFNγ production and IFNγR expression, several type 1 helper T cell markers were upregulated in *Nrp1*$^{-/-}$ T_{regs}, such as Tbet, Cxcr3, and Eomes (Fig. 8A–F) as well as downstream pSTAT1 in *Nrp1*$^{-/-}$ T_{regs} from *Nrp1*$^{L/L}$*Foxp3*$^{Cre\text{-}YFP/DTR\text{-}GFP}$ mice and pSTAT4 in all *Nrp1*$^{-/-}$ T_{regs} (Fig. 8G, H).

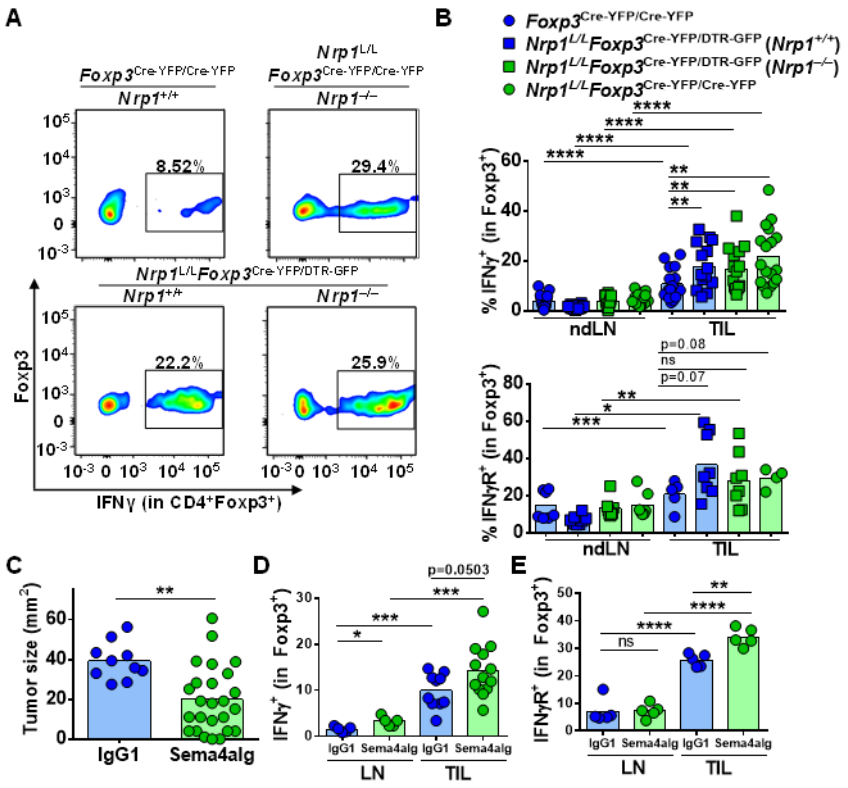

Figure 7: Nrp1$^{-/-}$ T$_{regs}$ display increased IFNγ in the tumor microenvironment.

Flow cytometry analysis. (**A-B**) *Foxp3*$^{Cre\text{-}YFP/Cre\text{-}YFP}$, *Nrp1*$^{L/L}$*Foxp3*$^{Cre\text{-}YFP/Cre\text{-}YFP}$, and *Nrp1*$^{L/L}$*Foxp3*$^{Cre\text{-}YFP/DTR\text{-}GFP}$ mice were injected with B16.F10 melanoma tumor cells ID on day 0 and sacrificed on day 12. Lymphocytes were isolated from ndLN and TIL of mice noted, stimulated and stained for IFNγ and IFNγR. (n=8-18). (**C-E**) C57BL/6 mice were injected with B16.F10 melanoma tumor cells ID on day 0. Mice were treated with either Sema4aIg or IgG1 every 3 days until sacrifice starting on day 5 (400ug, 200ug, 200ug, 200ug). (**C**) Tumors were measured on day 12 for prior to sacrifice (n=10-25). (**D**) Lymphocytes were isolated from ndLN and TIL, stimulated and stained for IFNγ (n=5-13). (**E**) Lymphocytes were isolated from ndLN and TIL, and stained for IFNγR (n=5). Data represent 3-4 independent experiments. Student unpaired t test was used. (*p<0.05, **p < 0.01, ***p < 0.001, ****p < 0.0001).

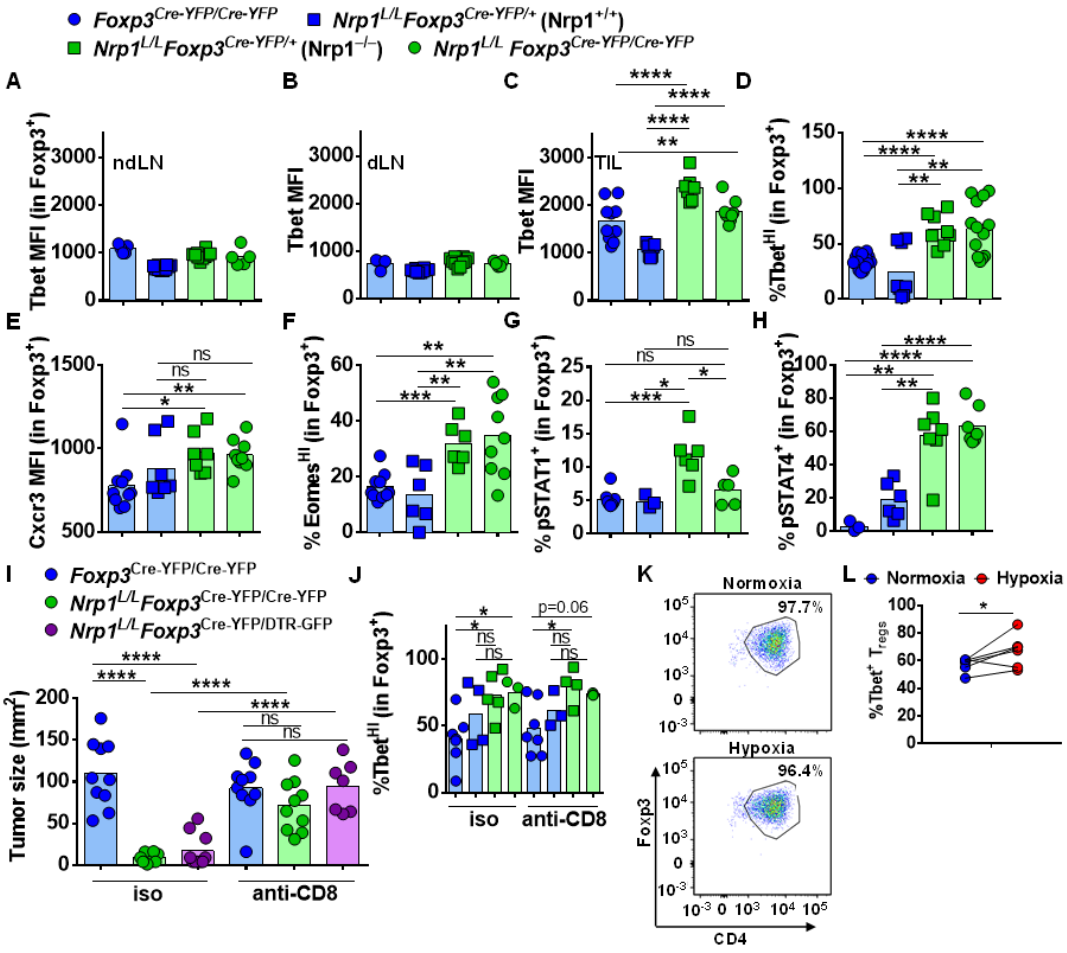

Figure 8: Nrp1 loss leads to an increase in TH1 markers.

Flow cytograms of markers indicated. (**A-H**) Lymphocytes were isolated from ndLN, dLN, or TIL of *Foxp3*$^{Cre\text{-}YFP/Cre\text{-}YFP}$, *Nrp1*$^{L/L}$*Foxp3*$^{Cre\text{-}YFP/Cre\text{-}YFP}$, *Nrp1*$^{L/L}$*Foxp3*$^{Cre\text{-}YFP/+}$ mice and stained. T_{regs} from *Nrp1*$^{L/L}$*Foxp3*$^{Cre\text{-}YFP/+}$ mice were stained with *Foxp3* and Nrp1^{+} and Nrp1^{-} T_{regs} were distinguished as YFP^{+}Foxp3^{+} (Nrp1^{-}) and YFP^{-}Foxp3^{+} (Nrp1^{+}) (n=5-15). (**I**) *Foxp3*$^{Cre\text{-}YFP/Cre\text{-}YFP}$ and *Nrp1*$^{L/L}$*Foxp3*$^{Cre\text{-}YFP/Cre\text{-}YFP}$ mice were injected with B16 on day 0 and treated with isotype or anti-CD8 (n=4-7). Lymphocytes were isolated from TIL and stained. (**J-K**) T_{regs} were isolated from *Foxp3*$^{Cre\text{-}YFP/Cre\text{-}YFP}$ and *Nrp1*$^{L/L}$*Foxp3*$^{Cre\text{-}YFP/Cre\text{-}YFP}$ mice and stimulated in hypoxia or normoxia for 3 days and stained (n=6). Data represent 3-6 independent experiments. Student unpaired t test was used. (ns, not significant, *p < 0.05, **p < 0.01, ***p < 0.001, ****p < 0.0001).

Surprisingly, I found that the majority of the IFNγ^{+} cells in the TIL of *Nrp1*$^{L/L}$*Foxp3*$^{\text{Cre-YFP}}$ and *Nrp1*$^{L/L}$*Foxp3*$^{\text{Cre-YFP/DTR-GFP}}$ were T_{regs} (Fig. 9A) and that the total percentage of IFNγ^{+} cells in TIL was small in the absence of T_{reg}-restricted Nrp1 deletion (Fig. 9B), raising the possibility that IFNγ production may be a dominant feature of T_{reg} fragility and thus could be affecting surrounding cells in the tumor microenvironment including *Nrp1*$^{+/+}$ T_{regs}.

While my data show that T_{regs} produced significant amounts of IFNγ in *Nrp1*$^{L/L}$*Foxp3*$^{\text{Cre-YFP}}$ and *Nrp1*$^{L/L}$*Foxp3*$^{\text{Cre-YFP/DTR-GFP}}$ mice, I could not rule out the possibility that IFNγ production by fragile T_{regs} was initially triggered, or potentiated by, the altered tumor microenvironment. Indeed, tumor size is greatly reduced and lymphocyte infiltration increased in *Nrp1*$^{L/L}$*Foxp3*$^{\text{Cre-YFP}}$ and *Nrp1*$^{L/L}$*Foxp3*$^{\text{Cre-YFP/DTR-GFP}}$ mice (Fig. 1E and Fig. 2A). In order to address this possibility, I blocked the anti-tumor immune response and prevented tumor shrinkage by depleting CD8^{+} T cells (using anti-CD8) in B16 tumor bearing mice, and assessed T_{reg} phenotype and function. I found that CD8^{+} T cell depletion had no effect on the suppressive capacity in *Nrp1*$^{L/L}$*Foxp3*$^{\text{Cre-YFP}}$ and *Nrp1*$^{L/L}$*Foxp3*$^{\text{Cre-YFP/DTR-GFP}}$ mice. Indeed, *Nrp1*$^{-/-}$ T_{regs} exhibited increased IFNγ and Tbet protein expression along with reduced in suppressive capacity in an *in vitro* suppression assay, suggesting that T_{reg} fragility due to *Nrp1* loss is primarily due to a cell intrinsic mechanism rather than an extrinsic environmental effect due to increased CD8^{+} T cell infiltration, the ensuing anti-tumor response, and tumor size (Fig. 8I-J and Fig. 9C-D). However, a role for CD8^{+} T cell-derived IFNγ in promoting T_{reg} fragility in this system cannot be ruled out.

Although cell-intrinsic processes downstream of *Nrp1* loss appeared to drive T_{reg} fragility, it is still possible that cell-extrinsic, environmental factors facilitated intratumoral T_{reg} fragility. Further analysis of my RNAseq data highlighted enhanced expression of *Hif1a* (hypoxia-inducible factor 1 alpha) in *Nrp1*$^{-/-}$ compared to *Nrp1*$^{+/+}$ intratumoral T_{regs} (Fig. 9E). Indeed, the percentage of Hif1α^{+} *Nrp1*$^{-/-}$ intratumoral T_{regs} and Hif1α protein expression within those T_{regs} was higher than their *Nrp1*$^{+/+}$ counterparts (Fig. 9F). Interestingly, Hif1α has been shown to be upregulated by Akt signaling which in turn led to increased IFN-γ production by T_{regs} [128, 129]. As Hif1α is upregulated in hypoxic conditions, I wondered whether hypoxia was capable of inducing T_{reg} fragility, analogous to the environment in which intratumoral T_{regs} reside. Remarkably, LN-derived T_{regs} from a naïve mouse showed increased IFN-γ and Tbet expression, and an elevated trend in Hif1α expression while retaining Foxp3 expression after being cultured for 3 days in hypoxic versus normoxic conditions (Fig. 9G and Fig. 8K and L). These data suggest that the hypoxia:Hif1α axis may prime T_{regs} to become functionally fragile in the tumor microenvironment.

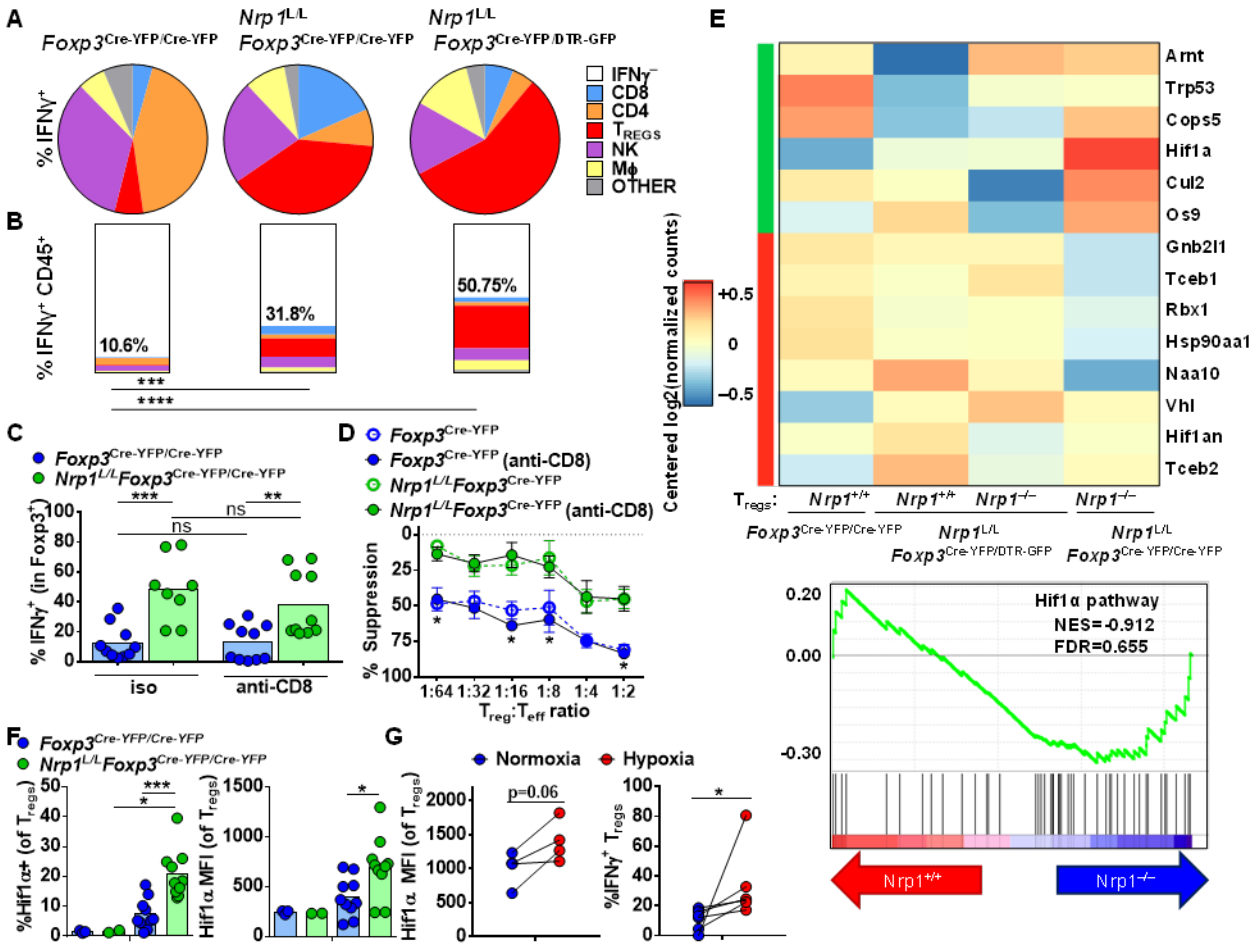

Figure 9: Hypoxia sensitizes intratumoral T_{regs} to IFNγ-mediated fragility.

(**A-B**) Flow cytometry of cell populations. *Foxp3*$^{Cre\text{-}YFP/Cre\text{-}YFP}$, *Nrp1*$^{L/L}$*Foxp3*$^{Cre\text{-}YFP/Cre\text{-}YFP}$, and *Nrp1*$^{L/L}$*Foxp3*$^{Cre\text{-}YFP/DTR\text{-}GFP}$ mice were injected with B16.F10 melanoma tumor cells ID on day 0 and sacrificed on day 12. Lymphocytes were isolated from TIL of mice noted, stimulated and stained for IFNγ (n=5). (**C-D**) Flow cytometry and suppression assay after CD8 depletion. Mice were treated with anti-CD8 or isotype (200ug) every 3 days starting on day 5. Tumor size was measured on day of sacrifice (D12), lymphocytes were isolated from TIL of mice noted, stimulated, and stained for IFNγ (n=7-10). (**E**) RNASeq analysis. Lymphocytes were isolated from mice noted and used in a microsuppression assay. (**F**) Flow cytometry analysis. T_{regs} were purified, processed, and analyzed as in Fig. 2 (n=5). Heatmap includes genes previously shown to be positive or negative regulators in the Hif1α pathway. Pathway analysis includes all genes in pathway. (**G**) Flow cytometry analysis after T_{regs} were cultured in hypoxia. *Foxp3*$^{Cre\text{-}YFP/Cre\text{-}YFP}$ and *Nrp1*$^{L/L}$*Foxp3*$^{Cre\text{-}YFP/Cre\text{-}YFP}$ mice were injected with B16.F10 melanoma tumor cells

ID on day 0 and sacrificed on day 12. Lymphocytes were isolated from ndLN and TIL and stained for Hif1α (n=10). (**H**) T_{regs} were isolated from LN of *Foxp3*$^{Cre\text{-}YFP/Cre\text{-}YFP}$ mice, stimulated for 3 days in hypoxia or normoxia, and stained (n=4-6). Data represent 2-5 independent experiments. Student unpaired t test was used. (*p<0.05, **p < 0.01, ***p < 0.001, ****p < 0.0001).

3.3.4 IFNγ is required and sufficient to drive intratumoral T_{reg} fragility

In order to test whether *Nrp1*$^{-/-}$ T_{regs} could directly impact the function of *Nrp1*$^{+/+}$ T_{regs}, and if this was mediated by IFNγ, I co-cultured ndLN- or tumor-derived *Nrp1*$^{+/+}$ T_{regs} from either Thy1.1 *Foxp3*$^{Cre\text{-}YFP}$ or *Ifngr1*$^{-/-}$*Foxp3*$^{Cre\text{-}YFP}$ mice (T_{regs} which lack the IFNγ receptor) with *Nrp1*$^{-/-}$ T_{regs} from Thy1.2 *Nrp1*$^{L/L}$*Foxp3*$^{Cre\text{-}YFP}$ mice prior to assessing their regulatory activity in a microsuppression assay (Fig. 10A). All cell populations were also cultured alone under the same conditions as controls, and as expected, T_{reg} populations cultured alone exhibited the expected suppressive capacity (Fig. 1H compared with Fig. 10B, left side columns). Note that APCs were not included in the 72h pre-culture prior to the T_{reg} microsuppression assay. Interestingly, TIL-derived *Nrp1*$^{+/+}$ T_{regs} that were co-cultured with tumor-derived *Nrp1*$^{-/-}$ T_{regs} lost their ability to suppress effector T cells, in contrast to ndLN-derived T_{regs} (Fig. 10B, right side columns). Loss of suppressive activity did not require cell-cell contact, but was dependent on IFNγR expression (Fig. 10B-D). In order to confirm that IFNγ was the sole cytokine responsible for *Nrp1*$^{+/+}$ T_{reg} fragility following co-culture with *Nrp1*$^{-/-}$ T_{regs}, I co-cultured *Nrp1*$^{+/+}$ and *Nrp1*$^{-/-}$ T_{regs} in the presence of different concentrations of anti-IFNγ for 72 hours, and then assessed the suppressive capacity of the purified *Nrp1*$^{+/+}$ T_{regs} in the absence of anti-IFNγ. IFNγ neutralization prevented the loss of tumor-derived *Nrp1*$^{+/+}$ T_{reg} suppression in a dose-dependent manner (Fig. 10E).

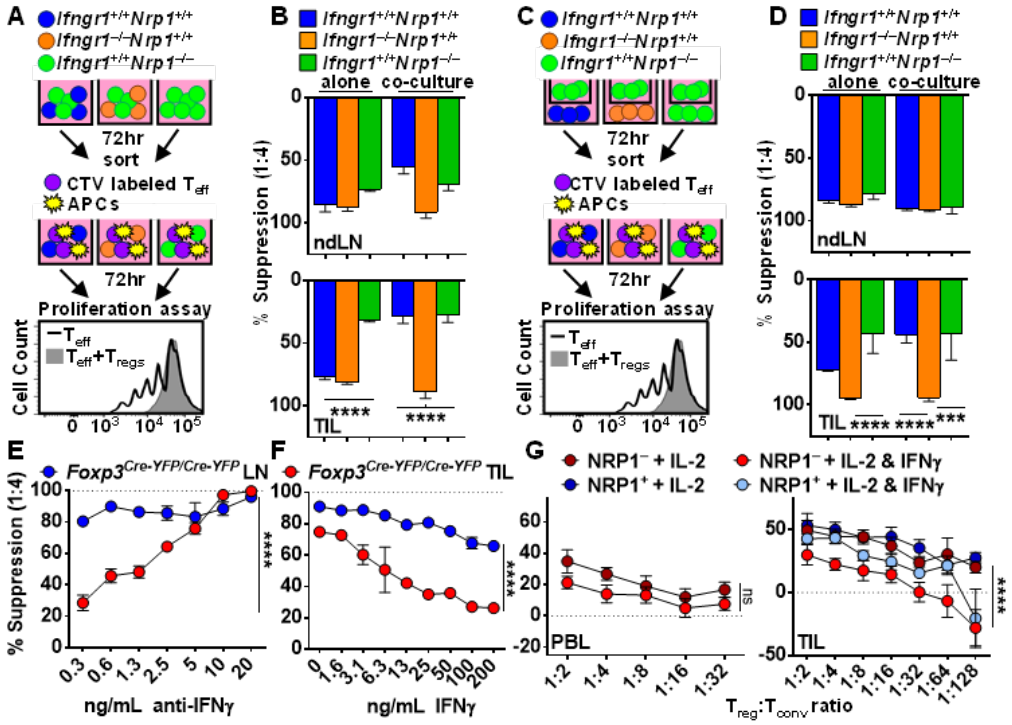

Figure 10: IFNγ reduces T_{reg} suppression.

In vitro cultures and suppression assays. (**A, B**) T_{regs} were isolated from ndLN and TIL of mice noted, stimulated with PMA and Ionomycin, cultured with IL-2 alone or with IL-2 and *Nrp1*$^{-/-}$ T_{regs} for 72 hours and used in a microsuppression assay in absence of cytokine (n=6-7). **(C, D**) T_{regs} were isolated and stimulated as in (**A**), cultured in the bottom of a transwell plate with IL-2 alone or with IL-2 and *Nrp1*$^{-/-}$ T_{regs} in the top well for 72 hours and used in a microsuppression assay in the absence of cytokine (n=6-7). (**E**) T_{regs} were isolated from ndLN and TIL of *Foxp3*$^{Cre\text{-}YFP/Cre\text{-}YFP}$ mice, co-cultured with Nrp1$^{-/-}$ T_{regs} and IL-2 in the presence or absence of anti-IFNγ, re-sorted and used in a microsuppression assay in the absence of cytokine (n=6). (**F**) T_{regs} were isolated from ndLN and TIL of *Foxp3*$^{Cre\text{-}YFP/Cre\text{-}YFP}$ mice, treated with IL-2 and IFNγ for 72 hours, re-sorted and used in a microsuppression assay in the absence of cytokine (n=6). (**G**) T_{regs} were isolated from HNSCC PBL and TIL, cultured with IL-2 +/- IFNγ for 3 days, then used in a microsuppression assay in the absence of cytokine (n=2-14). Data represent 3-5 experiments. Error bars represent the mean ± SEM. Student unpaired t test (**A-D**) and 2 Way Anova (**E-G**) were used. (*p<0.05, **p <0.01, ****p <0.0001).

While previous studies have suggested that IL-12 can impact T_{reg} suppression and induce IFNγ expression [130, 131], whether IFNγ has a direct effect on T_{regs} and if so what impact that might have in their function remains obscure. In order to determine whether IFNγ was sufficient to limit suppressive capacity, I treated *Nrp1*$^{+/+}$ T_{regs} from ndLN and TIL with IFNγ for 72 hours plus IL-2 in stimulating conditions prior to assessing their functional capacity in a microsuppression assay in the absence of cytokine. IFNγ substantially limited the suppressive capacity of TIL-derived, and to a lesser extent ndLN-derived, *Nrp1*$^{+/+}$ T_{regs} in a dose-dependent manner (Fig. 10F). Given that IFNγ limits the function of murine T_{regs}, I asked whether IFNγ could also impact human T_{regs} and whether this was enhanced by the human tumor microenvironment. Indeed, intratumoral human T_{regs} showed an increased sensitivity to IFNγ in comparison to PBL T_{regs} when cultured with the cytokine 72 hours prior to assessment of their suppressive capacity in the absence of cytokine (Fig. 10G). Furthermore, intratumoral NRP1^{+} T_{regs} appeared to be less sensitive to the effects of IFNγ than NRP1^{-} T_{regs}.

The increased sensitivity of tumor- versus ndLN-derived *Nrp1*$^{+/+}$ T_{regs} to *Nrp1*$^{-/-}$ T_{regs} appeared to correlate with IFNγR expression (Fig. 11A-B), and this effect was lost if *Ifngr1*$^{-/-}$ T_{regs} were used (Fig. 11C). Pre-treatment with IFNγ also induced IFNγ expression by WT T_{regs} but not *Ifngr1*$^{-/-}$ T_{regs} (Fig. 11D, and data not shown). Taken together, these data suggest that IFNγ can undermine the function of murine and human T_{regs} *in vitro*.

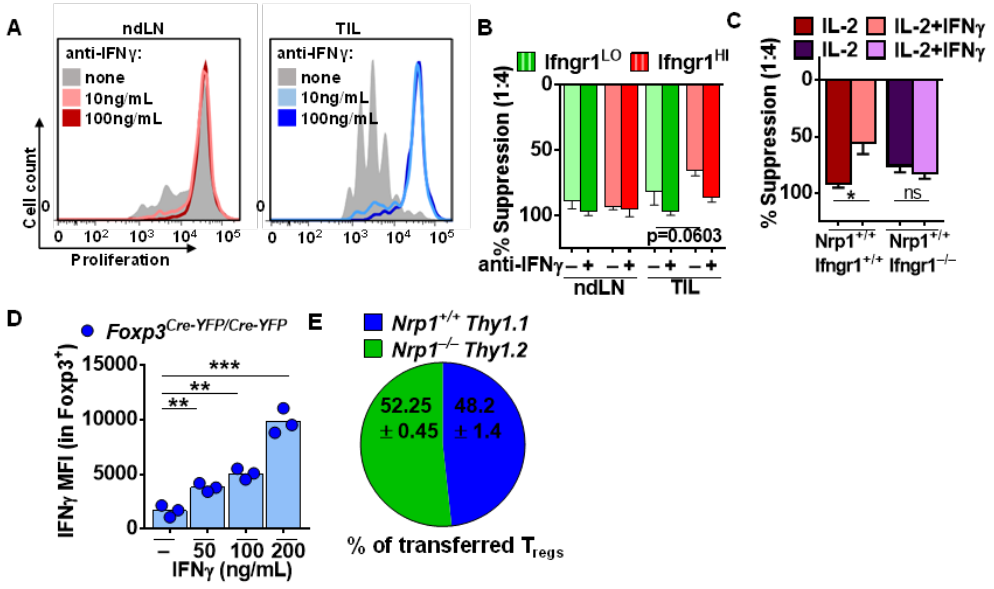

Figure 11: T_{reg} suppression is crippled by IFNγ.

(**A**) Microsuppression assay. T_{regs} were isolated from ndLN and TIL of *Foxp3*$^{Cre\text{-}YFP}$ mice, co-cultured with Nrp1$^{-/-}$ T_{regs} and IL-2 in the presence or absence of anti-IFNγ, resorted and used in a microsuppression assay (n=6). (**B**) Microsuppression assay. T_{regs} were isolated from the ndLN and TIL of *Foxp3*$^{Cre\text{-}YFP/Cre\text{-}YFP}$ mice, treated with IL-12 and IL-2 for 72 hours, sorted based on Ifngr1 expression, co-cultured with Nrp1$^{-/-}$ T_{regs} for 72 hours with or without anti-IFNγ, and re-isolated for a microsuppression assay (n=3). (**C**) Microsuppression assay. T_{regs} were isolated from ndLN and TIL of *Foxp3*$^{Cre\text{-}YFP}$ and *Ifngr1*$^{-/-}$*Foxp3*$^{Cre\text{-}YFP}$ mice, treated with IL-2 and IFNγ for 72 hours, resorted and used in a microsuppression assay (n=3-4). (**D**) IFNγ MFI by flow cytometry. T_{regs} were isolated from TIL of *Foxp3*$^{Cre\text{-}YFP}$ mice, treated with IFNγ and IL-2 for 72 hours, washed and stained (n=3). (**E**) Percent Nrp1$^{+/+}$ and Nrp1$^{-/-}$ T_{regs} post transfer. *Foxp3*$^{-/-}$ mice were injected with 10^6 of a 50:50 mix of *Nrp1*$^{+/+}$*Thy1.1* and *Nrp1*$^{-/-}$*Thy1.2* T_{regs} on day 2 post-birth. B16.F10 was injected ID on day 28. Lymphocytes were isolated and stained (n=3). Data represent 2-3 independent experiments. Error bars represent the mean ± SEM. Student unpaired t test was used. (ns, not significant, *$p < 0.05$, **$p < 0.01$, ***$p < 0.001$).

I next sought to determine if *Nrp1*$^{-/-}$ T_{reg}-derived IFNγ from could drive *Nrp1*$^{+/+}$ T_{reg} fragility *in vivo.* To address this, I used *Foxp3*$^{-/-}$ mice that lack T_{regs} and succumb to a scurfy-like phenotype if T_{regs} are not adoptively transferred within 48 hours of birth [34]. T_{regs} of a single genotype or a 50:50 mixture of two different T_{reg} genotypes were adoptively transferred into two-day-old *Foxp3*$^{-/-}$ mice. At 4 weeks of age, mice were injected with B16 melanoma and tumor growth assessed over time (Fig. 12A). Mice were monitored after T_{reg} injection and removed from study prior to B16 injection if any signs of autoimmunity were observed [34]. Tumor growth in *Foxp3*$^{-/-}$ mice that received either *Nrp1*$^{+/+}$ T_{regs}, *Nrp1*$^{-/-}$ T_{regs} or a 50:50 mixture of *Nrp1*$^{+/+}$ and *Nrp1*$^{-/-}$ T_{regs} phenocopied tumor growth in *Foxp3*$^{Cre\text{-}YFP/Cre\text{-}YFP}$, *Nrp1*$^{L/L}$*Foxp3*$^{Cre\text{-}YFP/Cre\text{-}YFP}$ and *Nrp1*$^{L/L}$*Foxp3*$^{Cre\text{-}YFP/DTR\text{-}GFP}$ mice, respectively (Fig. 1E and 12B-D and Fig. 11E). I then assessed the impact of T_{reg}-derived IFNγ on tumor growth by transferring either [a] *Nrp1*$^{+/+}$ T_{regs} that cannot respond to IFNγ with *Nrp1*$^{-/-}$ T_{regs} (50% *Nrp1*$^{+/+}$*Ifngr1*$^{-/-}$ + 50% *Nrp1*$^{-/-}$*Ifngr1*$^{+/+}$), or [b] *Nrp1*$^{-/-}$ T_{regs} that cannot produce IFNγ with *Nrp1*$^{+/+}$ T_{regs} (50% *Nrp1*$^{+/+}$*Ifng*$^{+/+}$ + 50% *Nrp1*$^{-/-}$*Ifng*$^{-/-}$). Strikingly, tumor growth was completely restored with either combination (Fig. 12E-H), revealing a critical role for IFNγ produced by fragile *Nrp1*$^{-/-}$ T_{regs} in mediating *Nrp1*$^{+/+}$ T_{reg} dysfunction, and thereby facilitating anti-tumor immunity and limiting tumor growth.

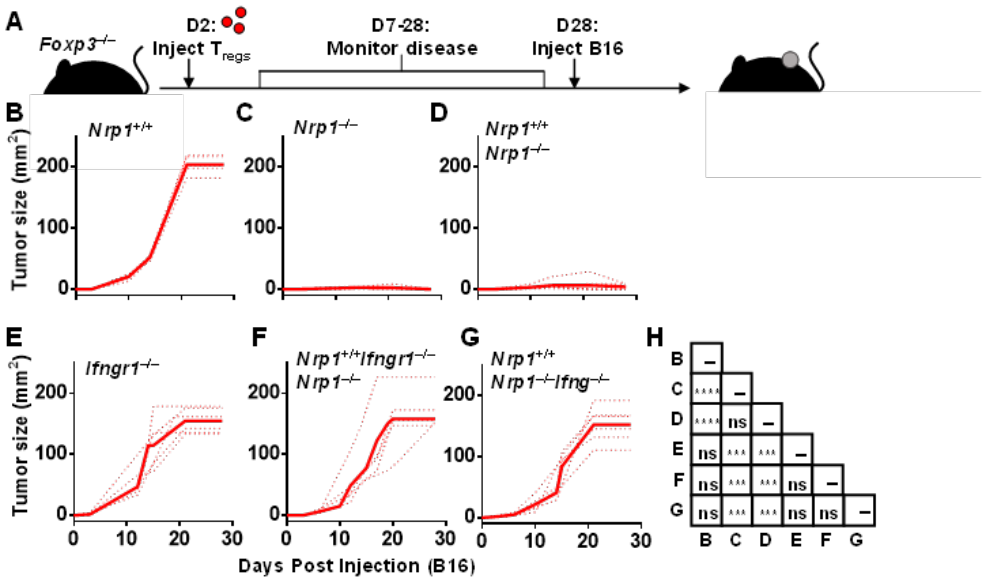

Figure 12: IFNγ uptake by T_{regs} is required for T_{reg} fragility and tumor clearance.

Tumor growth curves. (**A-G**) *Foxp3*$^{-/-}$ mice were injected with 10^6 T_{regs} on day 2 post-birth, and monitored for 28 days for the onset of any autoimmune symptoms [4 of 34 mice were removed from study], no more than 1 per experimental group. B16.F10 was injected ID on day 28 and tumor size was measured every 3 days. (**H**) Statistics of *Foxp3*$^{-/-}$ mice tumor growth. Data represent 5-7 independent experiments with 5-7 mice per experimental group. Error bars represent the mean ± SEM. 2 way ANOVA was used. (ns, not significant, ***$p < 0.001$, ****$p < 0.0001$).

3.4 DISCUSSION

In summary, my data highlight seven key observations. [i] A high proportion of human T_{regs} expressed NRP1 in two tumor types: melanoma and HNSCC. It is also noteworthy that PBL T_{regs} from these cancer patients also possessed a clear population of $NRP1^+$ T_{regs} in contrast to healthy donor PBL T_{regs}, which exhibited little to no NRP1 expression, suggesting that patient T_{regs} could be recirculating through the periphery. Interestingly, the percentage of intratumoral $NRP1^+$ T_{regs} appeared to correlate with poor disease prognosis. [ii] B16 tumors were rapidly cleared in mice harboring a 50:50 mixture of Nrp1-deficient and WT T_{regs} due to increased functional fragility and loss of suppressive activity of both T_{reg} populations without loss of *Foxp3* expression. This was the result of Nrp1-deficient T_{reg} fragility rather than the generation of $Foxp3^-$ ex-T_{regs}. [iii] T_{reg} fragility had a reciprocal impact on the transcriptomes of Nrp1-deficient and WT T_{regs}, highlighting the previously unappreciated fact that T_{regs} can impact other T_{reg} populations directly as well as many other cell types. [iv] The induction of IFNγ pathway genes was a dominant feature of T_{reg} fragility in tumors. Intratumoral T_{regs} were more susceptible to this functionally fragile phenotype due to the hypoxic tumor microenvironment, which led to increased Hif1α expression and IFNγ production [132]. While it is possible that IFNγ derived from other sources could lead to T_{reg} fragility, I have shown that hypoxia promoted IFNγ production and T_{reg} fragility. [v] IFNγ, exogenously-provided (human or mouse) or intratumoral *Nrp1*$^{-/-}$ T_{reg}-derived (mouse), was capable of driving the fragility of tumor-derived WT T_{regs} and loss of mouse and

human T_{reg} suppressive activity *in vitro*. This was a direct effect of IFNγ or *Nrp1*$^{-/-}$ T_{reg}-derived IFNγ as no other cells types were included in the *in vitro* experiments. Previous studies have suggested that IL-12 can impact T_{reg} suppression and induce IFNγ expression [130, 131, 133], while others show that IFNγ can limit T_{reg} expansion [134, 135, 136, 137]. However, the direct effect of IFNγ on T_{reg} function *in vivo* had surprisingly not been appreciated. While some studies have shown that IFNγ^{+} T_{regs} can maintain suppressive function, this seems to be largely disease specific and has not been carefully assessed in the context of the tumor microenvironment [138, 139]. It is possible that the tumor microenvironment plays a critical role in driving IFNγ-mediated T_{reg} fragility, as suggested by the role of Hif1α in this process. In addition, while I anticipate that IL-12 may be playing a role in this process given that I see increased pSTAT4 expression, I have shown that IFNγ is capable of driving T_{reg} fragility both *in vitro* and *in vivo* in tumor-derived T_{regs} exposed to a hypoxic environment, suggesting that IL-12 may not be essential. [vi] Intratumoral T_{reg} fragility was mediated by IFNγ derived from *Nrp1*$^{-/-}$ T_{regs} that acted on WT intratumoral T_{regs}, thereby leading to their fragility and loss of suppressive activity. This was supported by the fact that inclusion of WT T_{regs} that could not respond to IFNγ or *Nrp1*$^{-/-}$ T_{regs} that could not produce IFNγ restored T_{reg} function, block anti-tumor immunity, and promote tumor growth. While these data suggest that *Nrp1*$^{-/-}$ T_{reg}-derived IFNγ is required, I do not yet know if it is sufficient. These observations were consistent with a model in which fragile *Nrp1*$^{-/-}$ T_{regs} produce large amounts of IFNγ in the tumor microenvironment that directly promotes the fragility of intratumoral WT T_{regs} without loss of Foxp3 expression. Importantly, this occurred without any detectable peripheral T_{reg} fragility and without impacting their maintenance

of peripheral tolerance, suggesting that this was a proximally- and locally-driven event, likely induced by inflammation. While I only observed this in the context of the tumor microenvironment, it is possible that T_{reg} fragility could indeed occur in other inflammatory settings where exposure to IFNγ is increased. I would argue that the mechanism of IFNγ-induced T_{reg} fragility is mediated directly between *Nrp1*$^{-/-}$ and WT T_{regs} as either loss of IFNγ or IFNγR expression, respectively, impacts fragility. While it is possible that IFNγ derived from other cell populations, such as CD8$^+$ T cells or NK cells, or the ensuing anti-tumor response and altered tumor microenvironment contributed to T_{reg} fragility, it is noteworthy that the dominant IFNγ-producing cell type was *Nrp1*$^{-/-}$ T_{regs} and CD8$^+$ T cell depletion did not impact the enhanced IFNγ production and loss of suppressive activity observed.

A previous study had suggested that the absence of Nrp1 leads to reduced influx of T_{regs} into certain tumor types (*Vegfa*$^{+/+}$ or *Vegfa*$^{-/-}$ fibrosarcomas and *Ret* melanoma models) [122]. However, I did not observe any defect in the migration of Nrp1-deficient T_{regs} even in the competitive environment of B16 tumors in heterozygous *Nrp1*$^{L/L}$*Foxp3*$^{Cre\text{-}YFP/DTR\text{-}GFP}$ female mice. These discrepancies could be due to the different tumor models analyzed. Alternatively, their study primarily utilized *Nrp1*$^{L/L}$*CD4*^{Cre} mice in which Nrp1 would be removed in all T cells, which could have many direct and indirect effects on intratumoral T_{regs} [122]. Indeed, it has been previously shown that Nrp1 is expressed on a number of cell types, especially in the tumor [140] (data not shown).

The loss of Nrp1 not only results in T_{reg} fragility but also results in substantial IFNγ expression, which in turn induces fragility in other T_{regs} regardless of their Nrp1

expression in a feed-forward manner; a process I refer to as “infectious fragility”. My data suggest that loss of Nrp1 stabilizes Hif1α expression, which then binds *Ifng* and upregulates expression. While our data highlight the role of IFNγ acting through paracrine signaling, it is possible that it also acts in an autocrine fashion on the T_{reg}. As IFNγ production is a hallmark of a productive T cell-mediated immune response, my observations also raise the possibility that IFNγ-induced T_{reg} fragility may be a physiologically important regulatory mechanism to locally limit T_{reg} function and promote a productive immune response. Given the profound consequences of T_{reg}-derived IFNγ production, my data emphasize the importance of the Nrp1 pathway in limiting T_{reg} fragility in the tumor microenvironment but also highlights that this pathway can be overcome when sufficient IFNγ is induced. I speculate that the IFNγ pathway may drive T_{reg} fragility in certain inflammatory environments.

As a high frequency of intratumoral T_{regs} in cancer patients is largely considered a negative prognostic factor [105, 141, 142], identifying approaches to selectively target intratumoral T_{regs} while maintaining peripheral tolerance is critical. Although expression of NRP1 in peripheral, tissue-resident T_{regs} remains unclear, my findings highlight the surprisingly extensive and variable expression of NRP1 on human intratumoral T_{regs} [112, 143, 144, 145]. Importantly, given that my mouse model experiments suggest that NRP1 may not need to be targeted in all human intratumoral T_{regs} to derive a therapeutic effect, it is possible that targeting $NRP1^{+}$ intratumoral T_{regs} with an NRP1 mAb may be therapeutic. As I show that the impact of the IFNγ pathway on human T_{regs} is conserved, it is possible that by blocking NRP1 on T_{regs}, one could induce functional fragility in surrounding T_{regs} to further enhance the therapeutic effect and overall outcome. My

identification of IFNγ as the critical mediator of T_{reg} fragility highlights the potential importance of this mechanism in promoting anti-tumor immunity and provides a pathway to develop immunotherapeutic approaches that could lead to tumor reduction while maintaining peripheral tolerance.

3.5 AUTHOR CONTRIBUTIONS

Conceptualization, A.E.O.D. and D.A.A.V.; Formal Analysis, M.C., D.P.N., Y.S.; Investigation, H.Y., R.E.D., E.A.B., G.S., W.H., G.M.D., T.C.B.; Resources, J.M.M., C.S., J.M.K., R.L.F.; Writing, A.E.O.D. and D.A.A.V. Supervision, J.K.K., T.C.B., C.J.W., D.A.A.V.

4.0 THE ROLE OF T_{REG} FRAGILITY IMMUNOTHERAPEUTIC RESPONSE

Portions of this chapter (4.3) are included within a manuscript published in *Cell* in 2017 while other portions (4.4) are unpublished but are in preparation for submission.

4.1 SUMMARY

In chapter 3, I showed that T_{regs} can lose suppressive function, secrete IFNγ, but maintain Foxp3 expression, a term I refer to as 'T_{reg} fragility'. Indeed, T_{regs} treated with IFNγ were less suppressive; however, whether IFNγ-mediated T_{reg} fragility was required for a productive anti-tumor immune response, especially in the context of immunotherapy, remained unclear. In this chapter, I show that IFNγ-induced T_{reg} fragility is required for response to anti-PD1, and other immunotherapies are less effective in *Ifngr1*$^{L/L}$*Foxp3*$^{Cre\text{-}YFP}$mice. Taken together, these data suggest that cancer therapies promoting T_{reg} fragility may be efficacious.

4.2 INTRODUCTION

IFNγ^{+} T_{regs} have been observed previously in both human and mouse samples [44, 133, 146]. IFNγ^{+} T_{regs} were previously describe in human glioblastoma [146], and were found to be less suppressive and PD1^{Hi}. Interestingly, when patients were treated with anti-PD1, the percentage of IFNγ^{+} T_{regs} increased, suggesting that PD1 blockade could exert efficacy in part by skewing the T_{reg} population. While it has been previously shown that T_{regs} could lose suppressive function and secrete IFNγ while maintaining Foxp3 expression (T_{reg} fragility), the role of this in patient response to immunotherapy remains unclear.

4.3 T_{REG} FRAGILITY IS REQUIRED FOR EFFECTIVE RESPONSE TO ANTI-PD1

While my previous data suggested a prominent role for IFN-γ in driving T_{reg} fragility, the importance for this observation in the broader context of an immunotherapeutic response is unknown. I sought to address this question using mice that lack IFN-γR on T_{regs} (*Ifngr1*$^{L/L}$*Foxp3*$^{Cre\text{-}YFP}$) (Fig. 13A and B). *Ifngr1*$^{L/L}$*Foxp3*$^{Cre\text{-}YFP}$ or *Foxp3*$^{Cre\text{-}YFP}$ mice were injected with 5x10^{5} MC38 (an anti-PD1 sensitive tumor cell line) subcutaneously (SC) and then treated with either anti-PD1 or Armenian Hamster IgG control (200ug) on Days 6, 9 and 12 post-tumor injection. Strikingly, *Ifngr1*$^{L/L}$*Foxp3*$^{Cre\text{-}YFP}$ mice were completely resistant to PD1 blockade in comparison to *Foxp3*$^{Cre\text{-}YFP}$ mice, as exhibited by tumor growth and survival (Fig. 13C and Fig. 14A). Consistent with the loss of IFN-γR expression preventing the development of T_{reg} fragility, no increase in percentage of IFNγ^{+} T_{regs} was observed in *Ifngr1*$^{L/L}$*Foxp3*$^{Cre\text{-}YFP}$ mice in contrast to *Foxp3*$^{Cre\text{-}YFP}$ mice

following anti-PD1 treatment (Fig. 14B). Taken together, these data suggest that IFN-γ-induced T_{reg} fragility is required for an effective response to PD1-targeted immunotherapy.

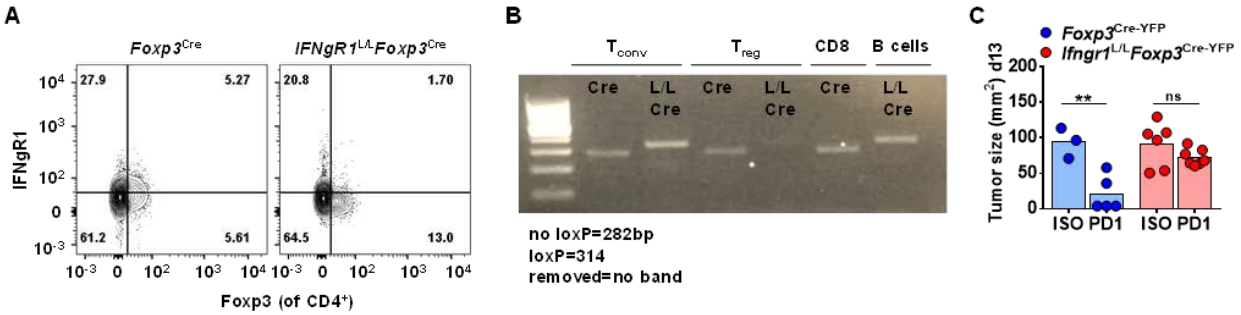

Figure 13: *Ifngr1*$^{L/L}$*Foxp3*$^{Cre\text{-}YFP}$ mice are non-responsive to PD1 blockade.

Ifngr1$^{L/L}$*Foxp3*$^{Cre\text{-}YFP}$ mouse analysis. (**A**) Lymphocytes were isolated from ndLN of *Foxp3*$^{Cre\text{-}YFP}$ or *Ifngr1*$^{L/L}$*Foxp3*$^{Cre\text{-}YFP}$ mice and stained for IFNγR (n=2). (**B**) T_{conv}, T_{regs}, CD8s, or B cells were isolated from LN and spleen of *Foxp3*$^{Cre\text{-}YFP}$ or *Ifngr1*$^{L/L}$*Foxp3*$^{Cre\text{-}YFP}$ mice, DNA was extracted for endpoint PCR testing for the presence or absence of the loxP sites or excision of loxP-targeted sequence (n=2). (**C**) *Foxp3*$^{Cre\text{-}YFP}$ or *Ifngr1*$^{L/L}$*Foxp3*$^{Cre\text{-}YFP}$ mice were injected with MC38 on day 0, sacrificed on day 13 (n=3-6). Data represent 2 experiments. Student unpaired t test was used. (ns, not significant, **p < 0.01).

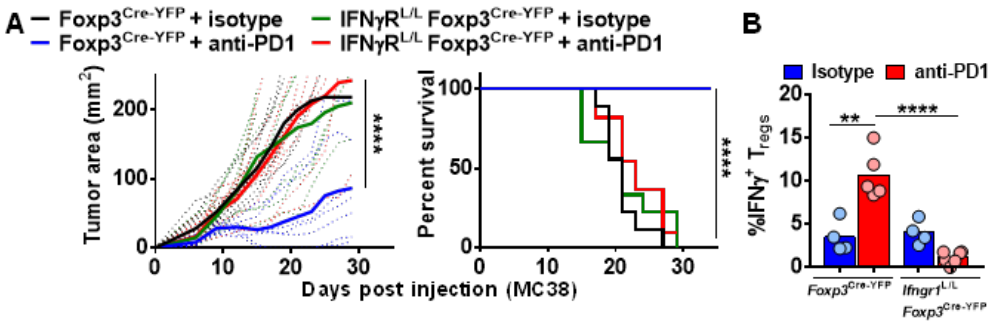

Figure 14: IFNγ-mediated T_{reg} fragility is required for anti-PD1 response.

(**A-B**) Tumor growth curve. *Foxp3*$^{Cre\text{-}YFP}$ and *Ifngr1*$^{L/L}$*Foxp3*$^{Cre\text{-}YFP}$ mice were injected with MC38 SC on day 0 and treated with either anti-PD1 or isotype on days 6, 9, and 12 (200ug, 200ug, 200ug). (**A**) Tumor growth was measured with digital calipers every three days. Mice were removed from study when tumor growth reached a diameter of 2cm in any direction or when necrosis was observed, and survival plots were generated. (**B**) Flow cytometry analysis of T_{regs}. Lymphocytes were isolated from TIL on day 12 from *Foxp3*$^{Cre\text{-}YFP}$ and *Ifngr1*$^{L/L}$*Foxp3*$^{Cre\text{-}YFP}$ mice and were stimulated and stained for IFNγ. Data represent 2 independent experiments with 4-11 mice per experimental group. 2 way ANOVA (Fig. 14A), Kaplan-Meier test (Fig. 14A), and Student unpaired t test (Fig. 14B) were used (**p < 0.01, ***p<0.001, ****p < 0.0001).

4.4 T_{REG} FRAGILITY WITHIN OTHER IMMUNOTHERAPIES

In order to determine whether the contribution of fragile T_{regs} to immunotherapeutic response was limited to anti-PD1, I sought to determine whether this was a conserved event across tumor and treatment types as well as determine whether PD-1 blockade affected T_{reg} function. I used three models to test this. First, I injected C57BL/6 mice with MC38 and treated with a combination of anti-PD1 and anti-LAG3. Similar to mice treated with anti-PD1 alone, *Ifngr1*$^{L/L}$*Foxp3*$^{Cre\text{-}YFP}$ mice were less susceptible to treatment compared to *Foxp3*$^{Cre\text{-}YFP}$ mice (Fig. 15).

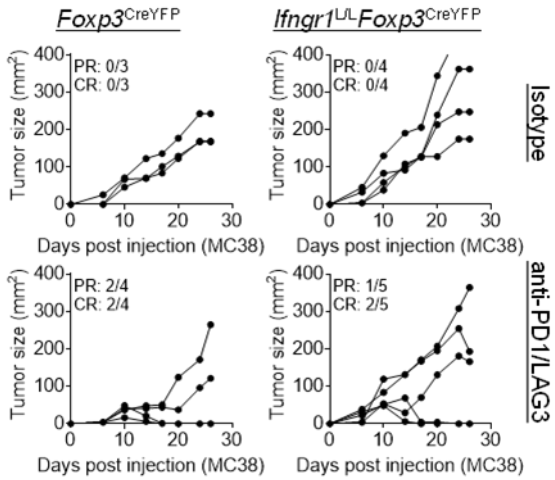

Figure 15: IFNγ induced T_{reg} fragility is required for response to PD1/LAG3 dual blockade.

Tumor growth curve of *Ifngr1*$^{L/L}$*Foxp3*$^{Cre\text{-}YFP}$ and *Foxp3*$^{Cre\text{-}YFP}$ mice that were injected with $5x10^6$ MC38 cells s.c. and treated with antiPD1 and antiLAG3 (200ug i.p. each) on days 6, 9, and 12. Tumors were measured every 3 days with electric calipers. Data represent 2 individual experiments.

To see if this effect would be maintained when other strategies were used, I treated B16 melanoma-bearing mice with the "AIPV" regimen, defined by Darrell Irvine [147]. Briefly, mice were given a high dose of B16 on day 0 ($1x10^6$ cells), and subsequently treated with a tumor specific antibody (anti-Trp1 "A"), mouse serum albumin fused IL-2 ("I"), anti-PD1 ("P"), and an amphiphile vaccine composed of peptide antigens and CpG DNA ("V") weekly for three weeks starting when tumors are 40-60mm^2, followed by "AI" treatment weekly for the remainder of the experiment. *Ifngr1*$^{L/L}$*Foxp3*$^{Cre\text{-}YFP}$ mice were less susceptible to treatment compared to WT; however, the difference was not as great in this model (Fig. 16).

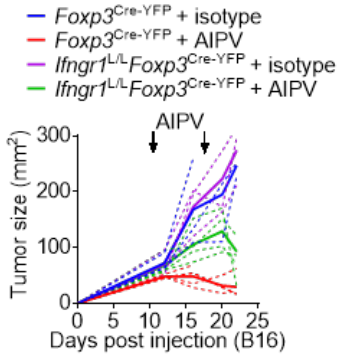

Figure 16: AIPV treatment efficacy is reduced upon deletion of *Ifngr1* in T_{regs}.

Tumor growth curve of *Ifngr1*$^{L/L}$*Foxp3*$^{Cre\text{-}YFP}$ and *Foxp3*$^{Cre\text{-}YFP}$ mice that were injected with $1x10^6$ B16 cells and treated with anti-Trp1 (100ug i.p.), MSA-IL-2 (30ug i.p.), anti-PD1 (200ug i.p.), and an amphiphile vaccine (1.24 nmol amph-CpG and 20ug amph-peptide s.c. at base of the tail) weekly for three weeks starting when tumors were 40-60mm^2, continued with anti-Trp1 and MSA-IL2 treatment weekly for the remainder of the experiment. Tumors were measured every 3 days with electric calipers. Data represent 3 independent experiments.

Two potential reasons for this are that “AIPV” treatment targets a variety of both adaptive and innate immune cells, which could diminish the effects on tumor growth by T_{reg} fragility or that other drivers of T_{reg} fragility are required to see an effect on tumor growth. Whether “AIPV” treatment increases IFNγ secretion by T_{regs} or reduces T_{reg} suppression remains unknown. Lastly, I used a model system where therapy targets the T_{reg} compartment through the use of an agonist anti-GITR antibody. In this system, *Ifngr1*$^{L/L}$*Foxp3*$^{Cre\text{-}YFP}$ mice were again less susceptible to treatment compared to WT; however, how this treatment affects the IFNγR^{-} T_{regs} in this system remains unknown (Fig. 17). Use of anti-GITR has been previously shown to reduce the T_{reg} frequency within the tumor microenvironment as well as reduce Foxp3 expression.

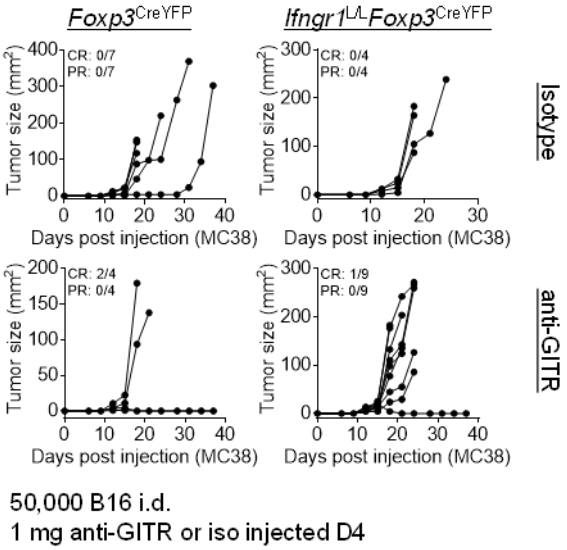

Figure 17: Treatments targeting T_{regs} require fragility for efficacy.

Tumor growth curves of *Ifngr1*$^{L/L}$*Foxp3*$^{Cre\text{-}YFP}$ and *Foxp3*$^{Cre\text{-}YFP}$ mice that were injected with 50,000 B16 cells and treated with anti-GITR (1mg, i.p.) on day 4. Tumors were measured every 3 days with electric calipers. Data represent 2 independent experiments.

To determine if immunotherapeutic treatment affected T_{reg} function in the TME, I performed a microsuppression assay with WT or *Ifngr1*$^{-/-}$ T_{regs} isolated from ndLN and TIL of MC38 tumor-bearing mice treated with anti-PD1. Although subtle, I did observe a trend showing that *Ifngr1*$^{-/-}$ T_{regs} remained more suppressive after PD1 blockade compared to WT T_{regs} from the TIL, while no differences were observed in the ndLN (Fig. 18). However, whether this difference (a) is a direct or indirect effect on T_{regs}, and (b) is exacerbated at later time points or in other immunotherapeutic settings remains to be determined. It would also be of interest to isolate T_{regs} from responders and non-responders to compare function in these two groups.

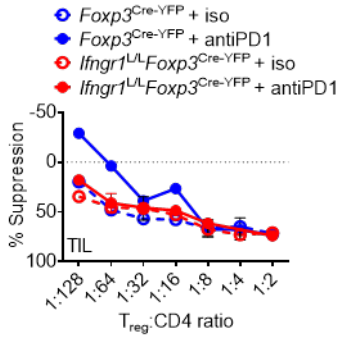

Figure 18: *Ifngr1*$^{-/-}$ T_{regs} maintain suppression after PD1 blockade.

Microsuppression assay after *Ifngr1*$^{L/L}$*Foxp3*$^{Cre\text{-}YFP}$ and *Foxp3*$^{Cre\text{-}YFP}$ mice were treated with anti-PD1 on D6, 9, 12. Tregs were pooled from 3 mice with 5-6 mice per group per experiment. Proliferation was measured and percent suppression was calculated as described in methods.

4.5 DISCUSSION

I have shown that IFNγR expression on intratumoral T_{regs} was required for an effective response to PD1 blockade. Strikingly, *Ifngr1*$^{L/L}$*Foxp3*$^{Cre\text{-}YFP}$ mice which like the IFNγ receptor on T_{regs} were completely resistant to anti-PD1 immunotherapy. Whereas WT T_{regs} showed a significant increase in IFNγ expression after PD1 blockade, *Ifngr1*$^{-/-}$ T_{regs} showed no increase in IFNγ, suggesting that IFNγ-driven T_{reg} fragility may need to be induced for an effective immunotherapeutic response.

Whether T_{reg} fragility is a feature of certain diseases and the extent to which this can be prevented or utilized therapeutically remains largely unknown and highly controversial [64, 69, 71, 73]. Indeed, my data show that the IFNγ response induced by PD1 blockade appears to be sufficient to drive intratumoral T_{reg} fragility despite expression of Nrp1. Loss of IFNγR expression on T_{regs} renders mice completely resistant to anti-PD1 immunotherapy and are partially resistant to other immunotherapies, including AIPV, anti-GITR, and anti-PD1/LAG3. This raises the provocative possibility that an essential component of effective immunotherapy (antibody or vaccine mediated) is to induce sufficient IFNγ in the tumor microenvironment to drive T_{reg} fragility. However, the impact of T_{reg} fragility and IFNγ expression by intratumoral T_{regs} on tumor growth and responsiveness to immunotherapy in murine and human tumors needs to be investigated further. Some underlying questions remain from these experiments: First, is Foxp3 expression reduced in WT or *Ifngr1*$^{-/-}$ T_{regs} after treatment? Second, is suppression differentially affected by various immunotherapies treatment in these two

T_{reg} populations? While *Ifngr1*$^{L/L}$*Foxp3*$^{Cre\text{-}YFP}$ mice are less responsive to all therapies in this chapter, the extent of responsiveness varies considerably, suggesting that different therapies have varying effects on T_{reg} fragility. This could occur due to the cell targeted by the therapy. For example, while anti-GITR targets T_{regs} directly, “AIPV” treatment targets a number of cell populations, both adaptive and innate. Thirdly, are there are other drivers of T_{reg} fragility? Indeed, it is possible that other cytokines may induce T_{reg} fragility in conjunction with IFNγ, as the TME has many secreted molecules that are unique to the tumor.

5.0 T_{REGS} MAINTAIN METABOLIC PLASTICITY AND FUNCTION THROUGH THE NRP1:HIF1A AXIS IN THE TUMOR MICROENVIRONMENT

This project is part of a collaboration between myself and the Delgoffe lab, with contributions from Ashley Menk and Greg Delgoffe. It has been compiled into a manuscript for submission in 2018.

5.1 SUMMARY

Regulatory T cells are required to maintain immune homeostasis and prevent autoimmunity; however, they act as a barrier to anti-tumor immunity and are considered a possible mechanism of resistance to immunotherapy. Therefore, it would be advantageous to uncover tumor T_{reg} specific targets. Neuropilin-1 (Nrp1) is required to maintain intratumoral T_{reg} stability but has no effect on peripheral T_{regs}. The tumor microenvironment is unique and is thought to support T_{regs} metabolically while starving other effector T cell subsets through ravenous glucose uptake and immunosuppressive metabolite secretion. I show that $Nrp1^{-/-}$ T_{regs} reside in areas of lower hypoxia, but maintain Hif1α. As a result of this sustained expression, $Nrp1^{-/-}$ T_{regs} are reliant on glycolysis and are less suppressive in low glucose environments both *in vivo* and *in vitro*. As a result, CD8 T cells from $Nrp1^{L/L}Foxp3^{Cre\text{-}YFP}$ mice are less metabolically

exhausted and contribute to reduced tumor growth or tumor clearance. Lastly, loss of both Nrp1 and Hif1α on T_{regs} leads to partial rescue of tumor growth. Taken together, my data indicate that Nrp1 maintains metabolic fitness and suppressive capacity in tumor-T_{regs} through restraint of Hifα.

5.2 INTRODUCTION

The tumor microenvironment is unique and supports immunosuppressive cells such as T_{regs} through both enhanced recruitment via chemokines and through altered metabolism. Cancer cells perform aerobic glycolysis, also known as the "Warburg effect", where they perform glycolysis even in the presence of oxygen, which is thought to provide them with the constant energy required for their rapid proliferation [148, 149]. Because of this, cancer cells act as a glucose "sink", depriving surrounding glucose-dependent cells, such as T_{eff} cells, of the nutrients they need to thrive in this environment [150, 151]. In addition this, the environment is hypoxic [152], lacks metabolites like glutamine [153], and has a surplus of immunosuppressive metabolites such as lactate [154, 155].

T_{regs} are distinct metabolically compared to other T cell subsets, which allows them to survive and proliferate better within the tumor microenvironment compared to other T cell subsets. Unlike other T cells, T_{regs} primarily utilize oxidative phosphorylation (OXPHOS) rather than glycolysis to fuel their energetic needs [156, 157]. T_{reg} metabolism is directly controlled by Foxp3-mediated suppression of Myc and the glycolysis pathway, thereby developing a metabolic advantage in areas of low glucose. In addition, T_{regs}

preferentially produce pyruvate from L-lactate rather than producing their own lactate, suggesting they may survive better in areas of high lactate, such as the tumor microenvironment. Indeed, the addition of L-lactate to T_{reg} cultures had no effect on their proliferation or function [158]. However, the majority of these studies were done *in vitro* with induced T_{regs} (iT_{regs}), so whether this occurs in the tumor remains unclear. I have previously shown that Nrp1 contributes to T_{reg} stability within the tumor microenvironment and in its absence, T_{regs} express higher levels of hypoxia inducible factor 1α (Hif1α), produce IFNγ, and lose suppressive function through downregulation of Hif1α and prevention of IFNγ secretion [44]. While Hif1α can be upregulated as a consequence of hypoxia, it can also be upregulated in normoxic conditions as a result of Akt activation [128, 159]; indeed, *Nrp1*$^{-/-}$ T_{regs} have increased Akt activity within the TME. However, many questions remain including: a) does Nrp1 restrain Hif1α in the tumor microenvironment? b) Does the downregulation of Hif1α affect T_{reg} metabolism? and c) Is loss of function in *Nrp1*$^{-/-}$ T_{regs} within the tumor microenvironment dependent on Hif1α?

5.3 RESULTS

5.3.1 Nrp1 restrains Hif1α in the TME

Previous studies have highlighted a role for Nrp1 in maintained T_{reg} stability within the tumor microenvironment, and in its absence, tumor-derived T_{regs} secrete IFNγ and contribute to anti-tumor immunity [43, 44]. In addition, Nrp1$^{-/-}$ T_{regs} expressed significantly

more Hif1α, suggesting that IFNγ secretion was controlled through this pathway. I hypothesize that in the absence of Nrp1, Akt activity is increased, leading to higher Hif1α expression and subsequent IFNγ secretion [128, 129]. As Hif1α expression can also be increased as a result of hypoxia, I first asked whether Nrp1$^{-/-}$ were located in areas of higher hypoxia within the tumor microenvironment. Surprisingly, Nrp1$^{-/-}$ were less hypoxic, as visualized by pimonidazole:Hypoxiprobe staining (Fig. 19 A, B), suggesting that Hif1α expression was being driven by an alternate mechanism. Interestingly, I found that Hif1α expression was significantly reduced in tumor-derived T_{regs} in WT mice compared to Nrp1$^{-/-}$ T_{regs} that either maintained or showed an increase in expression within the tumor (Fig. 19 C, D), suggesting that Nrp1 may restrain Hif1α in T_{regs} within the tumor microenvironment, and that in its absence, higher Hif1α leads to increased T_{reg} fragility and IFNγ secretion.

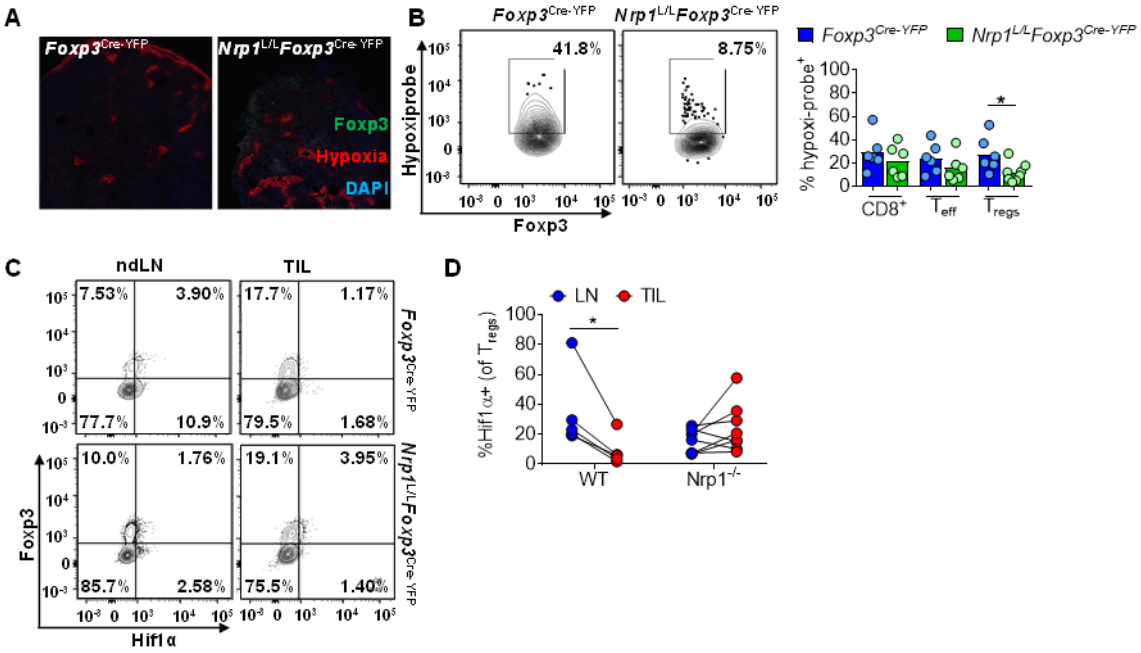

Figure 19: Nrp1$^{-/-}$ T_{regs} are less hypoxic but maintain Hif1α expression in the TME.

(**A**) Hypoxia staining. Tumors were harvested from *Foxp3*$^{Cre\text{-}YFP}$ and *Nrp1*$^{L/L}$*Foxp3*$^{Cre\text{-}YFP}$ mice on day 12, sectioned, and stained for Foxp3, Hypoxia via pimonidazole:Hypoxiprobe, and DAPI. (**B-D**) Flow cytograms of hypoxia and Hif1α. Lymphocytes were harvested from ndLN, dLN, and TIL of *Foxp3*$^{Cre\text{-}YFP}$ and *Nrp1*$^{L/L}$*Foxp3*$^{Cre\text{-}YFP}$ mice on day 12 and stained for hypoxia via pimonidazole:Hypoxiprobe or Hif1α. n=5-8. *p<0.05.

5.3.2 Nrp1$^{-/-}$ Tregs are glycolytic

Given that Hif1α has been previously shown to induce glycolysis through pyruvate dehydrogenase (PDK) activation [160, 161], I sought to determine whether the increase in Hif1α in Nrp1$^{-/-}$ T_{regs} in the tumor made them more glycolytic. While T_{eff} cells are largely dependent on glycolysis, T_{regs} rely primarily on fatty acid oxidation and oxidative phosphorylation. Tumor cells are thought to shift the tumor to an immunosuppressive microenvironment by taking up a majority of the glucose available and producing immunosuppressive metabolites such as lactate, thereby 'starving' T_{eff} and 'feeding' T_{regs} respectively [158, 162]. Therefore, I hypothesized that Nrp1$^{-/-}$ T_{regs} are reliant on glycolysis as a result of Hif1α and are less suppressive in the tumor microenvironment due to the lack of available glucose. Indeed, Nrp1$^{-/-}$ T_{regs} upregulated components of the glycolysis pathway (Fig. 20 A) and were less oxidative, as shown by a decrease in OCR, increase in ECAR (Fig. 20 B, C). In addition, Nrp1$^{-/-}$ appeared more metabolically exhausted as indicated by spare respiratory capacity (SRC) (Fig. 20 D) and had less ATP reserves (Fig. 20 E). To determine whether Nrp1$^{-/-}$ T_{regs} were reliant on glucose and therefore were less suppressive in its absence, I stimulated WT and Nrp1$^{-/-}$ T_{regs} in either high (25mM) or low (~5mM) glucose media for 3 days prior to re-isolating them for a suppression assay. Strikingly, Nrp1$^{-/-}$ T_{regs} were significantly less suppressive after culture in low glucose, while WT T_{regs} maintained function (Fig. 20 F) suggesting functional reliance on glucose. While 5mM glucose is lower than standard culture media, it is still considerably higher than levels found in the TME[163], so studies looking at even lower glucose levels is warranted.

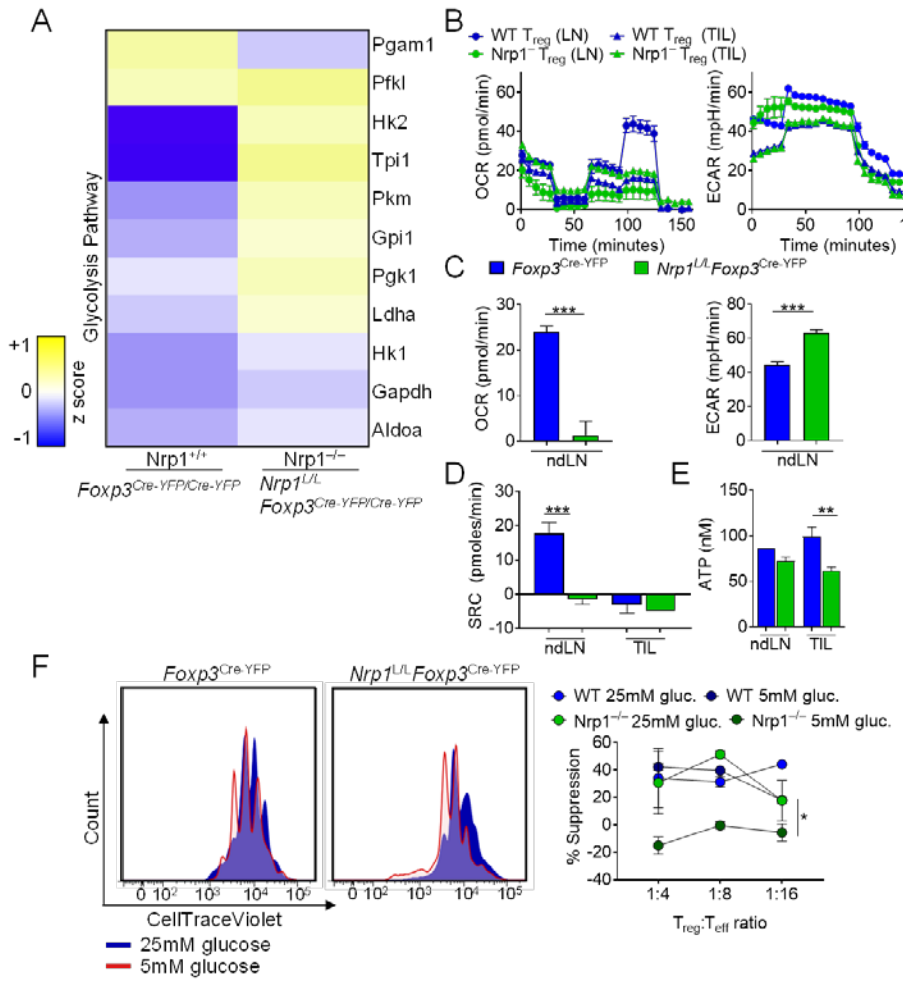

Figure 20: Nrp1$^{-/-}$ T$_{regs}$ are glycolytic.

(**A**) RNASeq analysis. T$_{regs}$ were purified based on CD4^{+}, and GFP or YFP expression from *Foxp3*$^{Cre-YFP/Cre-YFP}$, and *Nrp1*$^{L/L}$*Foxp3*$^{Cre-YFP/Cre-YFP}$ mice on D12, cDNA and libraries were generated using the Clontech SmartER Ultra-Low and Illumina Nextera XT Library Prep kits. Samples were normalized to 2nM and sequenced on a NextSeq500. A number of genes associated with the glycolysis pathway were upregulated in the *Nrp1*$^{-/-}$ samples. Data represent 5 independent experiments with 3-5 mice pooled per experiment. (**B-E**) Metabolic analysis. Lymphocytes were harvested from ndLN and TIL of *Foxp3*$^{Cre-YFP}$ and *Nrp1*$^{L/L}$*Foxp3*$^{Cre-YFP}$ mice on day 12 and used in a (**B-D**) Seahorse assay or an ATP determination assay (**E**). (**F**) Microsuppression assay. Lymphocytes were isolated as above and cultured in stimulating conditions in high or low glucose media for 3 days prior to being used a microsuppression assay. *p<0.05, **p<0.01, ***p<0.001.

Interestingly, Nrp1$^{-/-}$ T_{regs} did not show a significant reduction in mitochondrial mass or function (Fig. 21 A, B); however, both WT and Nrp1$^{-/-}$ T_{regs} showed a reduction in both mass and function over tumor progression, and this correlated with higher PD-1 expression (Fig. 21 C, D).

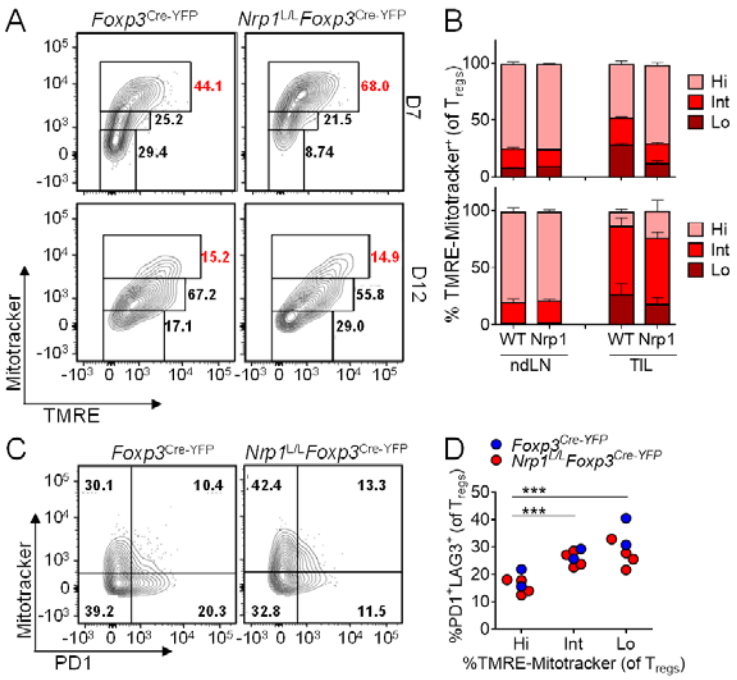

Figure 21: T_{regs} lose mitochondria and upregulate PD-1 in the tumor microenvironment.

Flow cytograms of mitochondrial mass and function in correlation with PD-1. (**A-C**) Lymphocytes were harvested from ndLN, dLN, and TIL of *Foxp3*$^{Cre\text{-}YFP}$ and *Nrp1*$^{L/L}$*Foxp3*$^{Cre\text{-}YFP}$ mice on day 12 and stained for mitotracker and TMRE to determine mitochondrial mass and function as well as PD-1. ***p<0.001.

5.3.3 Nrp1 supports OXPHOS through PGC1α expression

As Nrp1$^{-/-}$ T_{regs} were more glycolytic and less oxidative compared to WT T_{regs}, I asked whether there were also alterations within the OXPHOS pathway. PPAR-gamma coactivator 1 α (PGC1α) supports mitochondrial biogenesis and OXPHOS [164], and has been previously shown to be required for maintained T_{eff} function in the tumor microenvironment [165]. Interestingly, I found that PGC1α was downregulated in Nrp1$^{-/-}$ T_{regs} in comparison to WT T_{regs} within the ndLN but was similarly downregulated in both T_{reg} populations within the tumor microenvironment (Fig. 22 A-C), suggesting that there are Nrp1-driven changes in both the glycolytic and OXPHOS pathways that lead to altered T_{reg} metabolism within the tumor microenvironment. However, in order to determine the direct or indirect role of Nrp1 on PGC1α levels within the TME, one would need to perform genetic deletion experiments, and ideally, utilize a system where one could delete Nrp1 from T_{regs} while simultaneously overexpressing PGC1α.

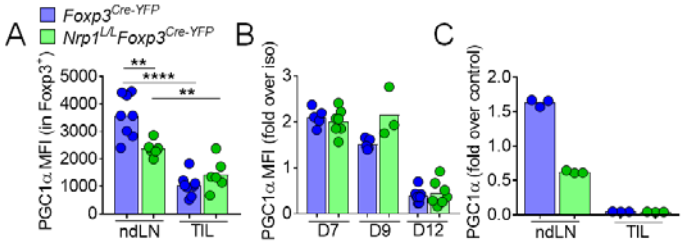

Figure 22: Nrp1 restrains PGC1α.

PGC1α expression levels by flow cytometry and qPCR. (**A-B**) Lymphocytes were harvested from ndLN, dLN, and TIL of *Foxp3*$^{Cre\text{-}YFP}$ and *Nrp1*$^{L/L}$*Foxp3*$^{Cre\text{-}YFP}$ mice on day 12 and stained. (**C**) Lymphocytes were harvested from ndLN, dLN, and TIL of *Foxp3*$^{Cre\text{-}YFP}$ and *Nrp1*$^{L/L}$*Foxp3*$^{Cre\text{-}YFP}$ mice on day 12, RNA was isolated, and qPCR was performed. **p<0.01, ****p<0.0001.

5.3.4 CD8^{+} T cells are more oxidative and less exhausted from *Nrp1*$^{L/L}$*Foxp3*$^{Cre-YFP}$ mice

Given that PGC1α has been shown to be required to prevent exhaustion and maintain function of CD8^{+} T_{eff} in the tumor microenvironment and that *Nrp1*$^{L/L}$*Foxp3*$^{Cre-YFP}$ mice have substantially reduced tumor growth that is dependent on CD8^{+} T cells [44, 165], I sought to determine whether the loss of Nrp1 on T_{regs} and subsequent metabolic deficiency affected intratumoral CD8^{+} T cell metabolic exhaustion. CD8^{+} T cells isolated from *Nrp1*$^{L/L}$*Foxp3*$^{Cre-YFP}$ mice (herein referred to as CD8^{Nrp1}) maintained mitochondrial mass and function within the tumor compared to those from *Foxp3*$^{Cre-YFP}$ mice (herein referred to as CD8^{WT}) (Fig. 23A). In addition, CD8^{Nrp1} T cells were less metabolically exhausted, as shown by higher OXPHOS levels (Fig. 23B).

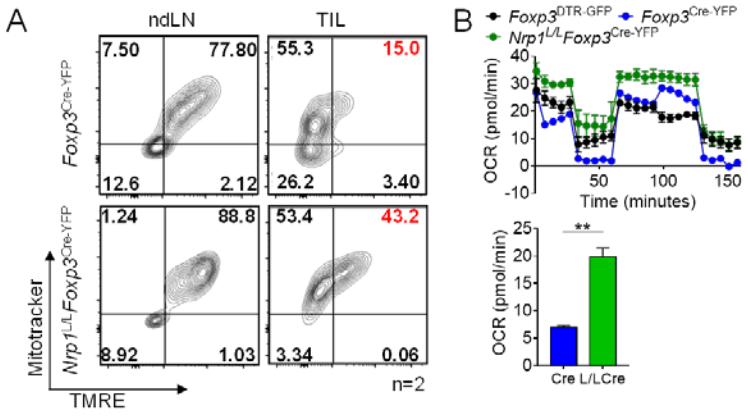

Figure 23: CD8^{+} T cells are less metabolically exhausted in *Nrp1*$^{L/L}$*Foxp3*$^{Cre-YFP}$ mice.

(**A-B**) Lymphocytes were harvested from ndLN and TIL of *Foxp3*$^{Cre-YFP}$ and *Nrp1*$^{L/L}$*Foxp3*$^{Cre-YFP}$ mice on day 12 and (**A**) stained or (**B**) used in a Seahorse assay. **p<0.01.

5.3.5 Hif1α restraint is required for Treg function in the TME

As Hif1α was decreased in WT T_{regs} but not *Nrp1*$^{-/-}$ T_{regs} within the TME, I reasoned that part of the reduction in tumor growth in *Nrp1*$^{L/L}$*Foxp3*$^{Cre\text{-}YFP}$ mice may indeed due to sustained Hif1α expression and subsequent IFNγ production by T_{regs}. In order to test this possibility, I injected *Nrp1*$^{L/L}$*Hif1a*$^{L/L}$*Foxp3*$^{Cre\text{-}YFP}$ mice with B16 to see if tumor growth was affected. *Nrp1*$^{L/L}$*Hif1a*$^{L/L}$*Foxp3*$^{Cre\text{-}YFP}$ mice showed partially restored tumor growth compared to *Nrp1*$^{L/L}$*Foxp3*$^{Cre\text{-}YFP}$ mice ($p<0.05$), suggesting that Nrp1 sustains T_{reg} function and stability in part by restraining Hif1α. However, whether (a) this effect is conserved across tumor types and (b) *Nrp1*$^{-/-}$*Hif1a*$^{-/-}$ T_{regs} are less fragile compared to *Nrp1*$^{-/-}$ T_{regs} remains to be determined.

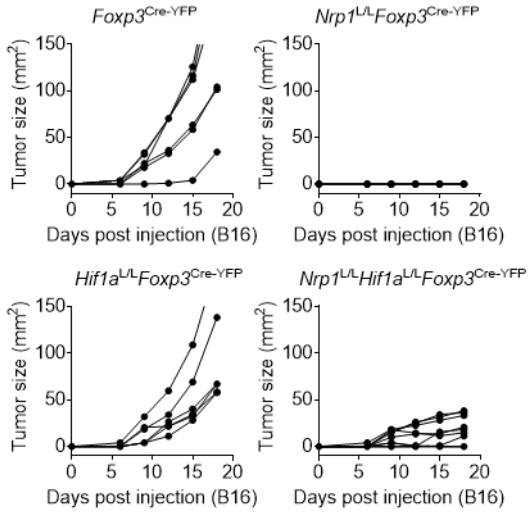

Figure 24: Loss of Nrp1 and Hif1α on T_{regs} partially rescues tumor growth.

Tumor growth curve. *Foxp3*$^{Cre\text{-}YFP}$, *Nrp1*$^{L/L}$*Foxp3*$^{Cre\text{-}YFP}$, *Hif1a*$^{L/L}$*Foxp3*$^{Cre\text{-}YFP}$, and *Nrp1*$^{L/L}$*Hif1a*$^{L/L}$*Foxp3*$^{Cre\text{-}YFP}$ mice were injected with B16 i.d. on day 0 and tumor growth was measured with digital calipers every three days. Mice were removed from study when tumor growth reached a diameter of 2cm in any direction or when necrosis was observed. n=4-10. Two way ANOVA was used.

5.4 DISCUSSION

In summary, my data show the following 5 observations: [i] Nrp1 restrains Hif1α in the tumor microenvironment. It is possible that this occurs to condition T_{regs} to better survive in a hypoxic environment as WT T_{regs} are more hypoxic than *Nrp1*$^{-/-}$ T_{regs}. [ii] *Nrp1*$^{-/-}$ T_{regs} are glycolytic unlike WT T_{regs} that primarily utilize OXPHOS. In addition, *Nrp1*$^{-/-}$ T_{regs} are dependent on glycolysis for function as they are no longer suppressive after culture in low glucose media while WT T_{regs} are not affected. [iii] Nrp1 directs T_{reg} OXPHOS through upregulation of PGC1α. Indeed, PGC1α expression is decreased in *Nrp1*$^{-/-}$ T_{regs} in the ndLN. However, PGC1α levels are similarly low in the TME in both WT and *Nrp1*$^{-/-}$ T_{regs}, suggesting that there could be unknown environmental effects that drive down expression within the TME. [iv] $CD8^+$ T cells are less metabolically exhausted in *Nrp1*$^{L/L}$*Foxp3*$^{Cre\text{-}YFP}$ mice as indicated by maintained mitochondrial mass and function and elevated basal oxidative phosphorylation. [v] *Nrp1*$^{-/-}$ T_{regs} contribute to anti-tumor immunity in part by increased Hif1α expression. Surprisingly, loss of both Nrp1 and Hif1α on T_{regs} led to an increase in tumor growth compared to loss of Nrp1 alone. This suggests that Hif1α restraint by Nrp1 on T_{regs} is required for maximal suppressive function and support of tumor growth; however, more studies are required to determine whether this is sufficient. Indeed, it is possible that other environmental changes are contributing to tumor growth in this system.

Previous studies have suggested that Hif1α binds to Foxp3 and acts as a switch between T_{H17} and T_{reg} development [128]; however, its role in T_{reg} function in the TME

remain unclear. Given that Nrp1 limits Akt activity, I speculate that Nrp1 restrains Hifα expression and sustains T_{reg} function and oxidative metabolism. In the absence of Nrp1 on T_{regs}, Hif1α expression is maintained in the TME, leading to increased IFNγ secretion and glucose dependency. It is possible that current immunotherapy efficacy could be improved by targeting T_{reg} metabolism, specifically limiting them to glycolysis either indirectly through Nrp1 blockade or directly through inhibition of oxidative phosphorylation. However, many questions remain: (1) does Nrp1 directly support OXPHOS within the TME? (2) What factors within in the TME drive down PGC1α in T_{regs}? (3) Are *Nrp1*$^{-/-}$*Hif1a*$^{-/-}$ T_{regs} less fragile than *Nrp1*$^{-/-}$ as determined by T_{reg} IFNγ production and reduced suppression? (4) Would *Nrp1*$^{L/L}$*Hif1a*$^{L/L}$*Ifngr1*$^{L/L}$*Foxp3*$^{Cre\text{-}YFP}$ mice harbor stable T_{regs} and therefore be completely resistant to immunotherapy? While subsequent studies are required, these data highlight the possibility that targeting T_{reg} fragility while skewing their metabolism within the TME may be efficacious in cancer therapies.

6.0 DISCUSSION

Parts of this discussion were derived from a review I have compiled and submitted to *Cancer Immunology Research*.

6.1 INTRODUCTION

T_{regs} function as the master regulators of the immune system, maintaining homeostasis and preventing autoimmunity; however, they also support tumor growth through the suppression of the anti-tumor immune response.

The tumor microenvironment is unique in that it is nutrient-poor, hypoxic, and acidic, making it a taxing environment for T_{eff} that are primarily glycolytic. In contrast to this, T_{regs} rely on oxidative phosphorylation and are thought to have an proliferative and functional advantage within hypoxic, acidic environments [155].

Increased T_{regs} have been observed in a variety of cancer patient peripheral blood and tumors, including non-small cell lung cancer, late stage ovarian cancer, breast cancer, and pancreatic cancer [166, 167]. Many cancer types show a positive correlation between higher T_{reg} percentages and poor prognosis in patients. T_{regs} percentages in the tumor mass increase with severity of stage in ovarian carcinoma patients [37]. In addition, higher T_{reg} percentages correlate with poorer disease-free

survival in germinal center-like diffuse large B-cell lymphoma, follicular lymphoma, and classical Hodgkin's lymphoma [38]. As a result, T_{regs} have been targeted in the clinic, albeit with limited success. Depletion strategies targeting the IL-2 pathway through use of antibodies or other small molecules led to off target effects such as depletion of effector T cells or loss of DC-mediated T cell activation, in addition to incomplete or transient depletion of T_{regs} [40, 41].

CTLA-4 blockade has been identified as a potential T_{reg} target due to high surface expression. Previous studies have shown that CTLA4 antibodies that had FcγR ADCC activity reduced T_{regs} in the TME, and that there was a positive correlation between reduced T_{regs} and CTLA-4 blockade response in bladder cancer patients [168]. It was initially thought that CTLA-4 blockade worked on T_{regs} through either depletion or by reducing suppression [169]; however, effects on both T_{eff} and T_{reg} compartments were required for full anti-tumor function [170]. Indeed, anti-tumor effects were thought to be due to enhanced $CD8^+$ T cell numbers rather than a decrease in T_{regs} within the tumor. Interestingly, blockade led to increased T_{regs} in the periphery; however, this also led to fewer T_{regs} in the tumor by both lack of accumulation and partial depletion due to higher CTLA-4 expression on intratumoral T_{regs} and the presence of FcγR-expressing macrophages. Subsequent studies suggested that CTLA-4 blockade led to increased T_{eff} in both the tumor and periphery [171].

Anti-CCR4 antibody (mogamulizumab; defucosylated to enhance ADCC) is in clinical trials currently and targets T_{regs} through the CCL22:CCR4 mediated recruitment to the tumor and has shown some clinical efficacy [172]. While encouraging, these strategies still show limited efficacy, thereby further highlighting the need to identify new

avenues with which to target T_{reg} function, potentially through destabilization of T_{regs} or by driving T_{reg} fragility specifically within the TME.

T_{reg} stability is defined as sustained Foxp3 expression, hypomethylation at the CNS2 locus, and maintained suppressive function; however, the prevalence and impact of T_{reg} instability remains controversial [45, 64, 71, 72, 73]. In contrast to T_{reg} instability, T_{reg} fragility has recently been defined as retention of Foxp3 expression with loss of suppressive function [44]. Fragile T_{regs} produce IFNγ, and upregulate the IFNγ receptor as well the transcription factor, Tbet. In addition, they have reduced expression of suppressive molecules, such as CD73 and IL-10 and are functionally less suppressive[44].

In this chapter, I will address the following questions: (1) How is T_{reg} stability maintained? (2) How is T_{reg} fragility induced? (3) Is responsiveness to immunotherapy dependent on T_{reg} fragility?

6.1.1 Building up: how is T_{reg} stability maintained?

T_{reg} stability has been discussed across many disease types in the past decade. T_{reg} instability was initially defined as loss of Foxp3 expression in cells and subsequent loss of suppressive function. This is thought to be in part due to lack of demethylation or remethylation at certain sites within the *Foxp3* locus [123]. Demethylation in this locus was first described in 2007 when a region in the 5' UTR of the *Foxp3* locus containing a number of conserved demethylated CpG motifs, was identified (known as the TSDR/CNS2) [45]. The demethylation pattern is observed in both thymic and mature peripheral T_{regs} in mice and peripheral blood of humans. In contrast, the *CNS2* is largely

methylated in effector $CD4^+$ T cells. Hypomethylation of the *Foxp3* locus is required for T_{reg} stability, but occurs independently of Foxp3 upregulation. Rather, hypomethylation is required for Foxp3 upregulation, and thus suppressive function and cell stability [48]. Interestingly, it has been shown that TGFβ-induced T_{regs} (iT_{regs}) display a somewhat hypermethylated *Foxp3* locus [48]; however, whether $Foxp3^+$ T_{regs} with a methylated *Foxp3* locus exist *in vivo* in sites of disease remains unclear. Indeed, IL-6 has been shown to lead to the remethylation of the *CNS2 in vitro* in a STAT3-dependent manner and also leads to reduced susceptibility of T_{conv} cells to T_{reg} suppression [173]. The possibility that there are other factors that lead to the remethylation of the locus in the TME warrants further investigation.

In addition to epigenetic alterations of the *Foxp3* locus, loss of Foxp3 expression is a hallmark of unstable T_{regs}. There are a number of factors involved in maintaining Foxp3 expression, including IL-2/STAT5 and Foxo1/3a. STAT5 binds to the *Foxp3* locus and in its absence T_{reg} development is reduced [77], while Foxo1 and Foxo3a translocate to the nucleus of T_{regs} and prevent effector functions [80]. Induction of Foxp3 and subsequent T_{reg} development can also be prevented by persistent TCR stimulation leading to constitutive activation of the PI3K/Akt/mTOR pathway [174], or in the absence of the microRNA processing enzyme, Dicer [175].

Loss of Foxp3 expression has also been reported in certain disease settings such as lymphopenia and autoimmune diabetes [71]. In these systems, fate-mapping mice were used to trace all cells that currently or previously expressed Foxp3, regardless of subsequent downregulation. In both cases, ex-$Foxp3^+$ cells, or 'exT_{regs}' upregulated IL7R, secreted IFNγ and IL17, took on a pathogenic role and worsened

disease [73]. Other groups have reported that Foxp3 expression is stable and that previously identified exT_{regs} were likely T cells that transiently upregulated Foxp3 during differentiation or activation [64, 74]. Indeed, very few exT_{regs} have been observed in mouse models of cancer [44], suggesting Foxp3 is largely stable in these models. Other studies have highlighted a role for Helios in maintaining Foxp3 expression and showed that in its absence, Foxp3 was reduced and Helios-deficient T_{regs} secreted IFNγ in the TME [176, 177]. However, whether unstable T_{regs} exist in patients is unknown and remains difficult to assess without cell lineage tracing capabilities.

6.1.2 Breaking down: how is T_{reg} fragility induced?

Multiple factors have been reported previously to be important for preventing T_{reg} fragility, including Nrp1, Foxo1 and Eos [43, 44] While Nrp1 can be expressed on a number of cell types, it is highly upregulated on T_{regs} and supports T_{reg} function through binding of Semaphorin-4a (Sema4a). Upon Sema4a:Nrp1 ligation, PTEN is recruited to the immunological synapse and limits Akt activity, thus increasing translocation of Foxo1/3a to the nucleus. Given that Foxo1 represses *Tbx21*, it is possible that the lack of Nrp1 and prevention of Foxo translocation leads to higher *Tbx21* (Tbet) and subsequent IFNγ secretion [81, 82, 178]. In the absence of Nrp1 signaling, either through Nrp1 blockade or genetic deletion (using *Nrp1*$^{L/L}$*Foxp3*$^{Cre\text{-}YFP}$ mice), intratumoral T_{regs} show reduced cell survival, reduced expression of suppressive markers (such as CD73, IL-10 and IL35), and significantly impaired suppressive function. Surprisingly this did not result in loss of Foxp3 expression. As a result, *Nrp1*$^{L/L}$*Foxp3*$^{Cre\text{-}YFP}$ mice cleared tumors similarly to mice lacking T_{regs}; however, the mice displayed no signs of autoimmunity. Nrp1^{+} T_{regs} are also

increased in metastatic melanoma and head and neck squamous cell carcinoma patients compared to healthy donors [44]. Furthermore, patients with a larger population of Nrp1^{+} T_{regs} correlated with reduced disease-free survival in comparison to those with a smaller population. It was later shown that Nrp1^{-} T_{regs} produced IFNγ and were less suppressive than WT T_{regs}, but maintained *Foxp3* expression. Secretion of IFNγ only occurred within the tumor microenvironment, likely as a result of sustained or increased Hif1a expression due to hypoxia and heightened Akt activity [43, 44, 128, 129]. Indeed, it is possible that the unique environment within tumors (hypoxic, acidic, nutrient poor) contributes to T_{reg} fragility and may underlie the preferential restriction of fragility to the tumor microenvironment.

Previous reports have shown that while Foxo1 is key for Foxp3 upregulation during T_{reg} development, the loss or mutation of Foxo1 from mature T_{regs} leads to a fragile phenotype rather than an unstable one. Specifically, Foxo1-deficient T_{regs} are less suppressive and secrete IFNγ; however, Foxp3 expression is maintained and in fact, the percentage of T_{regs} increases *in vivo*. Furthermore, Foxo1 deletion in T_{regs} leads to a lethal inflammatory phenotype that is dependent on IFNγ [81]. However, unlike the phenotype observed in the absence of Nrp1, wherein fragility appears to be restricted to the tumor microenvironment [43, 44] the loss of Foxo results in a fragile phenotype that is systemic, which leads to the inflammatory phenotype. Similarly, Eos is highly upregulated in T_{regs}, and when removed, Treg suppression is reduced, IFNγ and IL-2 are upregulated, but Foxp3 expression remains unchanged [84]. Interestingly, it has been reported that when LAG3 is deleted on T_{regs}, Eos is increased and leads to better suppressive function in an autoimmune diabetes setting [179]. Indeed, it is possible that

LAG3 limits Eos expression in T_{regs}, thereby promoting fragility; however, further studies are required.

6.1.3 Is response to immunotherapy dependent on T_{reg} fragility?

Intratumoral T_{regs} display a distinct profile, suggesting that there may be specific markers that one could target within the TME that might lead to T_{reg} instability (dysfunction and loss of Foxp3 expression) or T_{reg} fragility (dysfunction while maintaining Foxp3 expression). However, whether this (a) is observed in cancer patient intratumoral T_{regs} and (b) predicts patient responsiveness, remains unknown. I hypothesize that T_{regs} within the TME upregulate stabilizing molecules, such as NRP1, and that patients who respond to immunotherapy show a more fragile intratumoral T_{reg} phenotype.

T_{reg} fragility appears to be required for response to anti-PD1 in murine tumor models. In an adenocarcinoma mouse model (MC38) that is sensitive to PD-1 blockade, treatment of WT mice with anti-PD1 led to the upregulation of IFNγ$^+$ T_{regs}, consistent with an increased fragile phenotype. Strikingly, when T_{regs} were insensitive to IFNγ (through the use of an *Ifngr1*$^{L/L}$*Foxp3*$^{Cre\text{-}YFP}$ mouse), mice were completely resistant to PD-1 blockade in comparison to ~40% response in WT mice [44], suggesting a role of T_{reg} fragility in responsiveness to immunotherapy. Similarly, reduction of tumor burden through the use of a GITR agonist antibody (DTA-1) is due to an increase in IFNγ$^+$ T_{regs} and reduction in Helios expression [176, 180]. As mentioned, CD8:T_{reg} ratios have been shown to be indicative of patient response to therapy; however, the idea that T_{reg} fragility

is the key component to determining response to immunotherapy was previously unappreciated.

Similarly, previous studies have identified IFNγ^{+} T_{regs} in human samples in autoimmune diseases, such as multiple sclerosis and type 1 diabetes, where these cells have reduced suppression and altered methylation while maintaining Foxp3 expression, suggesting a fragile phenotype [48, 133, 181]. In addition, patients with malignant glioma (GBM) exhibit a higher percentage of circulating PD-1^{Hi} T_{regs} that are less suppressive and also express IFNγ. PD-1^{Hi} T_{regs} bear a distinct transcriptional profile, are phenotypically exhausted as defined by upregulation of LAG3 and Tim3, and show a minor reduction in CNS2 demethylation. Interestingly, when GBM patients were treated with anti-PD1 (Nivolumab), the exhausted PD-1^{+} IFNγ^{+} T_{reg} population increased [146]. This population has been observed in other tumor types, such as late advanced rectal cancer (LARC), where it correlated with poorer patient response [36].These data suggest that PD-1 blockade as well as other immunotherapies may act in part through inducing a fragile T_{reg} phenotype in patients. Whether this is a direct effect of anti-PD1 on T_{regs} or and indirect effect of increased IFNγ in the TME acting on T_{regs} to drive fragility remains to be determined.

Given that the impact of T_{reg} fragility in immunotherapy has not been fully elucidated in clinic, assessing the extent to which patient T_{regs} develop a fragile phenotype following immunotherapy could aid in both prediction of patient susceptibility to anti-PD1 as well as providing a rationale for patient responsiveness to immunotherapy. Sensitizing T_{regs} to become fragile may be an effective strategy to utilize alongside PD-1 blockade. While PD-1 blockade has been shown to upregulate

IFNγ in $CD8^+$ T cells, whether this directly affects T_{regs} remains unclear in the clinic. However, IFNγ-sensitive T_{regs} have been observed in patient samples, and were found to be less suppressive following IFNγ treatment [44]. While PD-1 blockade has been the primary focus thus far, it is certainly possible that T_{reg} fragility plays a key role in responsiveness to other immunotherapies currently in the clinic or perhaps the efficacy or any immunotherapy. One possibility would be to target a known driver of T_{reg} fragility prevention, such as Nrp1. I would argue that inducing T_{reg} fragility may be a preferred therapeutic strategy compared to T_{reg} depletion or destabilizing T_{regs} because the effect on T_{regs} seems to be restricted to the TME, thereby preventing autoimmune effects.

Identifying a way to target T_{reg} fragility while leaving T_{reg} stability intact may be critical, given the previously identified pathogenic nature of unstable T_{regs} or exT_{regs} in various diseases [71, 72, 73]. It is possible that local T_{reg} destabilization strategies may be efficacious; however, the potential systemic autoimmune effects of this are unknown. Furthermore, distinguishing between these two T_{reg} subsets can be challenging—while there are some clear markers of fragile T_{regs}, including Nrp1, PD-1 and IFNγR1, specific markers do not exist for unstable T_{regs}, that are often indistinguishable from Th-like cells. Furthermore, there may be more unappreciated markers of T_{reg} fragility. In addition, tracking the presence of exT_{regs} in patient samples is not feasible currently.

While I feel that targeting molecules that prevent T_{reg} fragility in the clinic represents the clearest step forward, many interrelated questions remain: (1) What are the markers of unstable or exT_{regs} in patients? (2) Are there other drivers of T_{reg} fragility? While IFNγ has been shown to drive T_{reg} fragility, it is possible that other cytokines or soluble factors could lead to a similar phenotype. (3) Do fragile T_{regs} display

hypermethylation at the *Foxp3 CNS2* locus, and does this lead to reduced suppressive function? While previous studies have suggested that hypomethylation is required for sustained *Foxp3* expression, our direct *ex vivo* methylation analysis (**Appendix B**) suggest that this is dispensable in the tumor microenvironment. (4) What is the level of T_{reg} fragility and instability in checkpoint blockade responders and non-responders, and do they correlate? (5) Is T_{reg} fragility a biomarker of patient response? and (6) Does patient response to immunotherapy depend on T_{reg} fragility? Indeed, while loss of Nrp1 and increased IFNγ sensitivity have been identified as drivers of T_{reg} fragility, there may be other molecules that contribute to this phenotype that have yet to be defined. I propose that the development of combinatorial immunotherapies that maximize T_{reg} fragility may maximize efficacy and improve patient response to immunotherapy.

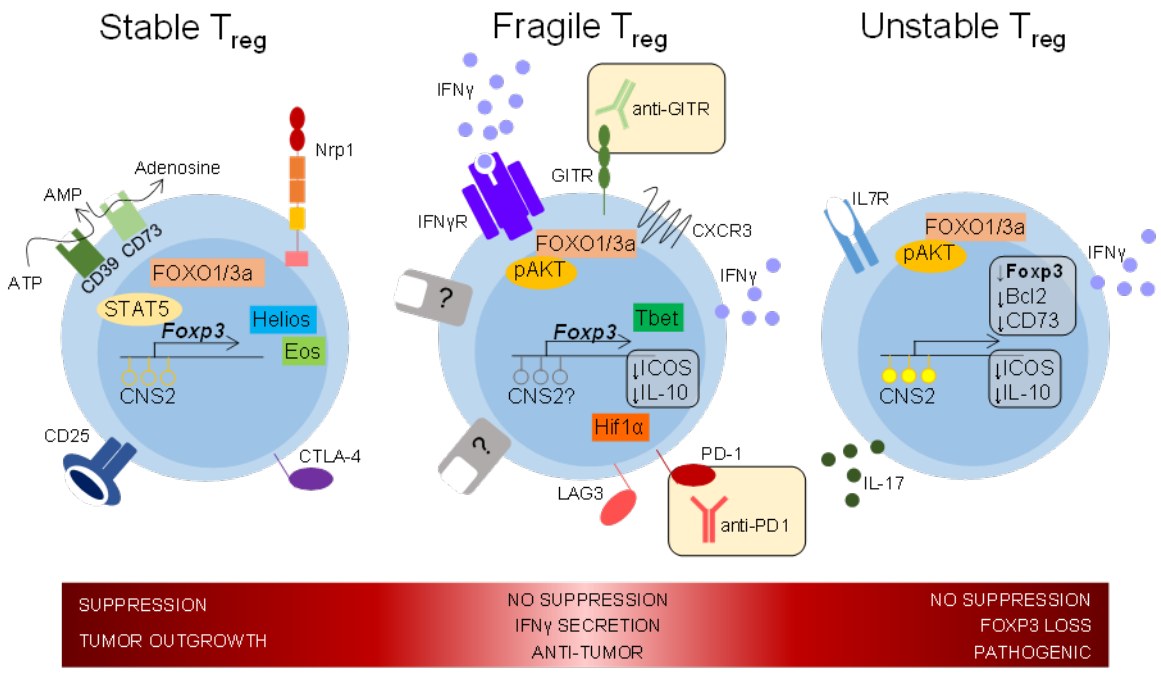

Figure 25: Schematic highlighting key distinctions between stable, fragile, and unstable T_{regs}

APPENDIX A

Stability and function of regulatory T cells is maintained by a neuropilin-1-semaphorin-4a axis

This is a collaborative project with many previous lab members and was published in *Nature* in 2013. I will introduce the primary observations with their permission as well as show data I generated in this appendix.

Neuropilin-1 (Nrp1) is a surface receptor expressed by many cells types; however, it is highly upregulated on T_{regs} and has been previously shown to bind to Semaphorin 3a and VEGF[49, 182]. Dr. Creg Workman performed a microarray on stimulated T_{regs} and compared this transcriptome to T_{conv} transcripts to identify possible molecules provided by T_{conv} cells that boost T_{reg} function. Sema4a was identified in this screen, and the lab reasoned that this may bind Nrp1 on T_{regs} and contribute to their function. In order to test this, the lab bred and used *Nrp1*$^{L/L}$*Foxp3*$^{Cre\text{-}YFP}$ mice in which Nrp1 is selectively removed on T_{regs} but remains intact in all other cells. Interestingly, *Nrp1*$^{L/L}$*Foxp3*$^{Cre\text{-}YFP}$ mice showed no autoimmune effects past one year of age, suggesting that Nrp1 is not required to maintain homeostatic T_{reg} function. To test how Nrp1 may affect T_{regs} under inflammatory conditions, Drs. Greg Delgoffe and Meghan

Turnis injected *Nrp1*$^{L/L}$*Foxp3*$^{Cre\text{-}YFP}$, *Foxp3*$^{Cre\text{-}YFP}$, and *Foxp3*$^{DTR\text{-}GFP}$ (in which T_{regs} are deleted upon diphtheria toxin administration) mice with a variety of transplantable tumor types, including B16 melanoma, MC38 adenocarcinoma, and EL4 thymoma. These tumor types were chosen because they are well characterized and have varying levels of aggressiveness and immunogenicity. While *Foxp3*$^{DTR\text{-}GFP}$ mice are resistant to tumor growth, the mice ultimately succumb to autoimmune effects shortly thereafter. In contrast, *Nrp1*$^{L/L}$*Foxp3*$^{Cre\text{-}YFP}$ mice show equal tumor resistance without any autoimmunity (Fig. 26 A-C). Similarly, C57BL/6 mice treated with Sema4a antibody, Nrp1 antibody (does not block Nrp1:VEGF), or Sema4a-IgG1 (soluble antagonist), showed reduced tumor growth (Fig. 26 D-F).

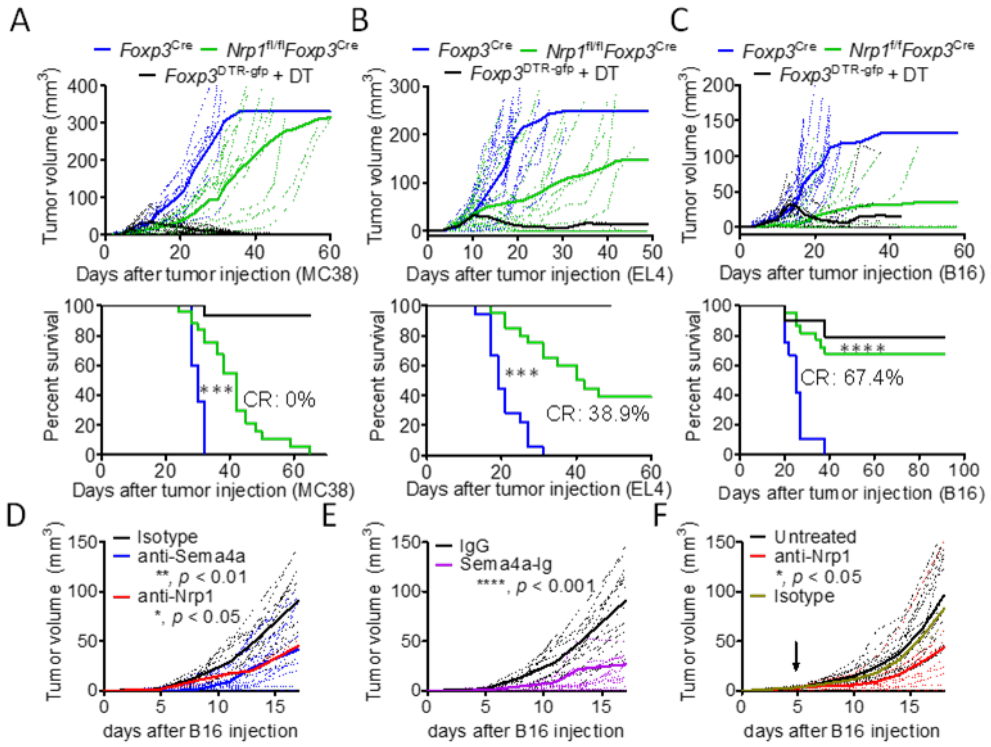

Figure 26: Nrp1-deficient Treg cells fail to suppress anti-tumor immune responses

Tumor growth curves and survival plots. (**A**) *Foxp3*^{Cre}, *Nrp1*$^{f/f}$*Foxp3*^{Cre}, or *Foxp3*$^{DTR\text{-}GFP}$ mice received 1.25×10^5 MC38 melanoma cells subcutaneously and (for *Foxp3*$^{DTR\text{-}GFP}$) 100 µg diphtheria toxin (DT) intraperitoneally, twice weekly. (**B**) As in (**A**), but mice received 1.25×10^5 EL4 thymoma i.d. (**C**) As in (**A**), but mice received 1.25×10^5B16 melanoma i.d. (**D**) Tumor growth curve of C57/BL6 mice receiving 1.25×10^5B16 melanoma i.d. concomitant with injections of isotype control, anti-Sema4a, or anti-Nrp1 (100 µg) twice weekly. (**E**) Tumor growth curve as in (**D**) except mice received Sema4a-IgG1 twice weekly. (**F**) Tumor growth curve of C57/BL6 mice receiving 1.25×10^5 B16 melanoma intradermally. When tumors were palpable (day 5, indicated by arrow), mice began receiving injections of anti-Nrp1 or its isotype control (400 µg initially, 200 µg every 3 days). Results represent 3-5 experiments. *$p < 0.05$, **$p < 0.01$, ***$p < 0.001$. One-way analysis of variance (ANOVA) was used. CR, complete response. Error bars indicate s.e.m

Dr. Greg Delgoffe then took a variety of approaches to determine the signaling pathway downstream of Nrp1:Sema4a ligation. The Akt/mTOR pathway has previously been shown to be critical for T_{reg} function (through restraining Akt signaling) and Nrp1 has been shown to modulate Akt activity. He further showed that pAKT was reduced upon Nrp1:Sema4a ligation in T_{regs} in a PTEN dependent manner. Given that Akt acts in part by preventing Foxo1/3a translocation to the nucleus, I sought to determine if this was the acting mechanism by which Nrp1 maintains Foxp3 stability. Indeed, Foxo1/3a nuclear translocation supports Foxp3 stability. Dr. Cliff Guy and myself found that Nrp1:Sema4a ligation supported Foxo1/3a nuclear translocation, as this was reduced in T_{regs} stimulated overnight in the absence of Sema4a and was rescued with the cells were stimulated with plate-bound Sema4a-IgG1 (Fig. 27 A-B).

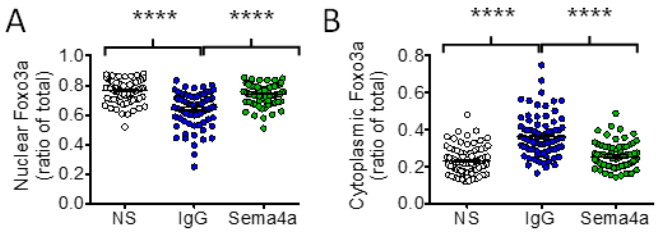

Figure 27: Ligation of Nrp1 by Sema4a promotes Treg-cell stability through modulation of Akt-mTOR signaling

Foxo3a nuclear (**A**) and cytoplasmic (**B**) localization signals, as defined by masking using actin and DNA staining. Arbitrary Units represent fluorescence intensity calculated volumetrically through 20 to 30 slices of T_{reg} cells. n = 70–93. US, unstimulated (control). Results represent at least three independent experiments. ****$p < 0.0001$. Student's unpaired t-test was used. Error bars indicate s.e.m.

APPENDIX B

Nrp1 supports T_{reg} hypomethylation in the tumor microenvironment

Foxp3 expression is the key characteristic of a stable T_{reg}. While there are many factors that contribute to Foxp3 stability, lack of methylation at the locus is considered the primary one. Initially described as the T_{reg} specific demethylated region (TSDR, later renamed the conserved non-coding sequence or CNS2), this locus consists of two regions: one upstream of the Foxp3 promoter and one in intron 7. $CD4^+$ T_{conv} show almost 100% methylation at these sites while T_{regs} show dramatically reduced methylation in the Foxp3 promoter region while they maintain methylation in intron 7, suggesting that this hypomethylation pattern is specific rather than global or random [45]. In addition, T_{reg} development requires both Foxp3 and hypomethylation at the promoter [48], and T_{reg} stability is lost in the absence of the CNS2 locus [183]. In order to determine whether Nrp1 was contributing to T_{reg} stability through epigenetic regulation, I performed bisulfite sequencing on T_{regs} and T_{conv} isolated from ndLN and TIL of *Foxp3*$^{Cre\text{-}YFP}$ and *Nrp1*$^{L/L}$*Foxp3*$^{Cre\text{-}YFP}$ mice. I hypothesized that $Nrp1^-$ T_{regs} would remain hypomethylation at the Foxp3 locus given that Foxp3 expression is not decreased in these cells, either by percentage or a per cell basis (MFI). Surprisingly, $Nrp1^{-/-}$ T_{regs} showed a striking

increase in methylation in the Foxp3 promoter locus compared to WT T_{regs} within the tumor, while both WT and Nrp1$^{-/-}$ T_{regs} remained hypomethylated in the ndLN (**Fig. 27**).

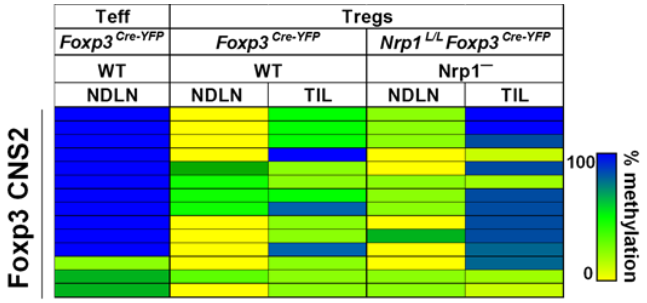

Figure 28: Nrp1-deficient T_{regs} are hypermethylated in the TME.

Methylation Analysis on ndLN T_{eff} and ndLN and TIL T_{regs} after bisulfite sequencing was performed on day 12 post B16 tumor inoculation.

There are two possibilities for this phenotype: 1) Nrp1$^{-/-}$ T_{regs} never become demethylated, possibly because of a reduction in TET proteins, or 2) Nrp1$^{-/-}$ T_{regs} become re-methylated due to changes in methyltransferases such as DNMT3a/b. TET proteins convert 5-methylcytosine to 5-hydroxymethylcytosine and are required for demethylation at the CNS2. When TET2/3 are removed from CD4^{+} T cells in mice through the use of a *TET2/3*$^{L/L}$*CD4*^{Cre} mouse, Foxp3 expression is reduced in the periphery, and TET2/3 DKO T_{regs} were unable to rescue RAG$^{-/-}$ mice, suggesting a role for TET proteins in maintaining T_{reg} stability [68, 184]. In addition, T_{reg} stability is maintained by downregulation of DNA methyltransferases (DNMTs) [66, 173]. While more studies are required to determine the cause of hypermethylation at the Foxp3 promoter while maintaining Foxp3 expression, I hypothesize that modifications in DNMTs within the

tumor microenvironment lead to *de novo* re-methylation of the Foxp3 locus in the absence of Nrp1. Interestingly, reduction of DNMTs via 5-azacytidine treatment led to increased Nrp1 expression on pDCs, suggesting a relationship between methylation status and Nrp1-driven T_{reg} stability; however, additional experiments dilineating expression of TETs and DNMTs are required to draw conclusions.

REFERENCES

1. Surveillance, Epidemiology, and End Results Program. [cited 2018]Available from: http://seer.cancer.gov

2. Hanahan D, Weinberg RA. Hallmarks of cancer: the next generation. *Cell* 2011, **144**(5)**:** 646-674.

3. Hanahan D, Weinberg RA. The hallmarks of cancer. *Cell* 2000, **100**(1)**:** 57-70.

4. Dunn GP, Old LJ, Schreiber RD. The three Es of cancer immunoediting. *Annual review of immunology* 2004, **22:** 329-360.

5. Hodge-Dufour J, Noble PW, Horton MR, Bao C, Wysoka M, Burdick MD*, et al.* Induction of IL-12 and chemokines by hyaluronan requires adhesion-dependent priming of resident but not elicited macrophages. *Journal of immunology* 1997, **159**(5)**:** 2492-2500.

6. Kaplan DH, Shankaran V, Dighe AS, Stockert E, Aguet M, Old LJ*, et al.* Demonstration of an interferon gamma-dependent tumor surveillance system in immunocompetent mice. *Proceedings of the National Academy of Sciences of the United States of America* 1998, **95**(13)**:** 7556-7561.

7. Shankaran V, Ikeda H, Bruce AT, White JM, Swanson PE, Old LJ*, et al.* IFNgamma and lymphocytes prevent primary tumour development and shape tumour immunogenicity. *Nature* 2001, **410**(6832)**:** 1107-1111.

8. Loeb LA, Loeb KR, Anderson JP. Multiple mutations and cancer. *Proceedings of the National Academy of Sciences of the United States of America* 2003, **100**(3)**:** 776-781.

9. Coley WB. II. Contribution to the Knowledge of Sarcoma. *Annals of surgery* 1891, **14**(3)**:** 199-220.

10. Hanna MG, Jr., Peters LC. Specific immunotherapy of established visceral micrometastases by BCG-tumor cell vaccine alone or as an adjunct to surgery. *Cancer* 1978, **42**(6)**:** 2613-2625.

11. Drake R. Prostate cancer. Novel technique for early detection of lymph node metastases. *Nature reviews Urology* 2010, **7**(9)**:** 475.

12. van den Eertwegh AJ, Versluis J, van den Berg HP, Santegoets SJ, van Moorselaar RJ, van der Sluis TM*, et al.* Combined immunotherapy with granulocyte-macrophage colony-stimulating factor-transduced allogeneic prostate cancer cells and ipilimumab in patients with metastatic castration-resistant prostate cancer: a phase 1 dose-escalation trial. *The Lancet Oncology* 2012, **13**(5)**:** 509-517.

13. Le DT, Wang-Gillam A, Picozzi V, Greten TF, Crocenzi T, Springett G*, et al.* Safety and survival with GVAX pancreas prime and Listeria Monocytogenes-expressing mesothelin (CRS-207) boost vaccines for metastatic pancreatic cancer. *Journal of clinical oncology : official journal of the American Society of Clinical Oncology* 2015, **33**(12)**:** 1325-1333.

14. Dranoff G. GM-CSF-secreting melanoma vaccines. *Oncogene* 2003, **22**(20)**:** 3188-3192.

15. Disis ML, Schiffman K, Guthrie K, Salazar LG, Knutson KL, Goodell V*, et al.* Effect of dose on immune response in patients vaccinated with an her-2/neu intracellular domain protein--based vaccine. *Journal of clinical oncology : official journal of the American Society of Clinical Oncology* 2004, **22**(10)**:** 1916-1925.

16. Palucka AK, Ueno H, Connolly J, Kerneis-Norvell F, Blanck JP, Johnston DA*, et al.* Dendritic cells loaded with killed allogeneic melanoma cells can induce objective clinical responses and MART-1 specific CD8+ T-cell immunity. *Journal of immunotherapy* 2006, **29**(5)**:** 545-557.

17. Rosenberg SA, Restifo NP, Yang JC, Morgan RA, Dudley ME. Adoptive cell transfer: a clinical path to effective cancer immunotherapy. *Nature reviews Cancer* 2008, **8**(4)**:** 299-308.

18. Porter DL, Levine BL, Kalos M, Bagg A, June CH. Chimeric antigen receptor-modified T cells in chronic lymphoid leukemia. *The New England journal of medicine* 2011, **365**(8)**:** 725-733.

19. Porter DL, Hwang WT, Frey NV, Lacey SF, Shaw PA, Loren AW*, et al.* Chimeric antigen receptor T cells persist and induce sustained remissions in relapsed refractory chronic lymphocytic leukemia. *Science translational medicine* 2015, **7**(303)**:** 303ra139.

20. Leach DR, Krummel MF, Allison JP. Enhancement of antitumor immunity by CTLA-4 blockade. *Science* 1996, **271**(5256)**:** 1734-1736.

21. Hodi FS, O'Day SJ, McDermott DF, Weber RW, Sosman JA, Haanen JB*, et al.* Improved survival with ipilimumab in patients with metastatic melanoma. *The New England journal of medicine* 2010, **363**(8)**:** 711-723.

22. Topalian SL, Hodi FS, Brahmer JR, Gettinger SN, Smith DC, McDermott DF*, et al.* Safety, activity, and immune correlates of anti-PD-1 antibody in cancer. *The New England journal of medicine* 2012, **366**(26)**:** 2443-2454.

23. Hamid O, Robert C, Daud A, Hodi FS, Hwu WJ, Kefford R*, et al.* Safety and tumor responses with lambrolizumab (anti-PD-1) in melanoma. *The New England journal of medicine* 2013, **369**(2)**:** 134-144.

24. Robert C, Long GV, Brady B, Dutriaux C, Maio M, Mortier L*, et al.* Nivolumab in previously untreated melanoma without BRAF mutation. *The New England journal of medicine* 2015, **372**(4)**:** 320-330.

25. Liu C, Workman CJ, Vignali DA. Targeting regulatory T cells in tumors. *The FEBS journal* 2016, **283**(14)**:** 2731-2748.

26. Kuniyasu Y, Takahashi T, Itoh M, Shimizu J, Toda G, Sakaguchi S. Naturally anergic and suppressive CD25(+)CD4(+) T cells as a functionally and phenotypically distinct immunoregulatory T cell subpopulation. *International immunology* 2000, **12**(8)**:** 1145-1155.

27. Fontenot JD, Gavin MA, Rudensky AY. Foxp3 programs the development and function of CD4+CD25+ regulatory T cells. *Nature immunology* 2003, **4**(4)**:** 330-336.

28. Abbas AK, Benoist C, Bluestone JA, Campbell DJ, Ghosh S, Hori S*, et al.* Regulatory T cells: recommendations to simplify the nomenclature. *Nature immunology* 2013, **14**(4)**:** 307-308.

29. Vignali DA, Collison LW, Workman CJ. How regulatory T cells work. *Nature reviews Immunology* 2008, **8**(7)**:** 523-532.

30. Bennett CL, Christie J, Ramsdell F, Brunkow ME, Ferguson PJ, Whitesell L*, et al.* The immune dysregulation, polyendocrinopathy, enteropathy, X-linked syndrome (IPEX) is caused by mutations of FOXP3. *Nature genetics* 2001, **27**(1)**:** 20-21.

31. Wildin RS, Ramsdell F, Peake J, Faravelli F, Casanova JL, Buist N*, et al.* X-linked neonatal diabetes mellitus, enteropathy and endocrinopathy syndrome is the human equivalent of mouse scurfy. *Nature genetics* 2001, **27**(1)**:** 18-20.

32. Brunkow ME, Jeffery EW, Hjerrild KA, Paeper B, Clark LB, Yasayko SA*, et al.* Disruption of a new forkhead/winged-helix protein, scurfin, results in the fatal lymphoproliferative disorder of the scurfy mouse. *Nature genetics* 2001, **27**(1)**:** 68-73.

33. Clark LB, Appleby MW, Brunkow ME, Wilkinson JE, Ziegler SF, Ramsdell F. Cellular and molecular characterization of the scurfy mouse mutant. *Journal of immunology* 1999, **162**(5)**:** 2546-2554.

34. Workman CJ, Collison LW, Bettini M, Pillai MR, Rehg JE, Vignali DA. In vivo Treg suppression assays. *Methods in molecular biology* 2011, **707:** 119-156.

35. Qin Z, Blankenstein T. CD4+ T cell--mediated tumor rejection involves inhibition of angiogenesis that is dependent on IFN gamma receptor expression by nonhematopoietic cells. *Immunity* 2000, **12**(6)**:** 677-686.

36. Twyman-Saint Victor C, Rech AJ, Maity A, Rengan R, Pauken KE, Stelekati E*, et al.* Radiation and dual checkpoint blockade activate non-redundant immune mechanisms in cancer. *Nature* 2015, **520**(7547)**:** 373-377.

37. Curiel TJ, Coukos G, Zou L, Alvarez X, Cheng P, Mottram P*, et al.* Specific recruitment of regulatory T cells in ovarian carcinoma fosters immune privilege and predicts reduced survival. *Nature medicine* 2004, **10**(9)**:** 942-949.

38. Tzankov A, Meier C, Hirschmann P, Went P, Pileri SA, Dirnhofer S. Correlation of high numbers of intratumoral FOXP3+ regulatory T cells with improved survival in germinal center-like diffuse large B-cell lymphoma, follicular lymphoma and classical Hodgkin's lymphoma. *Haematologica* 2008, **93**(2)**:** 193-200.

39. Kim JM, Rasmussen JP, Rudensky AY. Regulatory T cells prevent catastrophic autoimmunity throughout the lifespan of mice. *Nature immunology* 2007, **8**(2)**:** 191-197.

40. Onizuka S, Tawara I, Shimizu J, Sakaguchi S, Fujita T, Nakayama E. Tumor rejection by in vivo administration of anti-CD25 (interleukin-2 receptor alpha) monoclonal antibody. *Cancer research* 1999, **59**(13)**:** 3128-3133.

41. Dannull J, Su Z, Rizzieri D, Yang BK, Coleman D, Yancey D*, et al.* Enhancement of vaccine-mediated antitumor immunity in cancer patients after depletion of regulatory T cells. *The Journal of clinical investigation* 2005, **115**(12)**:** 3623-3633.

42. Wang C, Lee JH, Kim CH. Optimal population of FoxP3+ T cells in tumors requires an antigen priming-dependent trafficking receptor switch. *PloS one* 2012, **7**(1)**:** e30793.

43. Delgoffe GM, Woo SR, Turnis ME, Gravano DM, Guy C, Overacre AE*, et al.* Stability and function of regulatory T cells is maintained by a neuropilin-1-semaphorin-4a axis. *Nature* 2013, **501**(7466)**:** 252-256.

44. Overacre-Delgoffe AE, Chikina M, Dadey RE, Yano H, Brunazzi EA, Shayan G*, et al.* Interferon-gamma Drives Treg Fragility to Promote Anti-tumor Immunity. *Cell* 2017, **169**(6)**:** 1130-1141 e1111.

45. Floess S, Freyer J, Siewert C, Baron U, Olek S, Polansky J*, et al.* Epigenetic control of the foxp3 locus in regulatory T cells. *PLoS biology* 2007, **5**(2)**:** e38.

46. Sawant DV, Vignali DA. Once a Treg, always a Treg? *Immunological reviews* 2014, **259**(1)**:** 173-191.

47. Shevach EM, Thornton AM. tTregs, pTregs, and iTregs: similarities and differences. *Immunological reviews* 2014, **259**(1)**:** 88-102.

48. Ohkura N, Hamaguchi M, Morikawa H, Sugimura K, Tanaka A, Ito Y*, et al.* T cell receptor stimulation-induced epigenetic changes and Foxp3 expression are independent and complementary events required for Treg cell development. *Immunity* 2012, **37**(5)**:** 785-799.

49. Kolodkin AL, Levengood DV, Rowe EG, Tai YT, Giger RJ, Ginty DD. Neuropilin is a semaphorin III receptor. *Cell* 1997, **90**(4)**:** 753-762.

50. Parker MW, Guo HF, Li X, Linkugel AD, Vander Kooi CW. Function of members of the neuropilin family as essential pleiotropic cell surface receptors. *Biochemistry* 2012, **51**(47)**:** 9437-9446.

51. Pellet-Many C, Frankel P, Jia H, Zachary I. Neuropilins: structure, function and role in disease. *The Biochemical journal* 2008, **411**(2)**:** 211-226.

52. Tordjman R, Lepelletier Y, Lemarchandel V, Cambot M, Gaulard P, Hermine O*, et al.* A neuronal receptor, neuropilin-1, is essential for the initiation of the primary immune response. *Nature immunology* 2002, **3**(5)**:** 477-482.

53. Romeo PH, Lemarchandel V, Tordjman R. Neuropilin-1 in the immune system. *Advances in experimental medicine and biology* 2002, **515:** 49-54.

54. Yadav M, Louvet C, Davini D, Gardner JM, Martinez-Llordella M, Bailey-Bucktrout S*, et al.* Neuropilin-1 distinguishes natural and inducible regulatory T cells among regulatory T cell subsets in vivo. *The Journal of experimental medicine* 2012, **209**(10)**:** 1713-1722, S1711-1719.

55. Weiss JM, Bilate AM, Gobert M, Ding Y, Curotto de Lafaille MA, Parkhurst CN*, et al.* Neuropilin 1 is expressed on thymus-derived natural regulatory T cells, but not mucosa-generated induced Foxp3+ T reg cells. *The Journal of experimental medicine* 2012, **209**(10)**:** 1723-1742, S1721.

56. Farrar MA, Schreiber RD. The molecular cell biology of interferon-gamma and its receptor. *Annual review of immunology* 1993, **11:** 571-611.

57. Ealick SE, Cook WJ, Vijay-Kumar S, Carson M, Nagabhushan TL, Trotta PP*, et al.* Three-dimensional structure of recombinant human interferon-gamma. *Science* 1991, **252**(5006)**:** 698-702.

58. Bach EA, Aguet M, Schreiber RD. The IFN gamma receptor: a paradigm for cytokine receptor signaling. *Annual review of immunology* 1997, **15:** 563-591.

59. Dighe AS, Richards E, Old LJ, Schreiber RD. Enhanced in vivo growth and resistance to rejection of tumor cells expressing dominant negative IFN gamma receptors. *Immunity* 1994, **1**(6)**:** 447-456.

60. Gao J, Shi LZ, Zhao H, Chen J, Xiong L, He Q*, et al.* Loss of IFN-gamma Pathway Genes in Tumor Cells as a Mechanism of Resistance to Anti-CTLA-4 Therapy. *Cell* 2016, **167**(2)**:** 397-404 e399.

61. Koch MA, Tucker-Heard G, Perdue NR, Killebrew JR, Urdahl KB, Campbell DJ. The transcription factor T-bet controls regulatory T cell homeostasis and function during type 1 inflammation. *Nature immunology* 2009, **10**(6)**:** 595-602.

62. Zheng Y, Chaudhry A, Kas A, deRoos P, Kim JM, Chu TT*, et al.* Regulatory T-cell suppressor program co-opts transcription factor IRF4 to control T(H)2 responses. *Nature* 2009, **458**(7236)**:** 351-356.

63. Chaudhry A, Rudra D, Treuting P, Samstein RM, Liang Y, Kas A*, et al.* CD4+ regulatory T cells control TH17 responses in a Stat3-dependent manner. *Science* 2009, **326**(5955)**:** 986-991.

64. Rubtsov YP, Niec RE, Josefowicz S, Li L, Darce J, Mathis D*, et al.* Stability of the regulatory T cell lineage in vivo. *Science* 2010, **329**(5999)**:** 1667-1671.

65. Du J, Johnson LM, Jacobsen SE, Patel DJ. DNA methylation pathways and their crosstalk with histone methylation. *Nature reviews Molecular cell biology* 2015, **16**(9)**:** 519-532.

66. Wang L, Liu Y, Beier UH, Han R, Bhatti TR, Akimova T*, et al.* Foxp3+ T-regulatory cells require DNA methyltransferase 1 expression to prevent development of lethal autoimmunity. *Blood* 2013, **121**(18)**:** 3631-3639.

67. Nair VS, Oh KI. Down-regulation of Tet2 prevents TSDR demethylation in IL2 deficient regulatory T cells. *Biochemical and biophysical research communications* 2014, **450**(1)**:** 918-924.

68. Yang R, Qu C, Zhou Y, Konkel JE, Shi S, Liu Y*, et al.* Hydrogen Sulfide Promotes Tet1- and Tet2-Mediated Foxp3 Demethylation to Drive Regulatory T Cell Differentiation and Maintain Immune Homeostasis. *Immunity* 2015, **43**(2)**:** 251-263.

69. Sakaguchi S, Vignali DA, Rudensky AY, Niec RE, Waldmann H. The plasticity and stability of regulatory T cells. *Nature reviews Immunology* 2013, **13**(6)**:** 461-467.

70. Feuerer M, Hill JA, Mathis D, Benoist C. Foxp3+ regulatory T cells: differentiation, specification, subphenotypes. *Nature immunology* 2009, **10**(7)**:** 689-695.

71. Zhou X, Bailey-Bucktrout S, Jeker LT, Bluestone JA. Plasticity of CD4(+) FoxP3(+) T cells. *Current opinion in immunology* 2009, **21**(3)**:** 281-285.

72. Komatsu N, Okamoto K, Sawa S, Nakashima T, Oh-hora M, Kodama T*, et al.* Pathogenic conversion of Foxp3+ T cells into TH17 cells in autoimmune arthritis. *Nature medicine* 2014, **20**(1)**:** 62-68.

73. Zhou X, Bailey-Bucktrout SL, Jeker LT, Penaranda C, Martinez-Llordella M, Ashby M*, et al.* Instability of the transcription factor Foxp3 leads to the generation of pathogenic memory T cells in vivo. *Nature immunology* 2009, **10**(9)**:** 1000-1007.

74. Miyao T, Floess S, Setoguchi R, Luche H, Fehling HJ, Waldmann H*, et al.* Plasticity of Foxp3(+) T cells reflects promiscuous Foxp3 expression in conventional T cells but not reprogramming of regulatory T cells. *Immunity* 2012, **36**(2)**:** 262-275.

75. Zhou L, Lopes JE, Chong MM, Ivanov, II, Min R, Victora GD*, et al.* TGF-beta-induced Foxp3 inhibits T(H)17 cell differentiation by antagonizing RORgammat function. *Nature* 2008, **453**(7192)**:** 236-240.

76. Allan SE, Crome SQ, Crellin NK, Passerini L, Steiner TS, Bacchetta R*, et al.* Activation-induced FOXP3 in human T effector cells does not suppress proliferation or cytokine production. *International immunology* 2007, **19**(4)**:** 345-354.

77. Burchill MA, Yang J, Vogtenhuber C, Blazar BR, Farrar MA. IL-2 receptor beta-dependent STAT5 activation is required for the development of Foxp3+ regulatory T cells. *Journal of immunology* 2007, **178**(1)**:** 280-290.

78. Samstein RM, Arvey A, Josefowicz SZ, Peng X, Reynolds A, Sandstrom R*, et al.* Foxp3 exploits a pre-existent enhancer landscape for regulatory T cell lineage specification. *Cell* 2012, **151**(1)**:** 153-166.

79. Merkenschlager M, von Boehmer H. PI3 kinase signalling blocks Foxp3 expression by sequestering Foxo factors. *The Journal of experimental medicine* 2010, **207**(7)**:** 1347-1350.

80. Ouyang W, Beckett O, Ma Q, Paik JH, DePinho RA, Li MO. Foxo proteins cooperatively control the differentiation of Foxp3+ regulatory T cells. *Nature immunology* 2010, **11**(7)**:** 618-627.

81. Ouyang W, Liao W, Luo CT, Yin N, Huse M, Kim MV*, et al.* Novel Foxo1-dependent transcriptional programs control T(reg) cell function. *Nature* 2012, **491**(7425)**:** 554-559.

82. Kerdiles YM, Stone EL, Beisner DR, McGargill MA, Ch'en IL, Stockmann C*, et al.* Foxo transcription factors control regulatory T cell development and function. *Immunity* 2010, **33**(6)**:** 890-904.

83. Harada Y, Harada Y, Elly C, Ying G, Paik JH, DePinho RA*, et al.* Transcription factors Foxo3a and Foxo1 couple the E3 ligase Cbl-b to the induction of Foxp3 expression in induced regulatory T cells. *The Journal of experimental medicine* 2010, **207**(7)**:** 1381-1391.

84. Pan F, Yu H, Dang EV, Barbi J, Pan X, Grosso JF*, et al.* Eos mediates Foxp3-dependent gene silencing in CD4+ regulatory T cells. *Science* 2009, **325**(5944)**:** 1142-1146.

85. Sharma MD, Huang L, Choi JH, Lee EJ, Wilson JM, Lemos H*, et al.* An inherently bifunctional subset of Foxp3+ T helper cells is controlled by the transcription factor eos. *Immunity* 2013, **38**(5)**:** 998-1012.

86. Bruder D, Probst-Kepper M, Westendorf AM, Geffers R, Beissert S, Loser K*, et al.* Neuropilin-1: a surface marker of regulatory T cells. *European journal of immunology* 2004, **34**(3)**:** 623-630.

87. Hansen W, Hutzler M, Abel S, Alter C, Stockmann C, Kliche S*, et al.* Neuropilin 1 deficiency on CD4+Foxp3+ regulatory T cells impairs mouse melanoma growth. *The Journal of experimental medicine* 2012, **209**(11)**:** 2001-2016.

88. Collison LW, Pillai MR, Chaturvedi V, Vignali DA. Regulatory T cell suppression is potentiated by target T cells in a cell contact, IL-35- and IL-10-dependent manner. *Journal of immunology* 2009, **182**(10)**:** 6121-6128.

89. Rubtsov YP, Rasmussen JP, Chi EY, Fontenot J, Castelli L, Ye X*, et al.* Regulatory T cell-derived interleukin-10 limits inflammation at environmental interfaces. *Immunity* 2008, **28**(4)**:** 546-558.

90. Huang S, Hendriks W, Althage A, Hemmi S, Bluethmann H, Kamijo R*, et al.* Immune response in mice that lack the interferon-gamma receptor. *Science* 1993, **259**(5102)**:** 1742-1745.

91. Dalton DK, Pitts-Meek S, Keshav S, Figari IS, Bradley A, Stewart TA. Multiple defects of immune cell function in mice with disrupted interferon-gamma genes. *Science* 1993, **259**(5102)**:** 1739-1742.

92. Yang DH, Kim YK, Sohn SK, Chung JS, Joo YD, Lee JH*, et al.* Induction treatment with cyclophosphamide, thalidomide, and dexamethasone in newly diagnosed multiple myeloma: a phase II study. *Clinical lymphoma, myeloma & leukemia* 2010, **10**(1)**:** 62-67.

93. Dobin A, Davis CA, Schlesinger F, Drenkow J, Zaleski C, Jha S*, et al.* STAR: ultrafast universal RNA-seq aligner. *Bioinformatics* 2013, **29**(1)**:** 15-21.

94. Liao Y, Smyth GK, Shi W. featureCounts: an efficient general purpose program for assigning sequence reads to genomic features. *Bioinformatics* 2014, **30**(7)**:** 923-930.

95. Law CW, Chen Y, Shi W, Smyth GK. voom: Precision weights unlock linear model analysis tools for RNA-seq read counts. *Genome biology* 2014, **15**(2)**:** R29.

96. Ritchie ME, Phipson B, Wu D, Hu Y, Law CW, Shi W*, et al.* limma powers differential expression analyses for RNA-sequencing and microarray studies. *Nucleic acids research* 2015, **43**(7)**:** e47.

97. Wu D, Smyth GK. Camera: a competitive gene set test accounting for inter-gene correlation. *Nucleic acids research* 2012, **40**(17)**:** e133.

98. Battle A, Mostafavi S, Zhu X, Potash JB, Weissman MM, McCormick C*, et al.* Characterizing the genetic basis of transcriptome diversity through RNA-sequencing of 922 individuals. *Genome research* 2014, **24**(1)**:** 14-24.

99. picard. Picard [cited 2016]Available from: http://broadinstitute.github.io/picard/

100. Hill JA, Feuerer M, Tash K, Haxhinasto S, Perez J, Melamed R*, et al.* Foxp3 transcription-factor-dependent and -independent regulation of the regulatory T cell transcriptional signature. *Immunity* 2007, **27**(5)**:** 786-800.

101. Turnis ME, Sawant DV, Szymczak-Workman AL, Andrews LP, Delgoffe GM, Yano H*, et al.* Interleukin-35 Limits Anti-Tumor Immunity. *Immunity* 2016, **44**(2)**:** 316-329.

102. McMurchy AN, Levings MK. Suppression assays with human T regulatory cells: a technical guide. *European journal of immunology* 2012, **42**(1)**:** 27-34.

103. Miyara M, Sakaguchi S. Natural regulatory T cells: mechanisms of suppression. *Trends in molecular medicine* 2007, **13**(3)**:** 108-116.

104. Fontenot JD, Rasmussen JP, Williams LM, Dooley JL, Farr AG, Rudensky AY. Regulatory T cell lineage specification by the forkhead transcription factor foxp3. *Immunity* 2005, **22**(3)**:** 329-341.

105. Facciabene A, Motz GT, Coukos G. T-regulatory cells: key players in tumor immune escape and angiogenesis. *Cancer research* 2012, **72**(9)**:** 2162-2171.

106. Chaudhry A, Rudensky AY. Control of inflammation by integration of environmental cues by regulatory T cells. *The Journal of clinical investigation* 2013, **123**(3)**:** 939-944.

107. Im CK, Rha SY, Jeung HC, Ahn JB, Shin SJ, Noh SH*, et al.* A phase II study of a combined biweekly irinotecan and monthly cisplatin treatment for metastatic or recurrent gastric cancer. *American journal of clinical oncology* 2010, **33**(1)**:** 56-60.

108. Nishikawa H, Sakaguchi S. Regulatory T cells in tumor immunity. *International journal of cancer Journal international du cancer* 2010, **127**(4)**:** 759-767.

109. Jacobs JF, Nierkens S, Figdor CG, de Vries IJ, Adema GJ. Regulatory T cells in melanoma: the final hurdle towards effective immunotherapy? *The Lancet Oncology* 2012, **13**(1)**:** e32-42.

110. Drennan S, Stafford ND, Greenman J, Green VL. Increased frequency and suppressive activity of CD127(low/-) regulatory T cells in the peripheral circulation of patients with head and neck squamous cell carcinoma are associated with advanced stage and nodal involvement. *Immunology* 2013, **140**(3)**:** 335-343.

111. Saito T, Nishikawa H, Wada H, Nagano Y, Sugiyama D, Atarashi K*, et al.* Two FOXP3(+)CD4(+) T cell subpopulations distinctly control the prognosis of colorectal cancers. *Nature medicine* 2016, **22**(6)**:** 679-684.

112. Milpied P, Renand A, Bruneau J, Mendes-da-Cruz DA, Jacquelin S, Asnafi V*, et al.* Neuropilin-1 is not a marker of human Foxp3+ Treg. *European journal of immunology* 2009, **39**(6)**:** 1466-1471.

113. Xu B, Yuan L, Gao Q, Yuan P, Zhao P, Yuan H*, et al.* Circulating and tumor-infiltrating Tim-3 in patients with colorectal cancer. *Oncotarget* 2015, **6**(24)**:** 20592-20603.

114. Kao JY, Zhang M, Miller MJ, Mills JC, Wang B, Liu M*, et al.* Helicobacter pylori immune escape is mediated by dendritic cell-induced Treg skewing and Th17 suppression in mice. *Gastroenterology* 2010, **138**(3)**:** 1046-1054.

115. Luther J, Dave M, Higgins PD, Kao JY. Association between Helicobacter pylori infection and inflammatory bowel disease: a meta-analysis and systematic review of the literature. *Inflammatory bowel diseases* 2010, **16**(6)**:** 1077-1084.

116. Le DT, Uram JN, Wang H, Bartlett BR, Kemberling H, Eyring AD*, et al.* PD-1 Blockade in Tumors with Mismatch-Repair Deficiency. *The New England journal of medicine* 2015, **372**(26)**:** 2509-2520.

117. Oh SY, Kim WS, Lee DH, Kim SJ, Kim SH, Ryoo BY*, et al.* Phase II study of gemcitabine for treatment of patients with advanced stage marginal zone B-cell lymphoma: Consortium for Improving Survival of Lymphoma (CISL) trial. *Investigational new drugs* 2010, **28**(2)**:** 171-177.

118. Brahmer JR, Tykodi SS, Chow LQ, Hwu WJ, Topalian SL, Hwu P*, et al.* Safety and activity of anti-PD-L1 antibody in patients with advanced cancer. *The New England journal of medicine* 2012, **366**(26)**:** 2455-2465.

119. Lee JT, Bartolomei MS. X-inactivation, imprinting, and long noncoding RNAs in health and disease. *Cell* 2013, **152**(6)**:** 1308-1323.

120. Briggs SF, Reijo Pera RA. X chromosome inactivation: recent advances and a look forward. *Current opinion in genetics & development* 2014, **28:** 78-82.

121. Galupa R, Heard E. X-chromosome inactivation: new insights into cis and trans regulation. *Current opinion in genetics & development* 2015, **31:** 57-66.

122. Tahara T, Yamamoto E, Suzuki H, Maruyama R, Chung W, Garriga J*, et al.* Fusobacterium in colonic flora and molecular features of colorectal carcinoma. *Cancer research* 2014, **74**(5)**:** 1311-1318.

123. Overacre AE, Vignali DA. Treg stability: to be or not to be. *Current opinion in immunology* 2016, **39:** 39-43.

124. Hori S. Lineage stability and phenotypic plasticity of Foxp3(+) regulatory T cells. *Immunological reviews* 2014, **259**(1)**:** 159-172.

125. Pandiyan P, Zhu J. Origin and functions of pro-inflammatory cytokine producing Foxp3+ regulatory T cells. *Cytokine* 2015, **76**(1)**:** 13-24.

126. Duhen T, Duhen R, Lanzavecchia A, Sallusto F, Campbell DJ. Functionally distinct subsets of human FOXP3+ Treg cells that phenotypically mirror effector Th cells. *Blood* 2012, **119**(19)**:** 4430-4440.

127. Koenecke C, Lee CW, Thamm K, Fohse L, Schafferus M, Mittrucker HW*, et al.* IFN-gamma production by allogeneic Foxp3+ regulatory T cells is essential for preventing experimental graft-versus-host disease. *Journal of immunology* 2012, **189**(6)**:** 2890-2896.

128. Dang EV, Barbi J, Yang HY, Jinasena D, Yu H, Zheng Y*, et al.* Control of T(H)17/T(reg) balance by hypoxia-inducible factor 1. *Cell* 2011, **146**(5)**:** 772-784.

129. Lee JH, Elly C, Park Y, Liu YC. E3 Ubiquitin Ligase VHL Regulates Hypoxia-Inducible Factor-1alpha to Maintain Regulatory T Cell Stability and Suppressive Capacity. *Immunity* 2015, **42**(6)**:** 1062-1074.

130. Zhao J, Zhao J, Perlman S. Differential effects of IL-12 on Tregs and non-Treg T cells: roles of IFN-gamma, IL-2 and IL-2R. *PloS one* 2012, **7**(9)**:** e46241.

131. Couturier-Maillard A, Secher T, Rehman A, Normand S, De Arcangelis A, Haesler R*, et al.* NOD2-mediated dysbiosis predisposes mice to transmissible colitis and colorectal cancer. *The Journal of clinical investigation* 2013, **123**(2)**:** 700-711.

132. Ivanov, II, Frutos Rde L, Manel N, Yoshinaga K, Rifkin DB, Sartor RB*, et al.* Specific microbiota direct the differentiation of IL-17-producing T-helper cells in the mucosa of the small intestine. *Cell host & microbe* 2008, **4**(4)**:** 337-349.

133. Dominguez-Villar M, Baecher-Allan CM, Hafler DA. Identification of T helper type 1-like, Foxp3+ regulatory T cells in human autoimmune disease. *Nature medicine* 2011, **17**(6)**:** 673-675.

134. Olalekan SA, Cao Y, Hamel KM, Finnegan A. B cells expressing IFN-gamma suppress Treg-cell differentiation and promote autoimmune experimental arthritis. *European journal of immunology* 2015, **45**(4)**:** 988-998.

135. St Rose MC, Taylor RA, Bandyopadhyay S, Qui HZ, Hagymasi AT, Vella AT*, et al.* CD134/CD137 dual costimulation-elicited IFN-gamma maximizes effector T-cell function but limits Treg expansion. *Immunology and cell biology* 2013, **91**(2)**:** 173-183.

136. Visperas A, Shen B, Min B. gammadelta T cells restrain extrathymic development of Foxp3+-inducible regulatory T cells via IFN-gamma. *European journal of immunology* 2014, **44**(8)**:** 2448-2456.

137. Deligne C, Metidji A, Fridman WH, Teillaud JL. Anti-CD20 therapy induces a memory Th1 response through the IFN-gamma/IL-12 axis and prevents protumor regulatory T-cell expansion in mice. *Leukemia* 2015, **29**(4)**:** 947-957.

138. Isaacs C, Herbolsheimer P, Liu MC, Wilkinson M, Ottaviano Y, Chung GG*, et al.* Phase I/II study of sorafenib with anastrozole in patients with hormone receptor positive aromatase inhibitor resistant metastatic breast cancer. *Breast cancer research and treatment* 2011, **125**(1)**:** 137-143.

139. Kim SJ, Lee JW, Jung CW, Min CK, Cho B, Shin HJ*, et al.* Weekly rituximab followed by monthly rituximab treatment for steroid-refractory chronic graft-versus-host disease: results from a prospective, multicenter, phase II study. *Haematologica* 2010, **95**(11)**:** 1935-1942.

140. Diaz LA, Jr., Le DT. PD-1 Blockade in Tumors with Mismatch-Repair Deficiency. *The New England journal of medicine* 2015, **373**(20)**:** 1979.

141. Knol AC, Nguyen JM, Quereux G, Brocard A, Khammari A, Dreno B. Prognostic value of tumor-infiltrating Foxp3+ T-cell subpopulations in metastatic melanoma. *Experimental dermatology* 2011, **20**(5)**:** 430-434.

142. Ichihara F, Kono K, Takahashi A, Kawaida H, Sugai H, Fujii H. Increased populations of regulatory T cells in peripheral blood and tumor-infiltrating lymphocytes in patients with gastric and esophageal cancers. *Clinical cancer research : an official journal of the American Association for Cancer Research* 2003, **9**(12)**:** 4404-4408.

143. Battaglia A, Buzzonetti A, Monego G, Peri L, Ferrandina G, Fanfani F*, et al.* Neuropilin-1 expression identifies a subset of regulatory T cells in human lymph nodes that is modulated by preoperative chemoradiation therapy in cervical cancer. *Immunology* 2008, **123**(1)**:** 129-138.

144. Battaglia A, Buzzonetti A, Baranello C, Ferrandina G, Martinelli E, Fanfani F*, et al.* Metastatic tumour cells favour the generation of a tolerogenic milieu in tumour draining lymph node in patients with early cervical cancer. *Cancer immunology, immunotherapy : CII* 2009, **58**(9)**:** 1363-1373.

145. Chaudhary B, Khaled YS, Ammori BJ, Elkord E. Neuropilin 1: function and therapeutic potential in cancer. *Cancer immunology, immunotherapy : CII* 2014, **63**(2)**:** 81-99.

146. Lowther DE, Goods BA, Lucca LE, Lerner BA, Raddassi K, van Dijk D*, et al.* PD-1 marks dysfunctional regulatory T cells in malignant gliomas. *JCI insight* 2016, **1**(5).

147. Moynihan KD, Opel CF, Szeto GL, Tzeng A, Zhu EF, Engreitz JM*, et al.* Eradication of large established tumors in mice by combination immunotherapy that engages innate and adaptive immune responses. *Nature medicine* 2016, **22**(12)**:** 1402-1410.

148. Pfeiffer T, Schuster S, Bonhoeffer S. Cooperation and competition in the evolution of ATP-producing pathways. *Science* 2001, **292**(5516)**:** 504-507.

149. Warburg O. On the origin of cancer cells. *Science* 1956, **123**(3191)**:** 309-314.

150. Macintyre AN, Gerriets VA, Nichols AG, Michalek RD, Rudolph MC, Deoliveira D*, et al.* The glucose transporter Glut1 is selectively essential for CD4 T cell activation and effector function. *Cell metabolism* 2014, **20**(1)**:** 61-72.

151. Rathmell JC, Fox CJ, Plas DR, Hammerman PS, Cinalli RM, Thompson CB. Akt-directed glucose metabolism can prevent Bax conformation change and promote growth factor-independent survival. *Molecular and cellular biology* 2003, **23**(20)**:** 7315-7328.

152. Wilson WR, Hay MP. Targeting hypoxia in cancer therapy. *Nature reviews Cancer* 2011, **11**(6)**:** 393-410.

153. Altman BJ, Stine ZE, Dang CV. From Krebs to clinic: glutamine metabolism to cancer therapy. *Nature reviews Cancer* 2016, **16**(11)**:** 749.

154. Choi SY, Collins CC, Gout PW, Wang Y. Cancer-generated lactic acid: a regulatory, immunosuppressive metabolite? *The Journal of pathology* 2013, **230**(4)**:** 350-355.

155. Scharping NE, Delgoffe GM. Tumor Microenvironment Metabolism: A New Checkpoint for Anti-Tumor Immunity. *Vaccines* 2016, **4**(4).

156. Michalek RD, Gerriets VA, Jacobs SR, Macintyre AN, MacIver NJ, Mason EF*, et al.* Cutting edge: distinct glycolytic and lipid oxidative metabolic programs are essential for effector and regulatory CD4+ T cell subsets. *Journal of immunology* 2011, **186**(6)**:** 3299-3303.

157. Gerriets VA, Kishton RJ, Johnson MO, Cohen S, Siska PJ, Nichols AG*, et al.* Foxp3 and Toll-like receptor signaling balance Treg cell anabolic metabolism for suppression. *Nature immunology* 2016, **17**(12)**:** 1459-1466.

158. Angelin A, Gil-de-Gomez L, Dahiya S, Jiao J, Guo L, Levine MH*, et al.* Foxp3 Reprograms T Cell Metabolism to Function in Low-Glucose, High-Lactate Environments. *Cell metabolism* 2017, **25**(6)**:** 1282-1293 e1287.

159. Pore N, Jiang Z, Shu HK, Bernhard E, Kao GD, Maity A. Akt1 activation can augment hypoxia-inducible factor-1alpha expression by increasing protein translation through a mammalian target of rapamycin-independent pathway. *Molecular cancer research : MCR* 2006, **4**(7)**:** 471-479.

160. Takubo K, Nagamatsu G, Kobayashi CI, Nakamura-Ishizu A, Kobayashi H, Ikeda E*, et al.* Regulation of glycolysis by Pdk functions as a metabolic checkpoint for cell cycle quiescence in hematopoietic stem cells. *Cell stem cell* 2013, **12**(1)**:** 49-61.

161. Ito K, Suda T. Metabolic requirements for the maintenance of self-renewing stem cells. *Nature reviews Molecular cell biology* 2014, **15**(4)**:** 243-256.

162. Wang H, Franco F, Ho PC. Metabolic Regulation of Tregs in Cancer: Opportunities for Immunotherapy. *Trends in cancer* 2017, **3**(8)**:** 583-592.

163. Ho PC, Bihuniak JD, Macintyre AN, Staron M, Liu X, Amezquita R*, et al.* Phosphoenolpyruvate Is a Metabolic Checkpoint of Anti-tumor T Cell Responses. *Cell* 2015, **162**(6)**:** 1217-1228.

164. Finck BN, Kelly DP. PGC-1 coactivators: inducible regulators of energy metabolism in health and disease. *The Journal of clinical investigation* 2006, **116**(3)**:** 615-622.

165. Scharping NE, Menk AV, Moreci RS, Whetstone RD, Dadey RE, Watkins SC*, et al.* The Tumor Microenvironment Represses T Cell Mitochondrial Biogenesis to Drive Intratumoral T Cell Metabolic Insufficiency and Dysfunction. *Immunity* 2016, **45**(3)**:** 701-703.

166. Woo EY, Chu CS, Goletz TJ, Schlienger K, Yeh H, Coukos G*, et al.* Regulatory CD4(+)CD25(+) T cells in tumors from patients with early-stage non-small cell lung cancer and late-stage ovarian cancer. *Cancer research* 2001, **61**(12)**:** 4766-4772.

167. Liyanage UK, Moore TT, Joo HG, Tanaka Y, Herrmann V, Doherty G*, et al.* Prevalence of regulatory T cells is increased in peripheral blood and tumor microenvironment of patients with pancreas or breast adenocarcinoma. *Journal of immunology* 2002, **169**(5)**:** 2756-2761.

168. Liakou CI, Kamat A, Tang DN, Chen H, Sun J, Troncoso P*, et al.* CTLA-4 blockade increases IFNgamma-producing CD4+ICOShi cells to shift the ratio of effector to regulatory T cells in cancer patients. *Proceedings of the National Academy of Sciences of the United States of America* 2008, **105**(39)**:** 14987-14992.

169. Wing K, Onishi Y, Prieto-Martin P, Yamaguchi T, Miyara M, Fehervari Z*, et al.* CTLA-4 control over Foxp3+ regulatory T cell function. *Science* 2008, **322**(5899)**:** 271-275.

170. Peggs KS, Quezada SA, Chambers CA, Korman AJ, Allison JP. Blockade of CTLA-4 on both effector and regulatory T cell compartments contributes to the antitumor activity of anti-CTLA-4 antibodies. *The Journal of experimental medicine* 2009, **206**(8)**:** 1717-1725.

171. Simpson TR, Li F, Montalvo-Ortiz W, Sepulveda MA, Bergerhoff K, Arce F*, et al.* Fc-dependent depletion of tumor-infiltrating regulatory T cells co-defines the efficacy of anti-CTLA-4 therapy against melanoma. *The Journal of experimental medicine* 2013, **210**(9)**:** 1695-1710.

172. Ishida T, Joh T, Uike N, Yamamoto K, Utsunomiya A, Yoshida S*, et al.* Defucosylated anti-CCR4 monoclonal antibody (KW-0761) for relapsed adult T-cell leukemia-lymphoma: a multicenter phase II study. *Journal of clinical oncology : official journal of the American Society of Clinical Oncology* 2012, **30**(8)**:** 837-842.

173. Lal G, Zhang N, van der Touw W, Ding Y, Ju W, Bottinger EP*, et al.* Epigenetic regulation of Foxp3 expression in regulatory T cells by DNA methylation. *Journal of immunology* 2009, **182**(1)**:** 259-273.

174. Haxhinasto S, Mathis D, Benoist C. The AKT-mTOR axis regulates de novo differentiation of CD4+Foxp3+ cells. *The Journal of experimental medicine* 2008, **205**(3)**:** 565-574.

175. Liston A, Lu LF, O'Carroll D, Tarakhovsky A, Rudensky AY. Dicer-dependent microRNA pathway safeguards regulatory T cell function. *The Journal of experimental medicine* 2008, **205**(9)**:** 1993-2004.

176. Nakagawa H, Sido JM, Reyes EE, Kiers V, Cantor H, Kim HJ. Instability of Helios-deficient Tregs is associated with conversion to a T-effector phenotype and enhanced antitumor immunity. *Proceedings of the National Academy of Sciences of the United States of America* 2016, **113**(22)**:** 6248-6253.

177. Kim HJ, Barnitz RA, Kreslavsky T, Brown FD, Moffett H, Lemieux ME*, et al.* Stable inhibitory activity of regulatory T cells requires the transcription factor Helios. *Science* 2015, **350**(6258)**:** 334-339.

178. Rao RR, Li Q, Gubbels Bupp MR, Shrikant PA. Transcription factor Foxo1 represses T-bet-mediated effector functions and promotes memory CD8(+) T cell differentiation. *Immunity* 2012, **36**(3)**:** 374-387.

179. Zhang Q, Chikina M, Szymczak-Workman AL, Horne W, Kolls JK, Vignali KM*, et al.* LAG3 limits regulatory T cell proliferation and function in autoimmune diabetes. *Science immunology* 2017, **2**(9).

180. Schaer DA, Budhu S, Liu C, Bryson C, Malandro N, Cohen A*, et al.* GITR pathway activation abrogates tumor immune suppression through loss of regulatory T cell lineage stability. *Cancer immunology research* 2013, **1**(5)**:** 320-331.

181. McClymont SA, Putnam AL, Lee MR, Esensten JH, Liu W, Hulme MA*, et al.* Plasticity of human regulatory T cells in healthy subjects and patients with type 1 diabetes. *Journal of immunology* 2011, **186**(7)**:** 3918-3926.

182. Bruder D, Probst-Kepper M, Westendorf AM, Geffers R, Beissert S, Loser K*, et al.* Neuropilin-1: a surface marker of regulatory T cells. *European journal of immunology* 2004, **34**(3)**:** 623-630.

183. Zheng Y, Josefowicz S, Chaudhry A, Peng XP, Forbush K, Rudensky AY. Role of conserved non-coding DNA elements in the Foxp3 gene in regulatory T-cell fate. *Nature* 2010, **463**(7282)**:** 808-812.

184. Yue X, Trifari S, Aijo T, Tsagaratou A, Pastor WA, Zepeda-Martinez JA*, et al.* Control of Foxp3 stability through modulation of TET activity. *The Journal of experimental medicine* 2016, **213**(3)**:** 377-397.